INVESTIGATIONS ON MACHINING CHARACTERISTICS OF METAL MATRIX COMPOSITES USING ABRASIVE FLOW MACHINING

A thesis submitted

in fulfillment of the requirements

for the award of the degree of

DOCTOR OF PHILOSOPHY

By

SUSHIL KUMAR MITTAL

Registration No. 950908016

DEPARTMENT OF MECHANICAL ENGINEERING

THAPAR UNIVERSITY

PATIALA – 147 004, PUNJAB, INDIA

August, 2016

PREFACE

This research work was carried out by the author under the guidance of Dr. Vinod Kumar, Associate Professor, Department of Mechanical Engineering, Thapar University, Patiala and Dr. Harmesh Kumar, Professor and Head, Department of Mechanical Engineering, UIET, Panjab University Chandigarh. Abrasive Flow Machining set up developed at HCTM technical campus, Kaithal was used for the experimental work. Surface topography of specimens was analyzed using Scanning Electron Microscope (SEM) available at NIPER, Mohali and X-ray Diffraction (XRD) set up at IIT Ropar. Several research papers were published out of the present research work.

List of Journals/Conferences in which the papers find place is given below:

1. Sushil Mittal, Vinod Kumar and Harmesh Kumar, "**Experimental Investigation and Optimization of Process Parameters of Al/SiC MMCs finished by Abrasive Flow Machining**", Materials and Manufacturing Processes, Vol 30 (7), 2015, 902-911.
   (**SCI-Indexed; Thomson Reuters**) (Taylor & Francis, Publications, USA).
2. Sushil Mittal, Vinod Kumar and Harmesh Kumar "**Multi-Objective Optimization of Process Parameters of Al/SiC MMCs using Response Surface Methodology finished by Abrasive Flow Machining**", Proceedings of the Institution of Mechanical Engineers, Part L: Journal of Materials: Design and Applications, January 13, 2016, DOI: 10.1177/1464420715627292.
   (**SCI-Indexed; Thomson Reuters**) (SAGE Publications, UK)
3. Sushil Mittal, Harmesh Kumar and Vinod Kumar, "**Study of Machining Characteristics of MMC's using Abrasive Flow Machining**" International Journal of Surface Engineering and Materials Technology, Vol 2, July- Dec 2012, pp 29, ISSN No.2249-7250.
4. Sushil Mittal, Harmesh Kumar and Vinod Kumar,"**Study of machining characteristics of different materials using abrasive flow machining process: a review**" National Conference on Advances in Mechanical Engineering, UIET, Panjab University, Chandigarh, 2011.

ACKNOWLEDGEMENT

I am highly grateful to the authorities of Thapar University, Patiala for providing the opportunity to carry out the present research work. I acknowledge a deep sense of gratitude & humility, the inspiring help and guidance rendered by my supervisors, Dr. Vinod Kumar, Associate Professor, Department of Mechanical Engineering, Thapar University, Patiala and Dr. Harmesh Kumar, Professor and Head, Department of Mechanical Engineering, UIET, Panjab University Chandigarh for their interest and encouragement throughout the research work. Their deep insight into the problem and the ability to provide constructive suggestions have been of immense value in improving the quality of my research work at all stages.

Heartfelt thanks are due to Prof. Prakash Gopalan (Director, Thapar University, Patiala), Dr. O.P Pandey (Dean, Research and Sponsored Projects, Thapar University, Patiala), Dr. S. K. Mohapatra (Senior Prof. & Head, Mechanical Engineering Department, Thapar University, Patiala), Dr. V. P. Agrawal and Dr. Tarun Nanda for their encouragement and support during this research work. I am also thankful to the authors whose research has helped me a lot. I am thankful to Mr. Narender Kumar (Lab. Technician, Metrology Lab.) for providing help in using the Metrology instruments.

I avail the privilege to pour on paper my regards to my parents, family and my in-laws for their constant unconditional support both emotionally and financially. They had given me unequivocal support throughout, as always, for which my mere expression of thanks likewise does not suffice.

No amount of thanks is enough, finally, for my beloved wife Urvashi, who held the key to my success. Her patience and encouragement kept my motivation up. Despite all odds, she single handedly and intelligently managed all family matters as well as my two naughty kids (Arnav and Aarna). There were times during the past five years when everything seemed hopeless and I didn‘t have any hope. I can honestly say that it was only her determination and constant encouragement that ultimately made it possible for me to see this project through to the end. I thank all the souls who helped me in this herculean task. Finally, I bow my head to the ALMIGHTY for all the blessings he has showered on me.

(Sushil Kumar Mittal)

CERTIFICATE

Certified that the thesis entitled "**Investigations on Machining Characteristics of Metal Matrix Composites using Abrasive Flow Machining**" which is being submitted by Mr. Sushil Kumar Mittal, to the Department of Mechanical Engineering, Thapar University, Patiala, in the fulfillment of the requirements for the award of the degree of **DOCTOR OF PHILOSOPHY**, is a record of bonafide research work carried out by him under our guidance and supervision. The matter presented in this thesis has not been submitted either in part or full to any other University or Institute for the award of any degree.

25/8/16

Dr. Vinod Kumar
Associate Professor
Department of Mechanical Engineering
Thapar University, Patiala
Punjab, India

29.8.16

Dr. Harmesh Kumar
Professor and Head
Department of Mechanical Engineering
UIET, Panjab University
Chandigarh, India

ABSTRACT

In the era of non traditional finishing processes, it is of upmost importance that these processes can be applied to composite materials, as they have replaced traditional materials in many applications. It is hard to finish small slots in composite materials which have wide applications now days in aerospace, automobile, medical industries etc. Composite materials have replaced the traditional materials as their properties like light weight, good strength and good economy are of unique benefits. Abrasive Flow Machining (AFM) is an advanced finishing process suitable for machining difficult to reach and machine surfaces. In the literature, work has been reported on Abrasive Flow Machining of materials like Aluminium, Brass and EN8, etc. In the present work AFM set up has been designed and developed in the laboratory for experimental work. Composite materials with a high percentage of SiC (like 20-60 % SiC in Al/SiC composites) have been machined using abrasive flow finishing. Taguchi methodology is applied to find the effect of input parameters (Fluid pressure, percentage of oil in media, grit size, concentration of abrasives, work piece material and number of cycles) on the material removal rate (MRR), change in surface roughness (ΔRa) and surface topography. L27 array has been designed for experimental work. It is observed that extrusion pressure is the most significant factor for MRR and ΔRa. Optimization of response parameters (MRR and ΔRa) is done using Taguchi method. Further Response Surface Methodology (RSM) is also applied for experimental investigation. Box-Behnken design has been selected. Response parameters have been optimized using the desirability approach. The significance of different parameters is identified using ANOVA. An optimum combination of parameters is designed for the process. Mathematical modeling has been done for material removal rate using FEM and mechanism of material removal in abrasive flow machining has been also discussed. Specimens were examined and analyzed using scanning electron microscope and X- ray diffraction techniques. Work pieces cut by EDM process were finished by AFM process. It was observed that abrasive flow machining has removed the defects and improved the surface finish significantly.

LIST OF TABLES

LIST OF FIGURES

CONTENTS

CHAPTER 01

INTRODUCTION

1.0 INTRODUCTION

In the present era advanced industries require high strength materials with good finish. Composite materials have very good strength to weight ratio. If composite materials are finished to good surface finish, they can be used in advanced industries like aerospace, automobile, die finishing etc. It is hard to finish composite materials with intricate shapes. Machining means removal of certain parts of the work pieces to finished parts. Now, machining is being classified in two types: Conventional and Non-Conventional machining. In conventional machining tool is harder than the work piece to be machined. In this type of machining tool directly removes the material from work piece (Jain, 2012). A relative motion between the tool and work piece is responsible for the material removal (Pandey and Shan, 2005). When there is no direct contact between the tool and work piece and removal of material takes place indirectly, it is known as non-conventional machining (Weller, 1984). Non-conventional machining processes can be used to finish, intricate shaped composite materials (Hofy). Abrasive flow machining (AFM) is one of the non-conventional processes, which can be used to finish intricate shaped composite materials. The Abrasive Flow Machining process was developed in the 1960s by Extrude Hone Corporation, USA and this process is used to polish the areas that are difficult to reach (Jain et al. 1999). For the improved performance developments are taking place to improve the existing AFM process. Researchers have developed modified AFM machines as Magnetic Abrasive Finishing (MAF), Magnetic Float Polishing (MFP), Magnetorheological finishing (MRF), Magnetorheological Abrasive Flow Finishing (MRAFF), Rotational-Magnetorheological Abrasive Flow Finishing (R-MRAFF) (Sankar et al., 2011).

1.1 MACHINING OF COMPOSITE MATERIALS

1. The composite materials are advanced materials with desired properties obtained by combining two or more materials.

2. Machinability of silicon carbide particle reinforced aluminium alloy matrix composites has been discussed (Muller et al., 2001).

3. Categorized as Difficult-to-Machine material, due to its characteristics such as low elastic modulus, average thermal conductivity and chemical reactivity with other metals.
4. It is difficult to machine MMC with conventional tools as they are very hard, extensive tool wear is caused by very hard abrasives (Miracle et al., 2005) and (Basavarajappa et al., 2007).
5. Factors affecting tool wear are the percentage, size and density of the abrasive particles (Dabade U. et al., 2009).
6. Al/SiC MMC finished with processes like abrasive flow machining gives high and suitable surface finish, which have wide applications in the industry.

1.2 ABRASIVE FLOW MACHINING PROCESS

The AFM process has a great potential to polish, remove burrs, radius and remove recast layer of work piece. AFM processes are classified as: One way, two ways and orbital AFM. Two ways AFM process is the most common (Jain et al., 1999). In two-ways AFM, the abrasive medium flow up and down through passages formed by the work piece and fixture in two cylinders. Upper cylinder-piston arrangement pushes the abrasive medium downwards. When the abrasive medium is extruded through work piece held between the fixtures, finishing of the surface takes place. In upward stroke lower cylinder pushes the medium upwards. Hence, finishing also takes place in upward movement of abrasive media. AFM setup is shown in fig. 1.1.

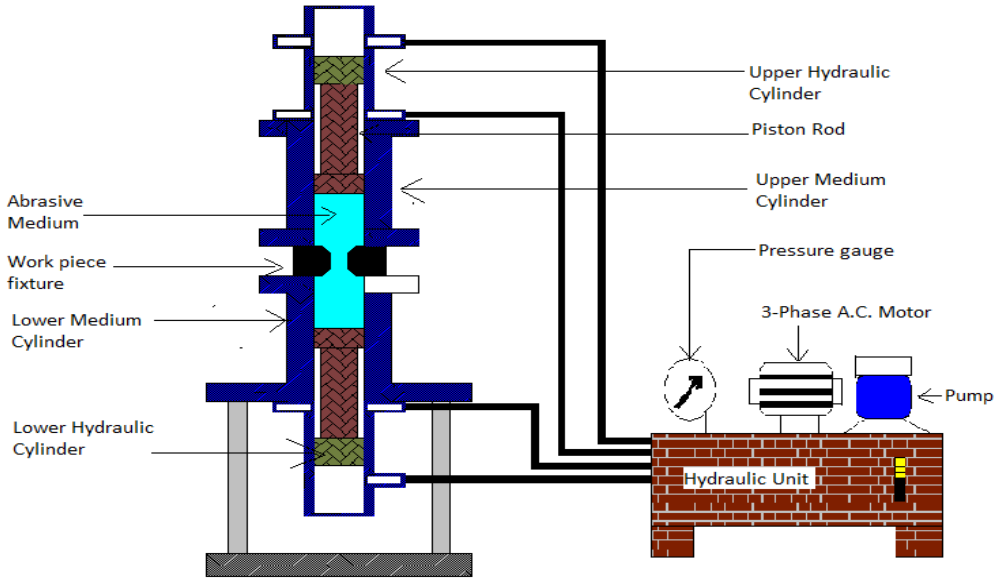

Fig. 1.1: Experimental setup of abrasive flow machining process

1.2.1 Basic Principle of AFM Process

AFM is a process in which a work piece is finished by passing a semisolid abrasive medium over the surface to be finished. Viscosity of media is so high that it can be held between the fingers. Fig. 1.2 shows the AFM process where the inner surface of a work piece is being machined by the medium passed through it (Sankar et al., 2011).

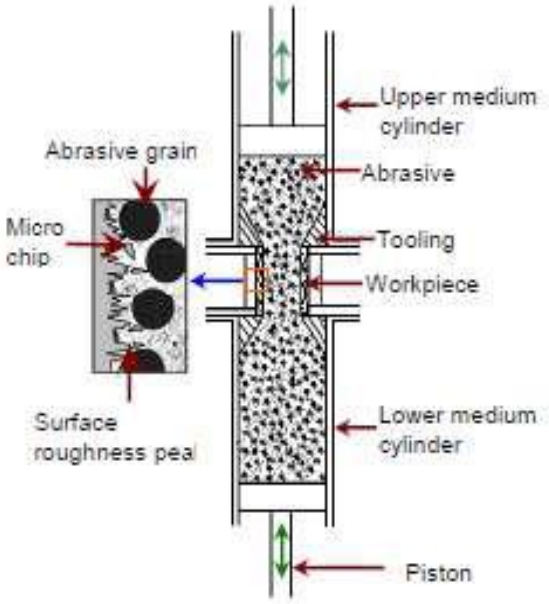

Fig. 1.2: Schematic diagram of two- way AFM process (Sankar et al., 2011)

Upper cylinder-piston arrangement pushes the abrasive media downwards. When the abrasive medium is extruded through work piece held between the holder/fixture, finishing of the surface takes place. Then the lower cylinder pushes the medium upwards. Hence finishing also takes place in upward movement of media.

1.2.2 Main components of AFM

The main components of abrasive flow machining are the following:

1.2.2.1 AFM setup

AFM setup is an important component for abrasive flow machining. It should be able to vary the process variables. Setup should have the capability to accommodate the required pressure.

1.2.2.2 Abrasive medium

Abrasive medium consists of three components: Abrasive particles, Polymer as carrier and oil. The abrasive particles may be such as Al_2O_3, SiC, B_4C etc. Polymer such as Silicone rubber, liquid silicone can be used. Oil such as hydraulic oil can be used.

1.2.2.3 Tooling and fixture

Tooling and fixture should be such that abrasive particles abrade the surface effectively. Fixture material should be selected so that it can be machined easily to the required shape. Passage area of the fixture should be increased gradually so that vibrations do not take place.

1.2.3 Material Removal Mechanism in AFM Process

In abrasive flow machining, the abrasive medium passes through the work piece and erodes the work piece. Abrasive particles in the media contact peaks on the surface of the work piece and remove them. The medium is forced through the work piece at high pressure using hydraulic energy. The maximum material removal takes place when passage of the medium is restricted; as the flow speed and pressure of the medium increases when its passage is restricted. Abrasive flow machining gives a very good surface finish.

1.2.4 Process variables affecting AFM

The process variables affecting the AFM process are Extrusion pressure, viscosity of medium, concentration of abrasives, grit size of abrasives, number of cycles, etc. These input process variables affect output responses like material removal rate and surface roughness. Effect of different process variables is discussed in detail in chapter number 3.

1.2.5 Advantages of AFM Process

- Excellent control of process
- Can finish, intricate shaped components
- Radius generation
- Faster change of work piece
- Faster changeover of media

1.2.6 Disadvantages of AFM Process

- Low finishing rate
- Incapability to correct the form geometry
- Abrasive materials tend to get embedded, if the work material is ductile
- Require closed environment
- Require start-up hole.

1.2.7 Applications of AFM Process

- Dies and Moulds
- Aerospace, need materials with high strength to weight ratio like MMCs
- In the automobile industry to make the body for passenger cars
- In defense for making bullet proof jackets
- Marine applications
- Medical industry
- Electronics
- Building construction

1.3 SCOPE OF THE WORK

These days; composite materials have overcome the traditional work piece materials. Composites have many advantages like these are light in weight and have more strength. Due to its many advantages, composite materials have wide applications in industry. However, fine machining and to attain a glass surface finish on surfaces of composites is a challenging task. (Ozden et al., 2007) reported the effect of the accumulation of reinforced particles in composite material. Due to unequal distribution and accumulation of particles resulted into reduction of toughness properties of the material. AFM process is an advanced method to get a good surface finish on MMCs. All these requirements necessitated us to take the present study. SiC/Al MMC (with 20, 40 and 60 percent SiC in Al as base material) has been selected as work material.

1.4 METHODOLOGY

1. **Survey of literature:** Extensive literature survey of AFM process has been conducted.
2. **Identification of Composite materials:** The SiC/Al MMC (with 20, 40, 60 percent SiC in Al as base material) has been identified and procured.

3. **Design and Development of experimental setup:** A new experimental setup has been designed and fabricated in the laboratory of Haryana College of Technology and Management, Kaithal.
4. **Procurement of abrasive medium:** Study of feasibility for different possible abrasive mediums has been done and procured.
5. **Experimentation:** The experiments have been designed using Taguchi method and Box Behnken approach of response surface methodology. Experiments have been conducted on experimental set up in the laboratory.
6. **Analysis of machined surface:** Results obtained have been analyzed using by applying ANOVA. The techniques Scanning Electron Microscopy (SEM) and XRD diffraction have been used for analysis of surfaces.
7. **Modelling:** A generalized mathematical model for MRR has been developed using FEM. MRR has been calculated after getting the values from the FLUENT software of ANSYS 15.
8. **Conclusions:** On the basis of results, different conclusions have been withdrawn.

1.5 ORGANIZATION OF THESIS

The write up of the thesis is divided into six chapters:

Chapter I: Introduction highlights the brief description of the non-traditional machining processes. Introduction to abrasive flow machining (AFM) process, working principle, mechanism of material removal, advantages, disadvantages and applications of AFM have been discussed. A brief introduction to composite materials is also presented. Scope, the overall methodology of the work and organization of thesis have also been described.

Chapter II: Literature Review presents an extensive research work carried out in the field of AFM, which leads to an understanding of various aspects of machining characteristics such as the material removal rate (MRR), surface roughness (SR) and surface topography. The effect of different machining input parameters on the machining characteristics has been discussed in detail. A review of research work on AFM of composite materials is presented in this chapter. Experimental methodologies for planning and analyzing the experiments have been discussed.

Various optimization techniques to optimize the input parameters are also discussed. After a detailed study of the published work on AFM process, it was observed that few studies have explained the machining characteristics of brass, aluminum work pieces. From the literature review, it can be concluded that little work has been reported on AFM of composite materials. It can also be concluded that no work has been reported on composite materials having high percentage of hard materials like SiC in the base material like aluminum. In the present research work above mentioned materials are taken for parametric and surface topographic study.

Chapter III: Design of study highlights pilot experimentation performed using one factor at a time approach to sort out the significant process parameters and to fix the range of these process parameters. The levels of the input parameters were finalized based on the results of pilot experimentations and literature survey. It was concluded that fluid pressure, viscosity of medium, mesh number of grit, concentration of abrasives, work piece material and number of cycles have a significant effect on MRR and SR. Taguchi method was used to design the experiments, L27 orthogonal array was used to find the effect of process parameters on output responses. Further response surface methodology was also used to find the effect of input parameters on responses and multi objective optimization is done using desirability approach.

Chapter IV: Experimentation describes the materials used in the present study. Design and development of experimental setup have been explained. Complete detail of experiments conducted in phases A and B is given. Three trials with two repetitions have been conducted for each experiment. This chapter also presents results of experiments conducted in tabulated form.

Chapter V: Results and discussion concentrates on analysis of results of main experimentation, in order to identify individuals as well as interaction effects of process parameters on various responses i.e. MRR and ΔRa. Effect of input parameters in terms of significance and the percentage contribution is discussed in detail on response parameters. Specimens were examined using SEM and XRD to understand the surface topography of machined surfaces. A Finite Element Method (FEM) based mathematical model of material removal has been proposed for AFM process. The purpose of the proposed model is to understand the abrasive action during the AFM process. A standard ANSYS package version 15

with FLUENT software has been employed to model the problem and to evaluate the rate and velocity of impingement and stress distributions in the work piece material.

Chapter VI: Conclusions present the conclusions of the research work carried out. This chapter is followed by references.

CHAPTER 02

LITERATURE REVIEW

2.1 INTRODUCTION

AFM was developed in the 1960s as a method to deburr, polish, and radius difficult to reach surfaces like intricate geometries and edges by passing an abrasive laden viscoelastic polymer over them. Literature survey has been categorized into two sections: Abrasive Flow Machining and Finite Element Modelling.

2.1.1 Abrasive flow machining

Jain R. K. et al. (1999) developed a model of material removal and surface roughness for abrasive flow machining process. Radial stresses have been predicted at the workpiece. Estimation of the material removal and surface roughness during AFM is also proposed on the basis of theoretical analysis. The theoretical results are compared with the experimental findings reported in the literature, and they are found to agree well.

Jain V. K. and Adsul S. G. (2000) reported the effects of different process parameters, such as number of cycles, concentration of abrasive, mesh size of abrasives and media flow speed, on material removal and surface finish for aluminium and brass work materials. The significant process parameter found was the concentration of abrasive, followed by mesh size, number of cycles, and media flow speed. Theoretical results were compared with experimental results. The machined surface was analyzed using scanning electron microscopy.

Jain R. K. et al. (2000) applied neural network for modeling and selection of optimum machining conditions in AFM. A four inputs, two outputs, and one hidden layer generalized back-propagation neural network has been used to establish the process model. Another network, which parallelizes the ALM algorithm, is used to determine the optimal machining. A good agreement was shown between simulation results and experimental results. For validation, optimization of the AFM process has also been carried out using genetic algorithm.

Jain N. K. and Jain V. K. (2001) developed various analytical and some semi-empirical/empirical material removal models (approximately 40) for different mechanical type advanced machining processes.

Jain R. K. et al. (2001) proposed a model for the determination of specific energy and tangential forces in AFM process. Process parameters like grain size, applied pressure, work piece material, numbers of cycles and number of active grains have been considered. Heat transfer to the work piece and medium has been analyzed. Theoretical results of work piece temperatures were compared with experimental observed values. The model also predicted the heat entering into the work piece and medium.

Singh S. and Shan H. S. (2002) applied a magnetic field around the work piece in AFM to improve the surface roughness and the material removal rate. A set-up was developed to study the effect of process parameters on the performance of the process by using a composite process termed as magneto abrasive flow machining (MAFM). Brass components were machined by this process and relationships were developed between the material removal rate and the percentage improvement in surface roughness of components. Analysis of variance has been applied to identify the significant parameters and test the adequacy of the models.

Gorana V. K. et al. (2003) investigated experimentally cutting forces and active grain density during abrasive flow machining. The results show that cutting force components and active grain density affects the surface roughness produced during the AFM process. The effects of three input variables (extrusion pressure, concentration of abrasives and grain size) on the responses (material removal, ΔRa value, cutting forces and active grain density) were analyzed. The machined surface was examined using a scanning electron microscope.

Jain R. K. et al. (2003) presented a simulation of active grain density in AFM process. Media topography is greatly influenced by the variables. Experimental observations obtained by a microscopic method were compared with simulation results.

Jeong D.K. and Kyung D. K. (2004) used spring collets made of chrome-molybdenum to test the deburring of the surface of collets, including crossed micro grooves by abrasive flow machining.

Singh D. K. et al. (2004) applied the Taguchi method to find out important parameters affecting the surface quality in Magnetic Abrasive Finishing. The parameters affecting the surface quality are applied voltage, working gap, speed of rotation of the magnet, and grit size. It has been reported that for ΔRa, voltage and working gap are the most significant parameters, then grit size and rotational speed.

Yan B. et al. (2005) investigated laser cutting of aluminium alloy reinforced with Al2O3 ceramic particles. They examined that higher quantity of reinforced particles have shown higher surface roughness as compared to lower quantity.

Gorana V. K. et al. (2006) presented a theoretical model for forces prediction during material deformation in abrasive flow machining. An experimental research has been carried out by measuring the axial force, radial force and active grain density during the AFM process. Results obtained from theoretical model have been compared with the experimental data of force and active grains obtained during AFM. Scratching experiments have also been performed to study the mechanism of material removal during the AFM process. It has been concluded that mechanism of material removal is rubbing and ploughing.

Gorana V. K. et al. (2006) in another study proposed an analytical model to predict the surface roughness for different machining conditions in AFM. Kinematics analysis was used to model the interaction between grain and work piece. Grain size, grain concentration and extrusion pressure were varied to study the AFM process with an initial surface finish of the work piece. The results of the proposed model are in good agreement with experimental results.

Sharma R. K. (2006) discussed a case-based approach in conjunction with standard tools, techniques and practices used to discuss various issues related with TPM implementation in a semi-automated cell. The findings indicate that TPM not only leads to increase in efficiency and effectiveness of manufacturing systems, measured in terms of OEE index, by reducing the wastages but also prepares the plant to meet the challenges put forward by globally competing economies to achieve world class manufacturing (WCM) status.

Singh et al. (2006) observed the effect of input parameters of AFM on the surface roughness of work pieces with the help of Taguchi technique. The optimum setting of various parameters affecting surface roughness has been reported.

Walia et al. (2006) proposed an analytical model for the velocity and the angle at which abrasive particles attack the work piece surface in AFM. Results of changing the parameters like shape and rotational speed of centrifugal force generating rod, extrusion pressure, number of process cycles and abrasive grit size have been discussed. The results indicate that all the input variables have a significant effect on the response parameters, like MR and SR.

Ko et al. (2007) applied a method of coolant supply and component of abrasive powder in magnetic abrasive flow machining to improve the surface roughness. Micro deburring of precision parts was done using magnetic abrasive flow machining.

Tzeng Hsinn-Jyh et al. (2007) developed a self-modulating abrasive medium whose viscosity and fluidity could be adjusted during the processing period. The complex micro channel was fabricated of the stainless steel (SUS304) using WEDM. The parameters (abrasive particle size, concentration, extrusion pressure and machining time) affecting AFM process were considered to study the machining characteristics of the micro channel.

Wang A. C. et al. (2007) developed the polymer abrasive gels for AFM process. Abrasive media with lower cost and good performance was developed to improve the roughness of the WEDM surface in this research. It has been reported that silicone rubber has good deformation, can flow through the complex holes easily and does not stick to the work piece surface after machining. In this study, abrasive particles and silicone rubber were used to become the flexible media. Then a surface, cut by WEDM, was polished in AFM.

Wang A. C. et al. (2007) used non-Newtonian flow to set up the abrasion mechanism of the abrasive media in AFM. A power law equation was used as a main equation of the non-Newtonian flow to describe the motion of the abrasive media. Viscosities vs. shear rates of different abrasive gels were used to establish the power law in CFD-ACE+ software. The relationships between the simulations and the experiments were obtained. The abrasive gel with high viscosity generated a larger shear force than the abrasive gel with low viscosity in the same area.

Das M. et al. (2008) attempted to analyze the medium flow in magneto rheological abrasive flow finishing (MRAFF) process. A capillary viscometer has been developed to study the effect

of magnetic field on the rheological properties of the medium. Microstructure of the mixture of ferromagnetic and abrasive particles in magneto rheological polishing fluid (MRPF) has been proposed, and normal force on the abrasive particles is calculated from the applied magnetic field. A model for the prediction of material removal and surface roughness has also been presented. Theoretical results have been compared with the experimental data available in the literature and was found in good agreement.

Fang L. et al. (2008) presented temperature as sensitive monitor for efficiency of work in abrasive flow machining. Mooney viscosity–temperature relation of media explains that temperature rise decreases media viscosity. CFD approach is applied to predict the abrasive particles movement tendency. A two-dimensional model is constructed for AFM process. The simulation results show that the temperature rise of media results in increasing the rolling tendency of abrasive particles which reduces work efficiency.

Jung D. et al. (2008) studied the effects of the AFM process on a direct injection diesel engine fuel injector nozzle. Microscopic variations inside the nozzle were measured by applying geometry characterization techniques. Empirically-based correlations had provided the geometry changes after finishing with AFM process. It could be clearly observed that AFM-processed injectors have improved engine performance and emissions.

Kamal K. Kar et al. (2008) studied performance evaluation and rheological characterization of butyl rubber based media for abrasive flow machining process. An attempt has been made to develop new viscoelastic media for fine finishing through the AFM process. The newly developed media was again characterized through rheological properties. Rheological properties have been affected by temperature, shear rate, creeping time and frequency and the percentage ingredients of media.

Fang L. et al. (2009) developed an analytical model of ellipsoidal geometry to determine particle movement patterns in AFM. C++ language was used to propose particle movement pattern. It was found that a seat position of ellipsoid was an easy grooving position for a particle and a large elasticity value predominantly increased grooving particle numbers.

Jain V.K. (2009) discussed Abrasive Flow Finishing (AFF), Magnetic Abrasive Finishing (MAF), Magneto rheological Finishing, Magneto rheological Abrasive Flow Finishing, Elastic Emission Machining (EEM) and Magnetic Float Polishing. Except AFF and EEM all other processes mentioned above use a medium whose properties can be controlled externally with the help of magnetic field. It also explained why a magnet used in MAF should have a slot in it even though the area under the slot has "non-machining" zone. Based on the experimental observations it has been elaborated why to use pulse D.C. power supply in MAF in place of smooth D.C. power supply.

Sankar M. R. et al. (2009) discussed R-AFF process where complete tooling was externally rotated and the medium reciprocated with the help of hydraulic actuators. Preliminary experiments have been conducted on Al alloy and Al alloy/SiC MMCs at different extrusion pressures. Effect of work piece rotational speed has been studied on ΔRa, MR, change in work piece hardness and surface topology.

Sankar M. R. et al. (2009) investigated experimentally mechanism of material removal in nano finishing of MMCs using abrasive flow finishing process. Metal matrix composite (MMC-aluminum alloy and its reinforcement with SiC) work pieces were initially ground to a surface roughness value in the range of 0.6±0.1 μm, and later were finished to the Ra value of 0.25±0.05 μm by using an Abrasive Flow Finishing process. The relationship between extrusion pressure and Ra shows an optimum value at about 6MPa. In the same way, the relationship between weight percentage of processing oil (plasticizer) and Ra also shows an optimum value at 10 percent weight. Further, an increase in work piece hardness requires more number of cycles to achieve the same level of improvement in Ra. Material removal also increases with an increase in extrusion pressure and the number of cycles, while it decreases with an increase in processing oil content in the medium. It is also concluded that the mechanism of finishing and material removal in case of alloys is different from that in case of MMC.

Uhlmann E. et al. (2009) modeled the abrasive flow machining process on advanced ceramic materials. It has been reported that it is possible to realize predefined edge rounding on any brittle or hard material using AFM. AFM is also suitable for advanced ceramic materials. An attempt has been made to discover the fundamental principles of AFM on advanced ceramic materials such as a relation between flow processes, surface formation and edge rounding. The

aim of this approach is to predict surface quality and edge rounding on any user-defined geometry.

Brar B. S. et al. (2010) presented a state of art paper on Abrasive Flow Machining. In this paper an overview of AFM technology, experimental and analytical research work undertaken has been discussed. This paper also highlights the range of AFM applications together with the development of hybrid machining processes. The trends for future AFM research have been discussed in this paper.

Lee H. S. et al. (2010) reported hybrid polishing mechanism of single crystal SiC using mixed abrasive slurry (MAS). Single crystal SiC is a hard and inert material used in optical land power devices. Hybrid polishing technique using MAS with colloidal silica and nano-diamond has been proposed. Optimization of material removal rate and good surface has been done for MAS.

Mali H.S & Manna A. (2010) used conventionally machined cylindrical surface of Al/15 wt% SiCp-MMC as work piece. It presented the utilization of robust design-based Taguchi method for optimization of AFM parameters. The influences of AFM process parameters on surface finish and material removal had been analyzed. The mathematical models for Ra, Rt, $f¢$Ra, and $f¢$Rt and material removal were established to investigate the influence of AFM parameters. Conformation test results verify the effectiveness of these models and optimal parametric combination within the considered range. Scanning electron micrographs testifies the effectiveness of AFM process in fine finishing of Al/15 wt% SiCp.

Sadiq and Shunmugam (2010) presented results of varying magnetic field in magneto-rheological abrasive honing process. They applied magnetic field on magnetic and non-magnetic specimens, the magnetic field near the non-magnetic specimens was increased.

Das M. et al. (2011) found experimentally that the improvement in out of roundness of Stainless Steel finished by Rotational–Magnetorheological Abrasive Flow Finishing process can be done by 2.04 µm. In this process, rotating motion and a simultaneous up and down motion is given to the polishing medium. Experiments have been designed using response surface methodology.

Kenda J. et al. (2011) investigated the machining characteristics of Abrasive Flow Machining of hardened tool steel AISI D2. It has been reported that AFM is capable to remove EDM damaged

surface and improve surface roughness to a significant value. High compressive residual stresses are induced to the machined surface, in a very thin sub layer of 10 μm. It is concluded that AFM is an efficient finishing process, for a good surface finish and productivity.

Yamaguchi H. et al. (2011) worked on magnetic abrasive finishing of cutting tools for machining of titanium alloys. Uncoated carbide tool surfaces are processed using MAF to improve the tool wear. Magnetic particle chains configuration plays an important role in surface finishing with minimal damage to the tool cutting edges. Roughness of less than 25 nm Ra on the flank and nose and less than 50 nm Ra on the rake can be achieved. In turning of Ti–6Al–4V alloy rods, tool life of MAF-processed tools increased up to two times.

Bahre D. et al. (2012) treated components of fuel injection systems to withstand higher internal pressures. Surface quality and reduction of stress concentrations at bore intersections have been investigated. Influence of medium pressure and lead time on the surface quality and form tolerance; have been studied for automotive steel AISI 4140. A measurement setup with axial force sensor was developed to measure the influence of the applied medium pressure on the machined part of the work piece.

Kamble P. D. et al. (2012) explored the recent increase in the use of hard, high strength and temperature resistant materials in engineering necessitated the development of newer machining techniques. Magneto abrasive flow machining is a new development in AFM. A set up has been developed for a composite process termed as magneto abrasive flow machining (MAMF). The effect of parameters on the performance of the process has been studied. Experimental results indicate significantly improved performance of MAMF over AMF.

Mali H.S. et al. (2012) applied artificial neural networks for modeling and simulation of response characteristics during the AFM process in finishing of Al/SiC MMCs components. A generalized back-propagation neural network with five inputs, four outputs, and one hidden layer was designed. Based upon the experimental data of the effects of AFM process parameters, e.g., abrasive mesh size, number of finishing cycles, extrusion pressure, percentage of abrasive concentration, and media viscosity grade, on performance characteristics, e.g., arithmetic mean value of surface roughness (Ra, micrometers), maximum peak–valley surface roughness height (Rt, micrometers), improvement in Ra (i.e., ΔRa), and improvement in Rt (i.e., ΔRt), the

networks were trained for finishing of Al/ SiC MMC cylindrical components. ANN models were compared with multivariable regression analysis models, and their prediction accuracy was experimentally validated.

Mulik and Pandey (2012) measured Normal force and finishing torque in ultrasonic assisted magnetic abrasive finishing process. It has been observed that supply voltage and finishing gap have influenced the finishing forces and torque. Mathematical models were developed to predict the force and torque dependence on voltage, machining gap and work piece hardness.

Sankar et al. (2012) created different media by using styrene butadiene based polymer, plasticizer and abrasives in the AFM process. Experiments were done to finish Al alloy and its MMCs using rotational abrasive flow finishing process. The effect of each parameter such as shear stress, percentage viscous component, modulus of stress relaxation and storage on the ΔRa and MRR was analyzed.

Singh R. et al. (2012) studied the parametric effect on ΔRa for Hybrid Centrifugal Force Assisted Abrasive Flow Machining Process. In recent years, hybrid-machining processes come into existence, to improve the efficiency of processes like abrasive flow machining. Centrifugal force has been applied for productivity enhancement in terms of surface roughness (Ra) of abrasive flow machining. Centrifugal force to the abrasive particles normal to the axis of work piece was produced using a rotating CFG rod inside the cylindrical work piece. The influence of important process parameters has been studied on the performance of a process.

Singh R. et al. (2012) in another study carried hybrid magnetic force assisted abrasive flow machining process for optimal material removal. The abrasive flow machining was hybridized with the magnetic force for improvement in MR. DC current is applied to the solenoid to generate the magnetic force around the length of the cylindrical work piece. This magnetic force is applied the abrasive particles normal to the axis of work piece. Effect of input parameters on the process has been studied.

Yin X. and Komvopoulos K. (2012) analyzed abrasive wear of a surface with low roughness sliding against a rough surface. Slip line theory of plasticity was applied. Numerical values of dependence of wear rate of abrasive and coefficient of wear on normal load, roughness of the surface, elastic plastic material properties of the surface and interfacial shear strength are

obtained. These are obtained for ceramic-ceramic, ceramic-metallic, and metal-metal sliding systems.

Brar B. S. et al. (2013) applied Taguchi's method to the developed Helical AFM process. Taguchi method has been applied to optimize the important parameters like abrasives/ media ratio, extrusion pressure and number of cycles, for characteristics of MR and the percentage improvement in the surface finish (ΔRa). Taguchi's experimental design based on L9 orthogonal array has been taken for the experimentation and on the basis of maximum Signal-to-Noise (S/N) ratio, the optimal parameters have been selected, leading to the robust AFM setup.

Cherian J. et al. (2013) investigated the effect of process variables in Abrasive Flow Machining. It is capable of machining areas which are difficult to reach by conventional machining and can be used to machine and improve surface finish of internal parts of intricate shapes. The effect of the work piece hardness, abrasive size, abrasive hardness, extrusion pressure and properties of carrier was investigated on the performance of AFM. The objective of the work was to study the effects of process variables on surface finish and material removal.

Judal et al. (2013) investigated process parameters i.e. vibration frequency, rotational speed, grit size and flux density on vibrating cylindrical magnetic abrasive finishing setup for aluminium workpieces.

Muguthu and Gao (2013) investigated tool wear, mechanism of wear, surface profile and accuracy for turning of Al2124SiCp (45%wt) MMC. Polycrystalline diamond and cubic boron nitride tools were used for machining. Results showed that tool wear mechanisms were abrasion, adhesion, chipping, and fracture. It is reported that in machining the MMC, PCD tools were the best then coated cubic boron nitride, and finally uncoated cubic boron nitride tools.

Tofigh A. et al. (2013) analyzed that addition of large sized B4C reinforced particles decreases the wear rate of metal matrix composite material.

Venkata B. et al. (2013) analyzed the machinability of various composite materials. They recommended the aluminum metal-matrix composite material by considering various parameters like radial force, cutting force and surface roughness.

Howard and Cheng (2014) developed a model using RSM for AFM to investigate the effect of input parameters on the surface of titanium alloy 6Al4V.

Kant G. and Sangwan K. S. (2014) provided a multi-objective predictive model for the optimization of power consumption and surface roughness in machining, using grey relational analysis coupled with principal component analysis and response surface methodology. ANOVA has been applied to test the significance of the proposed predictive model. It has been observed that feed is the most significant machining parameter, then depth of cut and cutting speed to reduce power consumption and surface roughness.

Sidhu et al. (2014) reported the results of MMCs machined with EDM process. SEM micrographs have been taken, and recast layer thickness has been studied.

Zhenlong W. et al. (2014) analyzed the surface of SiC/Al composites in WEDM process to overcome the problem of a recast layer usually found on machined surface processed by EDM process.

Paiva Rosa M. M. et al. (2015) presented a mixed numerical-experimental approach capable to predict and optimize the performance of the footwear adhesive joints, based on the weight composition of the used raw materials.

Ghosh R. et al. (2016) developed a machinable bioceramic composite by incorporation of a weak interphase material. Calcium phosphate (CaP) ceramics have high hardness that restricts the machinability of these materials and limits the wide applicability due to dimensional restrictions.

2.1.2 Finite Element Modelling

Jayswal et al. (2005) developed a finite element model to evaluate the distribution of magnetic forces on the work piece surface. The MAFF process removes a very small amount of material by indentation and rotation of magnetic abrasive particles in the circular tracks. A theoretical model for material removal and surface roughness is also proposed accounting for micro cutting by considering a uniform surface profile without statistical distribution. Numerical experiments are carried out by providing different routes of intermittent motion to the tool. The simulation results were validated with the experimental results available in the literature.

Bhondwe K. L. et al. (2006) developed a thermal model for the calculation of MRR during Electro-chemical spark machining (ECSM). First, temperature distribution within the zone of influence of single spark is obtained with the application of FEM. The nodal temperatures were further post processed for estimating MRR. The developed FEM based thermal model was validated with the experimental results. It has been concluded that an increase in electrolyte concentration due to ECSM of soda lime glass work piece material increases MRR.

Chunhua et al. (2006) proposed an approach using FEM to design tool in Electro Chemical Machining. This method is capable of designing three-dimensional free form surface tool from the scanned data of known work piece. It possesses high computing efficiency, good accuracy and flexible boundary treatment without the need for iterative procedure. This method is demonstrated as an example of tool design for turbine blade.

Gurgel A. G. et al. (2006) applied element-free Galerkin (EFGM) approximating functions to evaluate the properties of machined surfaces with cutting parameters when turning AISI 4140 steel using arbitrary sets of experimental values and the EFGM approximation functions, based on the moving least-squares method, in order to obtain the sensitivities through proper local derivations.

Lin H. et al. (2007) applied finite element software ABAQUS to analyze the age forming process and the spring-backs of 7B04 aluminum alloy plates. The effects of plate thickness and forming time on spring-backs are researched. The spring-backs decrease with the increase of plate thickness and forming time. The test results verify the reliability of the finite element method (FEM) analysis.

Rantatalo M. et al. (2007) applied a method for analysing lateral vibrations in a milling machine spindle is presented including finite-element modeling (FEM), magnetic excitation and inductive displacement measurements of the spindle response. The measurements were analysed and compared with the FEM simulations which incorporated a spindle speed sensitive bearing stiffness, a separate mass and stiffness radius and a stiffness radius sensitive shear deformation factor.

Wani et al (2007) developed a finite element model to find the magnetic potential distribution in magnetic abrasive flow finishing process.

Chen et al. (2008) studied stress, deformation and interaction mechanism of a bolt using FEM, especially with the ANSYS software, based on the updated Lagrangian law. The results show that the maximum stress on the inner wall of the bolt is consistent with an elastic analytic solution. The experimental results indicate that the maximum injection pressure in the bolt is 2.5 MPa without link enhancement and 8.3 MPa with the enhancement. This link enhancement effect is highly significant.

Davim P. et al. (2009) compared finite element model (FEM) simulations with experimental and analytical findings concerning precision radial turning of AISI D2 steel. Regarding the plastic strain, the differences between analytical calculations and FEM simulations (for the presented friction values) suggest that the finite element method is capable of predictions with reasonable precision.

Shuren Z. et al. (2009) introduced the self-designed Abrasive Flow Machine and Clamp. Abrasive flow medium selection and process parameter settings have been discussed. Experiments were conducted on 0.15 mm diameter hole. Experimental investigation has been done to select the best process parameters of the Abrasive Flow Machining of small hole.

Jain V.K. et al. (2009) analyzed the AFM process using finite element method for finishing of external surfaces. To study the material removal mechanism of AFM, finite element model of forces acting on a single grain had been developed. To carry out an experimental research to analyze the effect of extrusion pressure and number of cycles on material removal and surface finish, response surface method (RSM) was used. The experimental data obtained during AFM was compared with the results obtained from finite element analysis.

Mkaddem A. and Mansori M. E. (2009) presented a novel model for simulation of polymer-matrix composites (PMCs). The model is developed for orthogonal cutting configuration and finite element analysis (FEA). For enhancing chip formation simulation, adaptive mesh technique and dynamic explicit elements are used.

Sangwan K.S et al. (2015) presented an approach for examining the optimized parametric conditions to achieve the minimum surface roughness using Artificial Neural Network (ANN) and Genetic Algorithm (GA).

2.2 RESEARCH GAPS AND PROBLEM FORMULATION

From the literature survey, it has been observed that researchers have studied the effect of process parameters on aluminium and brass as work materials. But now a days; composite materials have been extensively used for various applications. Composites have many advantages like more strength. Due to these advantages, it is useful to use these materials. However, fine machining and to attain a glass surface finish on surfaces of composites is a challenging task. Moreover; the effect of AFM process parameters on composites needs to be investigated. Further; little work has been done on the machining mechanism of AFM of composites. All these parameters motivated us to take the present study for the research. From the extensive literature survey, following research gaps have been identified:

1. The studies of available literature, reveals that work has been reported on machining of materials as like aluminium and brass by AFM process.
2. Little work has been reported on machining characteristics of MMCs using AFM process.
3. No work has been reported on very hard MMCs (having high percentage of SiC in the base material like aluminium). In the present study high percentage of SiC was be taken in Aluminium as base material.
4. In the AFM process, parametric study of different input parameters is done for MMCs.
5. It is observed that little work has been reported on the machining mechanism of composite materials using AFM process, so there is scope to work in this field.
6. Analytical models for MRR using AFM have been presented by some researchers, but little work is reported using FEM.

2.3 OBJECTIVE OF THE STUDY

The study is aimed to investigate the machining characteristics of metal matrix composites under different parametric conditions in abrasive flow machining process. Objectives of present study are as follows:

1. To identify the metal matrix composites (MMC) of different compositions as work materials.

2. To design and develop an experimental setup of Abrasive Flow Machining in the laboratory. The experimental setup will be able to accommodate the change in process parameters.

3. To re-assess the effect of process variables (like fluid pressure, viscosity of medium, mesh number of grit, concentration of abrasives, work piece material, no of cycles) on machining characteristics of MMC in an AFM process on various output characteristics like MRR, SR & Surface Topography. To optimize the various input and output parameters involved in the machining of MMC by AFM using optimization techniques like Taguchi philosophy, Response Surface methodology etc.

4. To estimate the effect of process parameters using FEM by developing a generalized mathematical model for the results.

5. To analyze the process behavior of the AFM process on composite materials using FEM.

CHAPTER 03

PILOT EXPERIMENTATION AND DESIGN OF STUDY

3.0 INTRODUCTION

In the manufacturing process, machining or finishing methods have a very important role. It is also very important to select machines and materials. The selection of appropriate input parameters for machining of materials is of utmost importance. Metal Matrix Composites, which are difficult to-cut material, have been selected for the study. During the preliminary experimentation, various input process parameters can be varied that affect the machining performance in terms of material removal rate (MRR), change in surface roughness (ΔRa) and surface topography. One factor at a time approach has been applied in the pilot experimentations. Based on the results of a pilot study, final input parameters and their levels are finalized. Thereafter, based on Taguchi approach and response surface methodology, design of experiments is finalized. Effect of different process parameters in AFM process has been discussed in this chapter.

3.1 EFFECT OF PROCESS PARAMETERS

Input process parameters have been identified and their effect has been discussed on output responses. Different process parameters affecting AFM and associated processes have been summarized in the Ishikawa cause-effect diagram as shown in fig 3.1. In the present study following parameters have been identified.

3.1.1 Input Variables

- Fluid pressure
- Viscosity of medium
- Grain size
- Concentration of abrasives
- Work piece materials
- No. of cycles

3.1.2 Output Variables

- Material Removal Rate (MRR)
- Change in Surface Roughness (ΔRa)

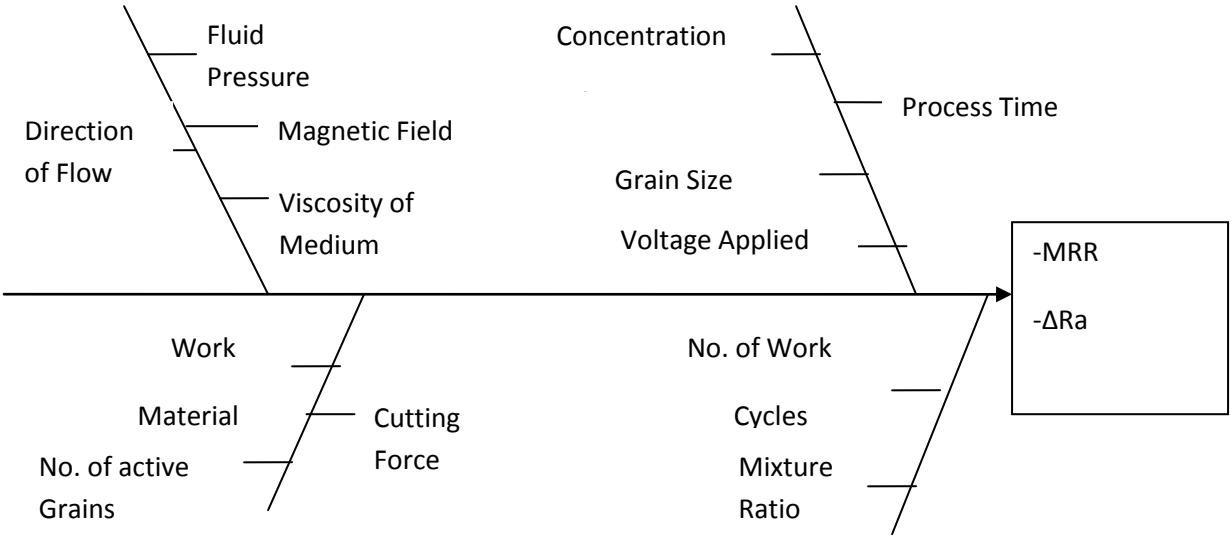

Fig. 3.1: Ishikawa cause effect diagram

3.2 DESIGN AND DEVELOPMENT OF AFM SETUP

AFM setup has been designed and developed in the laboratory. Setup is developed so that process variables can be varied as per process requirements.

3.2.1 Design requirements

1) Media cylinders and pistons
2) Work piece fixture
3) Hydraulic unit

3.2.1.1 Media cylinders and pistons

The primary job of media cylinders is to contain the sufficient media and guide the piston movement during reciprocating motion i.e. up and down movement. Keeping in mind the

constraints of availability of media, the required volume of cylinders is fixed as 300 cc approximately. Hydraulic cylinders are designed so that they can withstand maximum pressure up to 10 MPa. Cylinders are made up of EN8, composition of material is shown in table number 3.1. EN8 is a medium carbon steel, having good tensile strength and is often used in applications such as: shafts, gears, stressed pins, studs, bolts, keys etc.

Table 3.1: Chemical composition of EN8

Carbon	0.36 - 0.44 %
Silicon	0.10 - 0.40 %
Manganese	0.60 - 1 %
Sulphur	0.050 max
Phosphorus	0.050 max

Piston material is taken as gray cast iron to withstand desired pressure. Stroke length is taken as 250 mm so that sufficient displacement can be given to media to pass through the work piece. As shown in fig 3.2 cylinder internal diameter can be calculated as:

$$A = \Pi D^2/4 \quad (3.1)$$

Where A = cross sectional area of piston

D = Diameter of piston

Hence

$$D = \sqrt{\frac{4A}{\pi}} \quad (3.2)$$

Also, we know that

$$A = F/P \quad (3.3)$$

F = Force applied, P = Fluid pressure (10 MPa), as per our requirement.

Getting value of A from the equation (3) and putting in equation (2) we get piston diameter (D) as, 90 mm

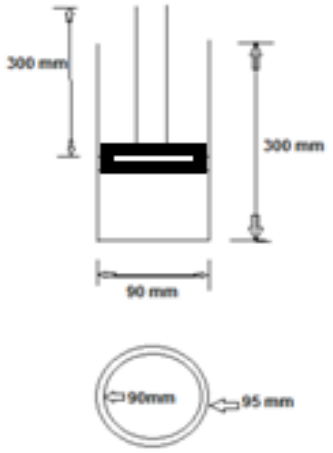

Fig 3.2: Cylinder and piston drawing

3.2.1.2 Work piece fixture

Design of work piece fixture also plays an important role as it guides the media to pass from work surface which is to be machined. Material of the work piece is taken as nylon so that it can be machined easily to get the desired shape. A slot has been cut in the fixture to hold the work piece which is exactly of the outer shape and size of work piece. Diameter in fixture is decreased gradually so that vibrations are avoided during machining. Pictorial view of nylon fixture is shown in fig 3.3.

Fig 3.3 Nylon fixture

3.2.1.3 Hydraulic unit

Hydraulic unit has been designed for the desired pressure up to 10 MPa. A hydraulic gear pump is used to pump the hydraulic oil from tank and supply it to the circuit. Flange type motor rated 2 HP, 1440 RPM has been used. Two direction control valves (DCV1 & DCV2-three position four ways, stainless steel) have been fixed on the hydraulic unit. DCV1 is used for actuation of up and down movement of hydraulic cylinders. Two pressure relief valves (PRV1 & PRV2, stainless steel) have been mounted to maintain the required pressure. Two pressure gauges of 3000 psi have been fixed to read the pressure in the circuit. The flow diagram of AFM setup is shown in figure 3.4.

Design considerations of hydraulic pump:

Our pressure requirement = 10 MPa ≈ 1450 psi

Power is given by the formula

$$P = \frac{Q \times p}{1714} \tag{3.4}$$

Hence,

$$p = \frac{P \times 1714}{Q} \tag{3.5}$$

Where, P = power in HP

Q = discharge (gpm)

p = pressure (psi)

Q can be calculated using

$$Q = n \times Vstroke \times \eta_{Vol} \tag{3.6}$$

$Vstroke$ = Volume swept = Cylinder volume

η_{Vol} = Volumetric efficiency (For gear pump it cab taken as 95 %)

V $stroke$ = Volume swept = Cylinder volume = $\Pi r^2 h$

= 3.14 x 45 x 45 x 250

= 1589625 mm^3

= 0.0015 m^3

Hence, Q = 1/10 x 0.0015 x 0.95

= 0.00014 m^3/s = 2.22 gpm

Now putting the value of q in equation (5) we get, pressure:

$$p = \frac{2 \times 1714}{2.22}$$

= 1544 psi

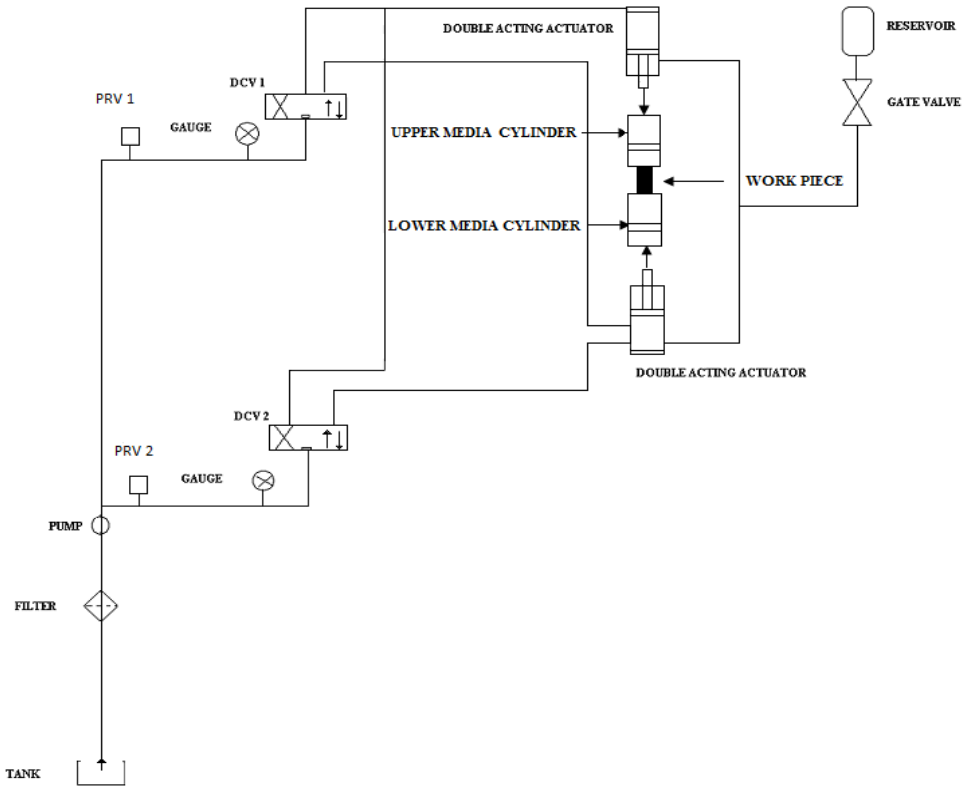

Fig 3.4: Flow diagram of AFM set up

The electric motor driven gear hydraulic pump draws hydraulic oil from the tank through the filter and delivers it to two manually actuated direction control valves DCV1 and DCV2 through

pressure relief valves PRV1 & PRV2. The main function of pressure relief valves is to limit the pressure in the system to a desired value. During downward stroke pressure in the upper hydraulic cylinder is kept high by varying it with PRV1 and low in upper cylinder using PRV2. Keeping knob of DCV2 in central position, downward stroke is completed by actuating DCV1. After completion of downward stroke pressure in lower cylinder is maintained at a high level using PRV2 and upper cylinder at low pressure using PRV1. Positions of DCV1 and DCV2 have been reversed. In this way one cycle is completed by completing the upward stroke. Two pressure gauges have been used to read the pressure in the system.

Experimentation is done based on L27 orthogonal array and Box-Behnken design at different parameter settings. Work piece material is taken as SiC/Al MMC (20, 40, 60 percent SiC in Al as base material). Input parameters, fluid pressure, viscosity (percentage of oil in the media), grit size (mesh number of abrasives), concentration of abrasives, work piece material and number of cycles were varied at three levels each to find their effect on response parameters. Three readings were taken for each run to minimize the deviation in the results. Significance and the percentage contribution of process parameters have been found out and analyzed. Experimental setup has been designed and developed as shown in figure 3.5. Work piece surfaces finished with AFM are shown in fig 3.6.

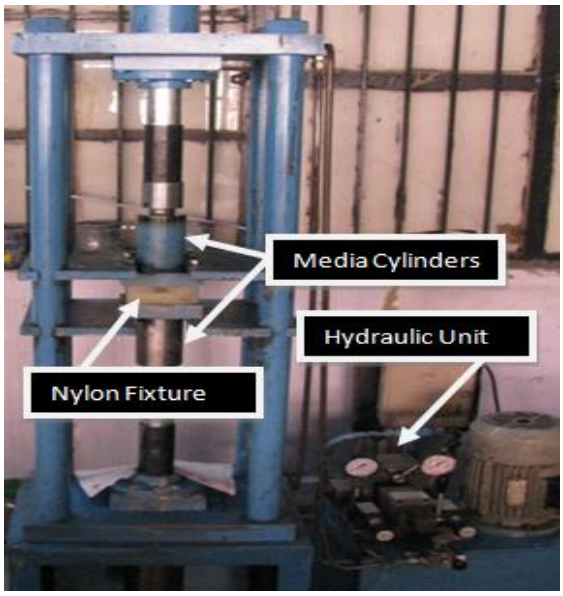

Fig 3.5: Experimental set up of AFM process

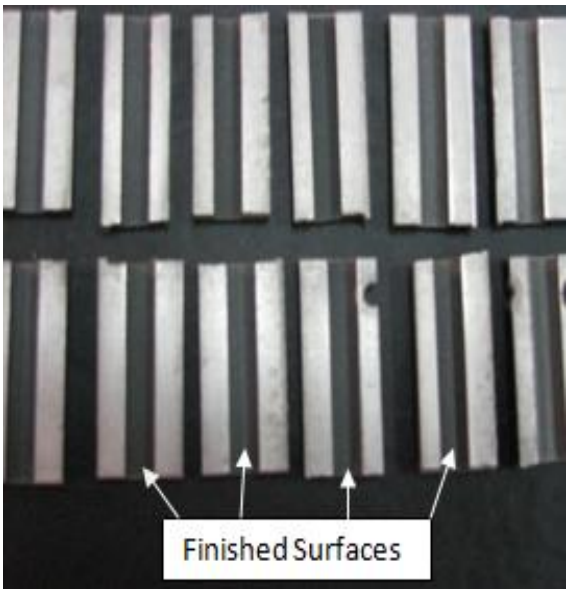

Fig 3.6: Samples finished by AFM process

3.3 MATERIALS USED IN EXPERIMENTATION

Metal Matrix Composite having a different percentage of SiC in Al as base material (20, 40 and 60 percent SiC in Al) has been taken in the present study. Percentage composition is shown in table 3.2. The Rockwell hardness tester is used for indentation at 5 different points selected randomly to calculate average hardness. Diamond indentor at 150 Kgf is used. MMC with 20% SiC has Rockwell hardness 40 HRC, with 40 % SiC 50 HRC and with 60 % SiC has 60 HRC. Slots have been cut by wire EDM then finished by AFM.

Table 3.2: Percentage composition of elements in work piece materials

Elements	**Work piece 1 (20% SiC in Al/SiC)**	**Work piece 2 (40% SiC in Al/SiC)**	**Work piece 3 (60% SiC in Al/SiC)**
Cu	0.016	1.56	<0.004
Mg	0.478	0.263	0.103
Si	20.238	38.45	62.8
Fe	2.94	0.958	0.218
Ni	0.010	0.035	0.018
Mn	0.019	0.011	0.004
Zn	0.038	0.527	0.031
Pb	0.039	0.060	0.023
Sn	0.017	0.062	0.014
Ti	<0.016	0.076	0.03
Cr	0.023	0.016	0.007
Al	Balance	Balance	Balance

3.4 PILOT EXPERIMENTATION

One factor at a time approach (OFTA) has been applied in the pilot experimentation (Montgomery, 2002). Effect of input parameters like fluid extrusion pressure, viscosity of medium (varied by varying the percentage of oil in abrasive medium), mesh number of grit, concentration of

abrasives, work piece material, no of cycles has been studied on machining characteristics of MMCs like MRR, SR & Surface topography.

3.5 EFFECT OF PROCESS VARIABLES

3.5.1 Effect of process variables on MRR

3.5.1.1 Extrusion pressure

Keeping other parameters constant, extrusion pressure is varied from 2 Mpa to 10 Mpa. It can be observed from the plot that MRR increases with increase in extrusion pressure as shown in fig 3.7. It can be also observed that the slope of the curve gets decreased near 7-8 MPa. This is because active grain density increases with extrusion pressure up to 7 MPa and then decreases as reported in [20]. Hence the extrusion pressure range of 3.5 to 7 MPa was considered.

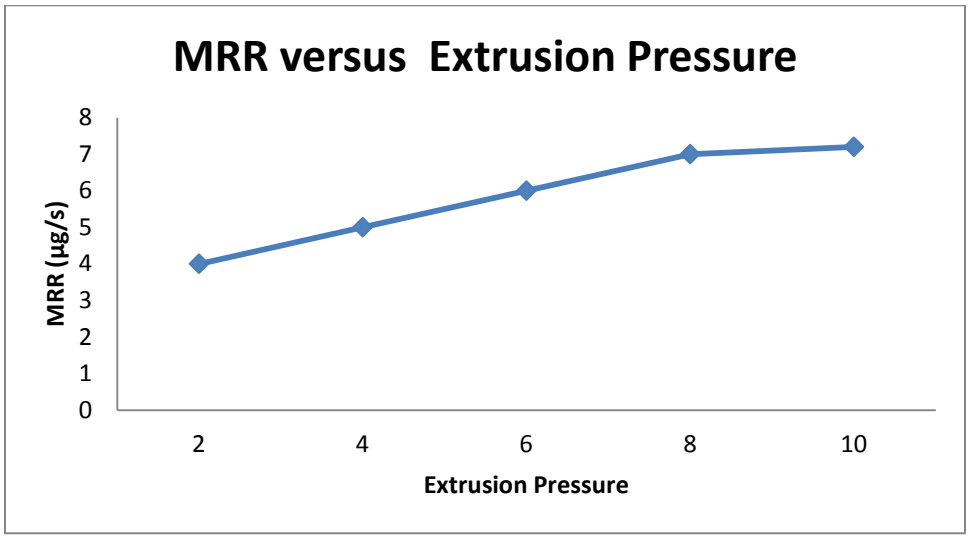

Fig 3.7: Effect of extrusion pressure on MRR, at percentage of oil = 10 %, mesh number of abrasives = 150, concentration of abrasives = 60 %, work piece material (SiC %) = 20, No. of cycles = 200

3.5.1.2 Percentage of oil in medium

As a percentage of oil increases in abrasive medium, viscosity decreases. It can be concluded from the plot that MRR decreases with increase in percentage of oil in the medium as shown in fig 3.8. However, it has very little effect on MRR. This is because with increase in percentage of oil in media it becomes more smooth and percentage concentration of abrasives decreases to some extent. Hence number of cutting edges decreases and MRR gets decreased.

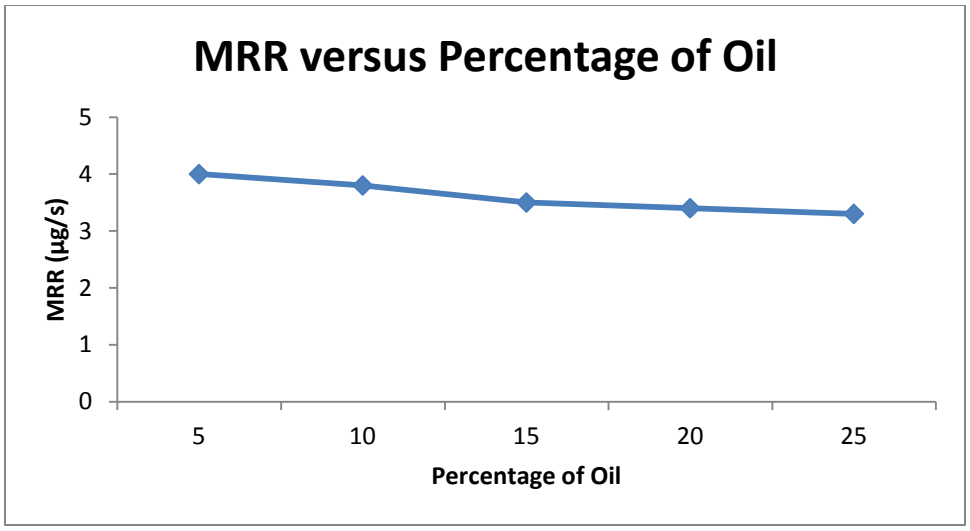

Fig 3.8: Effect of percentage of oil on MRR, at extrusion pressure = 3.5 MPa, mesh number of abrasives = 150, concentration of abrasives = 60 %, work piece material (SiC %) = 20, No. of cycles = 200

3.5.1.3 Mesh number of abrasives

It can be observed from the plot that MRR decreases with increase in the mesh number of abrasives as shown in fig 3.9. The grit size decreases with increase in mesh size, hence smaller the grit size lesser is MRR. Area of penetration of grit decreases with decrease in size, so lesser volume of material is removed [31].

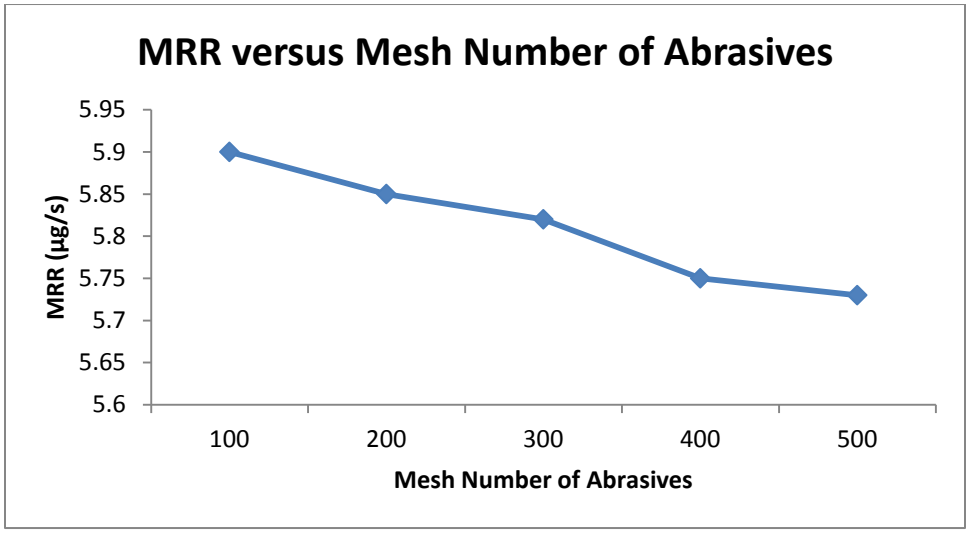

Fig 3.9: Effect of mesh no of abrasives on MRR, at extrusion pressure = 3.5 MPa, percentage of oil = 10 %, concentration of abrasives = 60 %, work piece material (SiC %) = 20, No. of cycles = 200

3.5.1.4 Concentration of abrasives:

MRR gets increased with the increase in concentration of abrasives in the medium as shown in fig 3.10. As more number of abrasive particles are there in the medium, more number of particles come in contact with work piece surface. Higher concentration of abrasives permits the media to sustain large cutting forces [33].

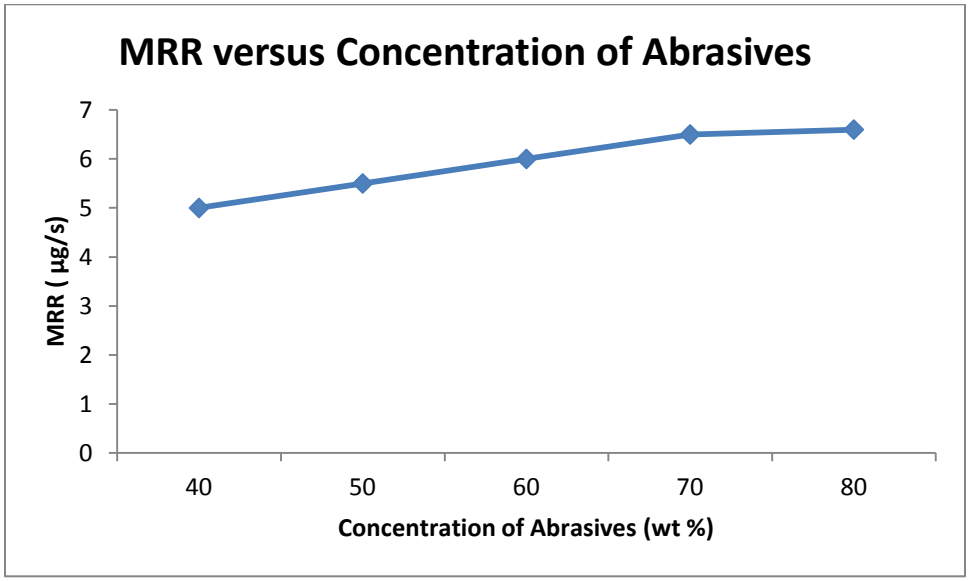

Fig 3.10: Effect of concentration of abrasives on MRR, at extrusion pressure = 3.5 MPa, percentage of oil = 10 %, mesh number of abrasives = 150, work piece material (SiC %) = 20, No. of cycles = 200

3.5.1.5 Work piece materials

With the increase in percentage of SiC (20-60) in SiC/Al MMC, MRR gets decreased as shown in fig 3.11. This is because with the increase in percentage of SiC work piece material gets harder. Hence, more MRR gets decreased keeping other parameters constant [33].

3.5.1.6 Number of cycles

As the number of cycle increases, MRR gets increased as shown in figure. As illustrated in the plot in fig 3.12 slope gets decreased near 300 cycles, because here after there are lesser peaks and valleys to be finished. Material removal increases non linearly with increase in number of cycles. Initially MRR is more and decreases later because initially number of peaks and valleys are more which are dissolved and becomes less later [33].

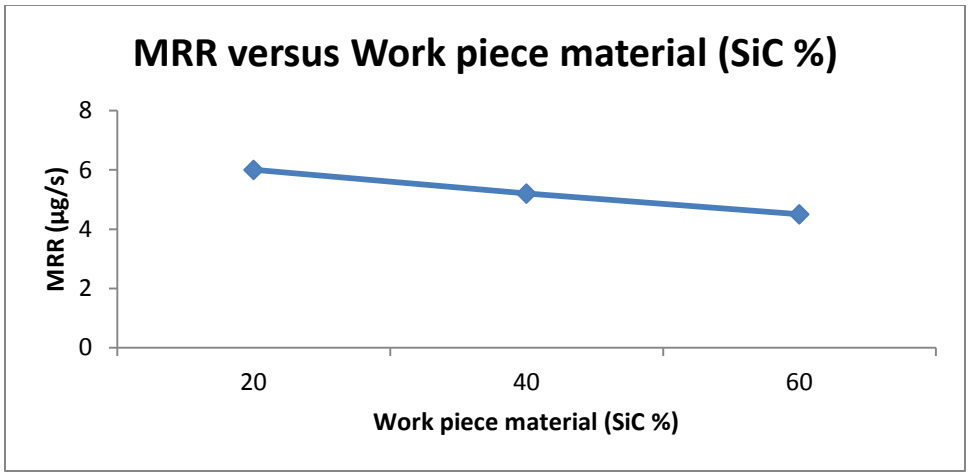

Fig 3.11: Effect of work piece material (SiC %) on MRR, at extrusion pressure = 3.5 MPa, percentage of oil = 10 %, mesh no of abrasives = 150, concentration of abrasives = 60 %, No. of cycles = 200

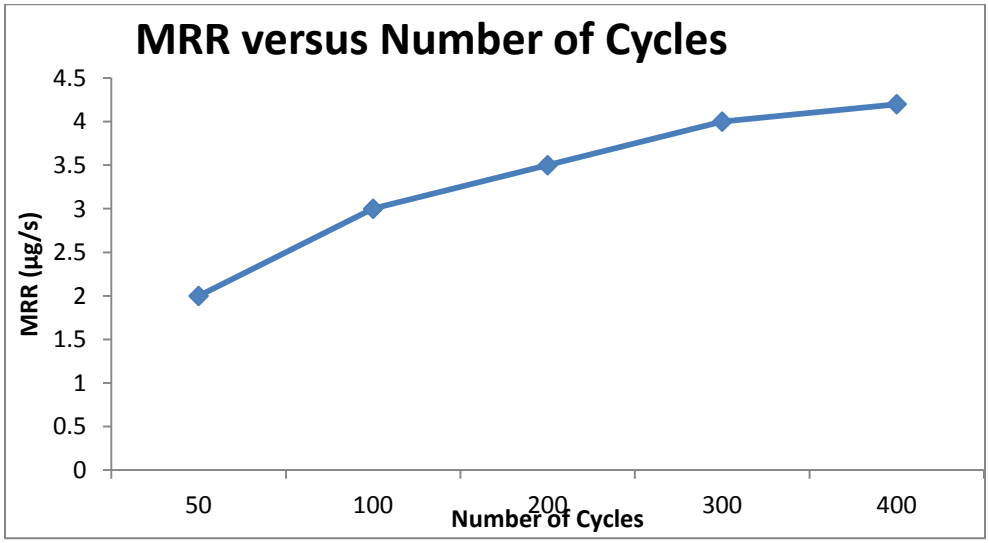

Fig 3.12: Effect of no. of cycles on MRR, at extrusion pressure = 3.5 MPa, percentage of oil = 10 %, mesh number of abrasives = 150, concentration of abrasives = 60 %, work piece material (SiC %) = 20

3.5.2 Effect of process variables on ΔRa

Effect of input process parameters have been discussed on response parameters.

3.5.2.1 Extrusion pressure

Keeping other parameters constant extrusion pressure is varied from 2 Mpa to 10 Mpa. It can be observed from the plot shown in fig 3.13, that ΔRa increases with increase in extrusion pressure. As grain density increases with increase in extrusion pressure, more peaks gets dissolved hence ΔRa increases.

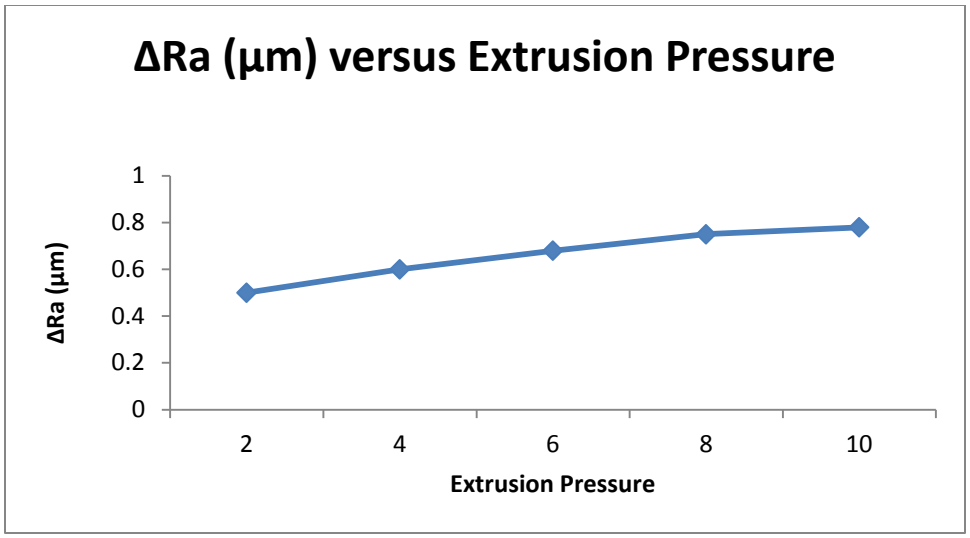

Fig 3.13: Effect of extrusion pressure on ΔRa, at percentage of oil = 10 %, mesh number of abrasives = 150, concentration of abrasives = 60 %, work piece material (SiC %) = 20, No. of cycles = 200

3.5.2.2 Percentage of oil in medium

It can be concluded from from the plot that ΔRa decreases with the increase in percentage of oil in the medium as shown in fig 3.14. This is because number of cutting edges decreases.

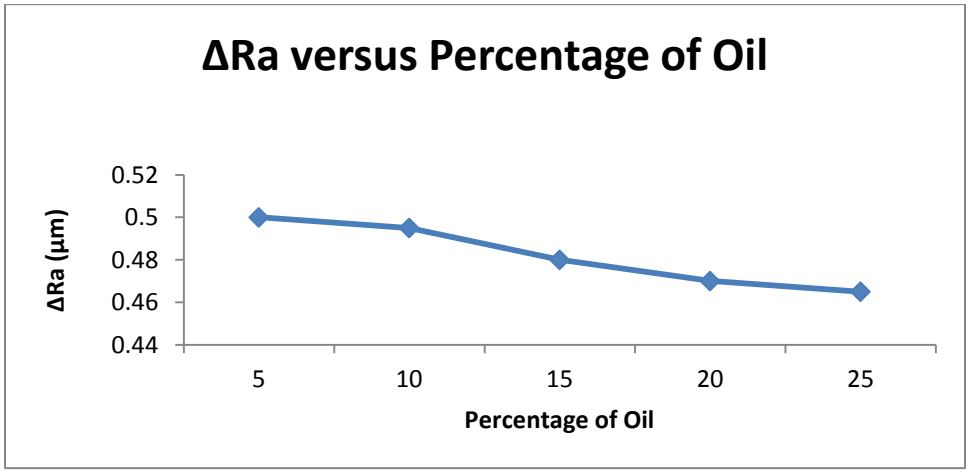

Fig 3.14: Effect of percentage of oil on ΔRa, at extrusion pressure = 3.5 MPa, mesh number of abrasives = 150, concentration of abrasives = 60 %, work piece material (SiC %) = 20, No. of cycles = 200

3.5.2.3 Mesh number of abrasives

ΔRa gets decreased with an increase in the mesh number of abrasives as illustrated in the plot in fig 3.15. As less material is removed with increase in mesh number, ΔRa gets decreased.

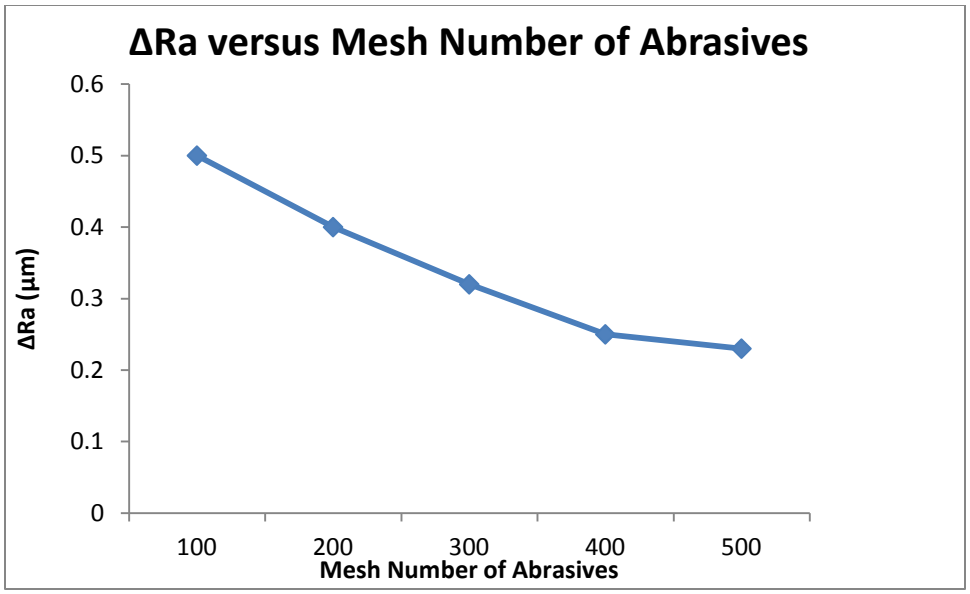

Fig 3.15: Effect of mesh no of abrasives on ΔRa, at extrusion pressure = 3.5 MPa, percentage of oil = 10 %, concentration of abrasives = 60 %, work piece material (SiC %) = 20, No. of cycles = 200

3.5.2.4 Concentration of abrasives

With the increase in concentration of abrasives, ΔRa gets increased as shown in fig 3.16. With increase in concentration of abrasives grain density (number of cutting edges) is increased hence ΔRa increases.

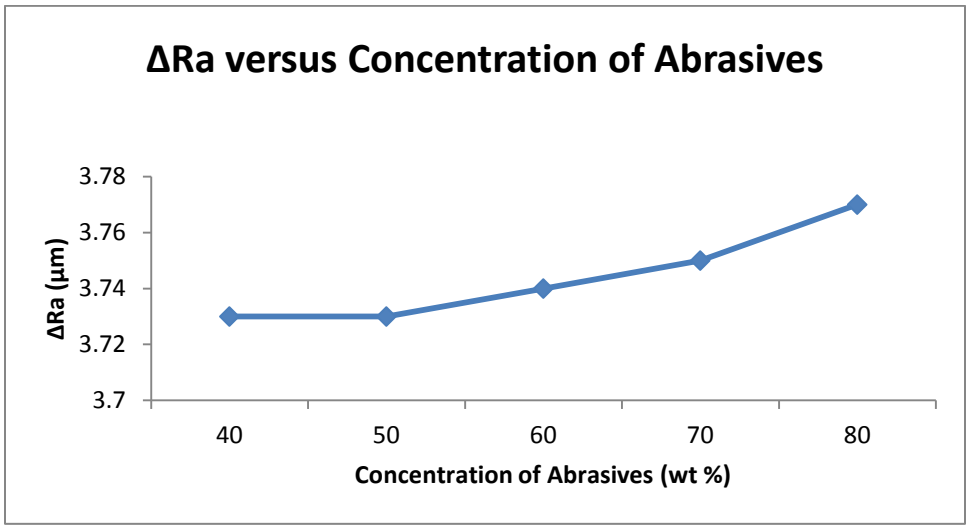

Fig 3.16: Effect of concentration of abrasives on ΔRa, at extrusion pressure = 3.5 MPa, percentage of oil = 10 %, mesh number of abrasives = 150, work piece material (SiC %) = 20, No. of cycles = 200

3.5.2.5 Work piece materials

As SiC percentage increases in the work piece with aluminium as base material, it is difficult to cut/ finish, because hardness gets increased. Hence, ΔRa gets decreased as shown in fig 3.17.

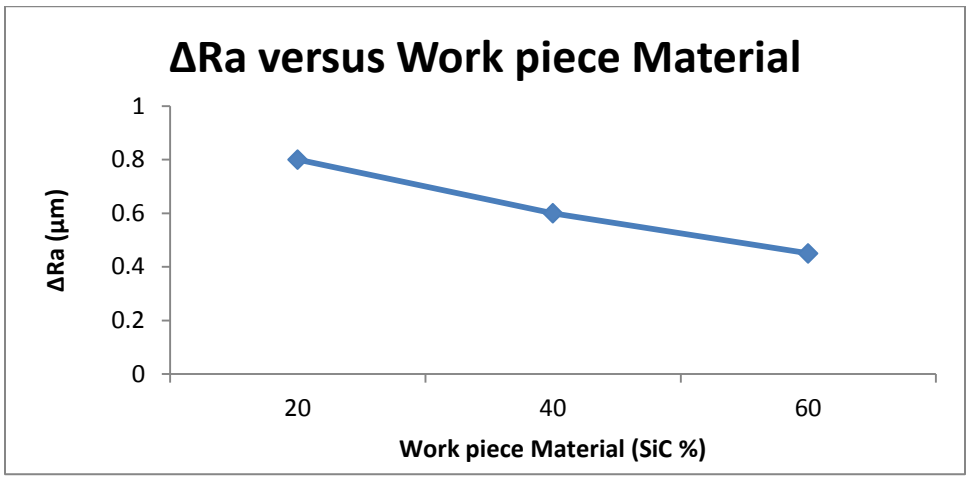

Fig 3.17: Effect of work piece material (SiC %) on ΔRa, at extrusion pressure = 3.5 MPa, percentage of oil = 10 %, mesh no of abrasives = 150, concentration of abrasives = 60 %, No. of cycles = 200

3.5.2.6 Number of cycles

As the number of cycle increases, ΔRa gets increased as shown in fig 3.18. Initially surface roughness improves more, but becomes less with further increase in the number of cycles. This is because initially there are more peaks and valleys.

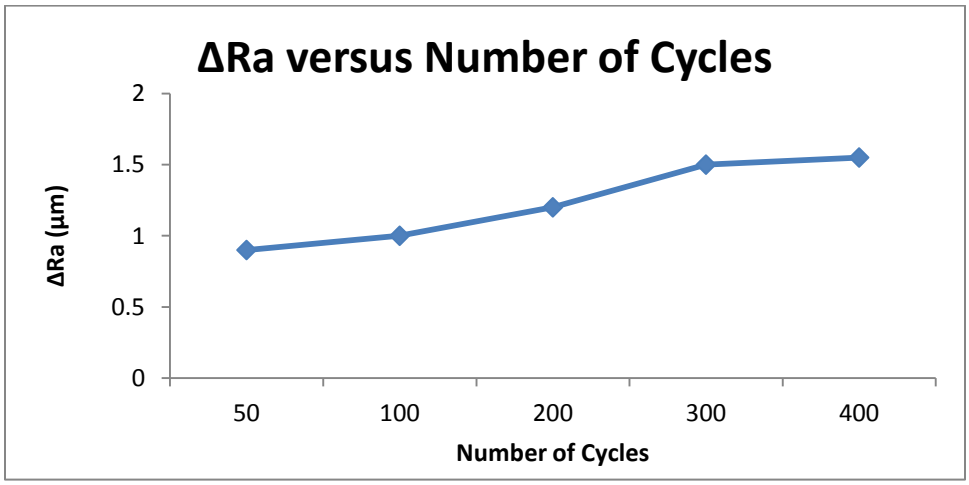

Fig 3.18: Effect of no. of cycles on ΔRa, at extrusion pressure = 3.5 MPa, percentage of oil = 10 %, mesh number of abrasives = 150, concentration of abrasives = 60 %, work piece material (SiC %) = 20

3.6 DESIGN OF EXPERIMENTS (PHASE A for Taguchi method)

With due time, there were number of scientific approaches developed which used the basic theory of design of experiments (DOE). Various methodologies such as Response Surface methodology (RSM), full factorial designs, Taguchi methodology etc have some of advantages over the basic DOE approach. These approaches are one of the most useful and significant in current industrial era to carrying out the various optimized process.

3.6.1 Selection of Input Process Parameters

On the basis of experimental results obtained during pilot experimentation, input process parameters and their levels have been finalized (Antony, 2003). Process parameters and their levels for phase A experimentation based on L27, OA are listed in the table 3.3.

Table 3.3: Input parameters and their levels

Symbol	Factors	Level 1	Level 2	Level 3
A	Extrusion pressure (MPa)	3.5	5	7
B	Percentage of oil in Media	10	12.5	15
C	Mesh Number	100	150	220
D	Concentration of abrasives (weight %age of abrasives)	50	55	60
E	Work piece material (percentage of SiC in Al/SiC)	20	40	60
F	Number of Cycles	100	200	300

3.6.2 Selection of Orthogonal Array (OA)

The DOE approach has a number of positive facts like the reduced number of experiments, due to which it is commonly used in many problems (Ferreira et al., 2007). In the present study, total six input process parameters were selected as shown in table 3.1. Since the selected input parameters have three levels each, the degrees of freedom (DOF) of three levels factor is 2 (number of levels - 1), hence total DOF for the experiments is 12. The DOF of selected OA for an experiment must be more than or equal the total DOF for that experiment. Therefore,

Taguchi's experimental design with orthogonal array L_{27} was finalized. L_{27} orthogonal array contains total six columns and 27 rows. The selected array has been shown in table 3.4.

Table 3.4: L27 Orthogonal Array

	Factors					
Experiment No.	A	B	C	D	E	F
1	1	1	1	1	1	1
2	1	2	1	1	2	2
3	1	3	1	1	3	3
4	1	3	2	2	1	2
5	1	1	2	2	2	3
6	1	2	2	2	3	1
7	1	2	3	3	1	1
8	1	3	3	3	2	1
9	1	1	3	3	3	2
10	2	2	2	3	1	1
11	2	3	2	3	2	2
12	2	1	2	3	3	3
13	2	1	3	1	1	2
14	2	2	3	1	2	3
15	2	3	3	1	3	1
16	2	3	1	2	1	3
17	2	1	1	2	2	1
18	2	2	1	2	3	2
19	3	3	3	2	1	1
20	3	1	3	2	2	2

	Factors					
Experiment No.	A	B	C	D	E	F
21	3	2	3	2	3	3
22	3	2	1	3	1	2
23	3	3	1	3	2	3
24	3	1	1	3	3	1
25	3	1	2	1	1	3
26	3	2	2	1	2	1
27	3	3	2	1	3	2

3.6.3 Signal-to-Noise Ratio for Response Characteristics

The signal-to-noise ratio (S/N ratio) can be found using Taguchi's methodology. The S/N ratio, which condenses the multiple data points within a trial, depends on the type of characteristic being evaluated. The change in quality characteristic of a product under examination in response to a factor introduced in the experimental design is the 'signal' represents the desirable value (mean). However, when an experiment is performed, different external factors influence the response characteristics; these external factor effects the outcome of quality characteristic is termed as 'noise' represents the undesirable value. S/N ratio measures the sensitivity of the quality characteristic being investigated in a controlled manner, to those external influencing factors (noise factors) not under control. Thus, the S/N ratio represents the amount of variation present in the performance characteristic.

The aim of any experimental study is always to determine the highest possible S/N ratio for the result irrespective of the quality characteristics. A high value of S/N ratio implies that the signal is much higher than the random effects of noise factors. The highest S/N ratio always yields the optimum quality with minimum variance.

There are three different types of performance characteristics, namely lower-the better, higher-the-better and nominal-the-best, application of each characteristic depends upon the performance

characteristic. Right selection of an S/N ratio is essential for optimization of the output characteristics. The three possible categories to measure quality characteristics can be described as follows:

- **Higher-the-better**

$$HB: S/N\ ratio = -10\log_{10}\left[\frac{1}{n}\sum_{i=1}^{n} yi^{-2}\right] \tag{3.7}$$

- **Lower-the-better**

$$LB: S/N\ ratio = -10\log_{10}\left[\frac{1}{n}\sum_{i=1}^{n} yi^{2}\right] \tag{3.8}$$

- **Nominal-the-better**

$$NB: S/N\ ratio = 10\log_{10}\left[\frac{\bar{y}^{2}}{s^{2}}\right] \tag{3.9}$$

Where yi represents the experimentally observed value of the ith experiment, n is the trials of each experiment, $\bar{y}$ is the mean of samples and s is the sample standard deviation of n observations in each run. The unit of calculated, S/N ratio from the observed values is decibel (dB) and is denoted by η.

In the present study, Higher-the-better type of quality characteristics has been selected as the objective function for MRR and ΔRa, as both the characteristics are desirable to be maximized.
The Mean Standard Deviation (MSD) is a statistical quantity that reflects the deviation from the target value. For nominal-the-best characteristic, the standard definition of MSD is used. For smaller-the-better, the unstated target value is zero. For larger-the-better, inverse of each large value becomes a small value and again the unstated target value is zero. For that reason, for all the three MSD expressions, the smallest magnitude of MSD is being sought. The constant 10 has been purposely used to magnify S/N ratio for each analysis and negative sign is used to set the S/N ratio of larger-the-better type relative to the square deviation of smaller-the-better type.

3.6.4 Analysis of Variance (ANOVA)

ANOVA is a statistical tool which is used to determine the significance of the input parameters of a process. This technique enables to find out the amount of variance attributed to various parameters and make a decision whether or not the parameters have produced any significant effect on output performance. The percent contribution of each factor for the results of the experiment has been determined by using the ANOVA technique. It calculates various parameters, namely the sum of squares (SS), pure SS, degree of freedom, variance, F-ratio and the percentage contribution of each factor. By using the F-test the significant parameter is determined by comparing $F_A > F_{0.05,n1,n2}$ at 95% confidence interval with n_1 and n_2 degree of freedom (Rss Roy). In view of the fact that the procedure of ANOVA is very complicated and makes use of considerable statistical formulae, only a brief explanation is included here. The Sum of Squares (SS_T) is a measure of the deviation of the experimental data from the mean value of the data as given in equations as:

$$SS_T = \sum_{i=1}^{N} y_i^2 - \frac{T^2}{N} \tag{3.10}$$

$$SS_T = \sum_{i=1}^{N} \left(y_i - \overline{T} \right)^2 \tag{3.11}$$

$$SS_A = \sum_{i=1}^{N} \frac{A_i^2}{n_{Ai}} - \frac{T^2}{N} \tag{3.12}$$

Let ‘A’ be a factor taken for present work

N = Number of response observations, is the mean of all observations

Factor Sum of Squares = Squared deviations of factor (A) averages from the overall average

A_i =Sum of observations under level

n_{Ai} =number of observations under Ai level

A_i = average of observations under Ai level = A_i/n_{Ai}

N = Total number of observations

T =Sum of all observations

$\overline{T}$ =Average of all observations = T/N

k_A = Number of Levels of Factor A

Error Sum of Squares (SS_e) = Squared deviations of observations from factor (A) averages

$$SS_e = \sum_{j=1}^{k_A} \sum_{i=1}^{n_{Ai}} \left(y_i - \overline{A_j} \right)^2 \qquad (3.13)$$

3.7 DESIGN OF EXPERIMENTS (PHASE B for RSM)

Various DOE approaches have some disadvantages as follows:

I. The location (mean) and dispersion (variance) effects provide typical data using Taguchi's methodology. However, this approach also uses the signal to noise ratios (S/N ratios) data to carry out the detailed analyses work.

II. With the help of Taguchi's methodology, the information about the interaction effects cannot not be attained and considered as negligible. Due to this effect optimum design of the whole process cannot be attained efficiently.

III. Using Taguchi's methodology, the optimized solutions cannot be obtained and also it does not pursue the sequential experimentation.

IV. This approach also not able to develop the mathematical models which have many applications for analyzing the process.

V. The multi or simultaneous optimization of various parameters cannot be attained till other technique is applied.

Due to consideration of all these disadvantages the present research work is based on response surface methodology for conducting the experimentation work on AFM process. The detailed introduction of response surface methodology is given below:

3.7.1 Response surface methodology

Response surface methodology uses mathematical and statistical techniques to optimize a process. It was developed by Box and Wilson in 1951. The RSM approach uses the response surface as a multivariate function, whereas it also determines the polynomial coefficients. This approach also measures the relationship between the controllable input parameters and obtained response surfaces (Kwak, 2005).

If all control factors are assumed to be measurable, the response surface can be expressed as follows:

$$y = f(x_1, x_2, x_3, \ldots, x_n) \quad (3.14)$$

y = output response

x_i = i^{th} independent variable (process parameter)

The main objective is to obtain the optimized value of the response parameter y. It is assumed that to attain the approximation of the model the existence of relationship between response surface and independent variables is necessary. In the RSM for the interaction of two control variables, a second order surface is applied (Gunaraj et al., 1999) and is given by the equation as shown below:

$$y = \beta_0 + \sum_{i=1}^{k} \beta_i x_i + \sum_{i=1}^{k} \beta_{ii} x_i^2 + \sum_{i<j} \beta_{ij} x_i x_j + \varepsilon \quad (3.15)$$

ε = random error

β = regression coefficient

y = output response

x_i = i^{th} control factor

3.7.2 Evaluation of Regression Coefficients

The method of least squares is typically used to estimate the regression coefficients in a multiple linear or quadratic regression model (Gunaraj and Murugan, 1999). Equation (3.16) can be written in matrix form.

$$y = X\beta + \varepsilon \quad (3.16)$$

Where y is defined to be a matrix of measured values, X to be a matrix of independent variables. The matrixes β and ε consist of coefficients and errors, respectively.

$$y = \begin{bmatrix} y_1 \\ y_2 \\ . \\ . \\ y_n \end{bmatrix} \quad X = \begin{bmatrix} 1 & X_{11} & X_{21} & . & X_{1k} \\ 1 & X_{21} & X_{22} & . & X_{2k} \\ . & . & . & . & . \\ . & . & . & . & . \\ 1 & X_{n1} & X_{n2} & . & X_{nk} \end{bmatrix} \quad \beta = \begin{bmatrix} \beta_0 \\ \beta_1 \\ . \\ . \\ \beta_k \end{bmatrix} \quad \varepsilon = \begin{bmatrix} \varepsilon_0 \\ \varepsilon_1 \\ . \\ . \\ \varepsilon_n \end{bmatrix}$$

In general, y is an n×1 vector of observations, X is an n×k matrix of levels of independent variables, β is a k×1 vector of regression coefficients and ε is an n×1 vector of random errors. The aim is to find the vector of least square estimators, b that minimizes L that is as follows:

$$L = \sum_{i=1}^{n} \varepsilon_i^2 = \varepsilon'\varepsilon = (y - X\beta)'(y - X\beta)$$
$$= y'y - \beta'X'y - y'X\beta + \beta'X'X\beta$$
$$= y'y - 2\beta'X'y + \beta'X'X \qquad (3.17)$$

Since $\beta'X'y$ is a 1×1 matrix, or scalar, and its transpose $(\beta'X'y)' = y'X\beta$ is the same scalar. The least square estimators must satisfy

$$\left.\frac{\partial L}{\partial \beta}\right|_b = -2X'y + 2X'Xb = 0$$
$$X'Xb = X'y \qquad (3.18)$$

Equation 3.18 is set of normal equations in matrix form. Multiply both sides of this by inverse of $X'X$. Thus, least square estimator of β is (Kwak, 2005; Gunaraj and Murugan 1999):

$$b = (X'X)^{-1}X'y \qquad (3.19)$$

The fitted regression model is

$$\hat{y} = Xb \qquad (3.20)$$

Where $\hat{y}$ = estimate of y

3.7.3 Terms used for checking adequacy of model

Model adequacy checking is necessary to (a) Examine the fitted model to ensure that it provides an adequate approximation to the true system and (b) to verify that none of the least square assumptions are violated. The various techniques used for it are described below (Myers, 2002).

3.7.4 Sum of Squares of Residuals Technique

The difference between observation y_i and fitted value $\hat{y}$ is called residual (e). The n×1 vector of residuals is denoted by

$$e = y - \hat{y} \tag{3.21}$$

The method of least squares produces an unbiased estimator of the parameter β in the multiple regression models. The important parameter is the sum of squares of the residuals (SS_E)

$$SS_E = \sum_{i=1}^{n} (y_i - \hat{y})^2 = \sum_{i=1}^{n} (e_i)^2 = e'e \tag{3.22}$$

From (3.21 and 3.22) substituting $e = y - \hat{y} = y - Xb$,

$$ss_E = (y - Xb)'(y - Xb)$$
$$= y'y - b'X'y \tag{3.23}$$

The above equation is called error or residual sum of squares with n-k-1 degrees of freedom.

Total sum of squares (SS_T) is given by following equation with n-1 degrees of freedom

$$SS_T = y'y - \left(\sum_{i=1}^{n} y_i\right)^2 \Big/ n$$

It is necessary to test for significance of the model. This test procedure involves partitioning the total sum of squares into the sum of squares due to model (regression) and sum of squares due to error (Myers, 2002).

$$SS_T = SS_R + SS_E$$

$SS_R = b'X'y - \left(\sum_{i=1}^{n} y_i\right)^2 / n$ with k degrees of freedom (3.24)

3.7.5 Test for Significance of Regression

F statistics is a test for comparing model variance with residual (error) variance. It is the ratio of mean square of regression (MS_R) to the mean square of error (MS_E).

Where

$$MS_R = \frac{SS_R}{k} \quad (3.25)$$

$$MS_E = \frac{SS_E}{n-k-1} \quad (3.26)$$

If model F value exceeds $F_{\alpha,k,n-k-1}$, then the model is considered valid. Alternatively, p-value approach to hypothesis testing can be utilized, according to which, if p-value of the F statistics of the model is lower than the confidence interval (α), the model is considered valid.

R^2 is a measure of the amount of reduction in the variability of y obtained by using the variables x_1, x_2,..,x_n in the model and is defined by ratio of sum of squares due to regression to the total sum of squares ($\frac{SS_R}{SS_T}$) . The domain for R^2 = 0 to 1. A larger value of R^2 does not necessarily imply that regression model is a good one. Adding a variable to the model will always increase R^2, regardless of whether the additional variable is statistically significant or not. Thus, it is preferred to use an adjusted R^2 statistics that is defined as follows:

$$R^2_{adj} = 1 - \frac{SS_E/(n-k)}{SS_T/(n-1)} \quad (3.27)$$

Adjusted R^2 is a measure of the amount of variation around the mean explained by the model, adjusted for the number of terms in the model. The adjusted R-square decreases as the number of terms in the model increases, if those additional terms don't add value to the model.

Adequate Precision is a term that measures signal to noise ratios. It compares the range of the predicted values at the design points to the average prediction error. Ratios greater than 4 indicate adequate model discrimination.

3.7.6 Test for Lack of Fit

It is frequently useful to obtain two or more observations (replicates) on the response at the same settings of independent variables. As replicates of the central point are made, it is possible to estimate pure error associated with repetitions. Thus, the sum of the square for residuals can be dismembered into two more parcels: the sum of the square due to pure error (SS_{PE}) and the sum of the square due the lack of fit (SS_{LOF}), as shown below:

$$SS_{RES} = SS_{PE} + SS_{LOF} \quad (3.28)$$

Where,

$$SS_{PE} = \sum_{i=1}^{m}\sum_{j=1}^{n_i}(y_{ij} - \bar{y}_i)^2 .$$

$$SS_{LOF} = \sum_{i=1}^{m} n_i.(\bar{y}_i - \hat{y}_i)^2$$

$$MS_{PE} = \frac{SS_{PE}}{n_i - 1}$$

$$MS_{LOF} = \frac{SS_{LOF}}{m - k}$$

y_{ij} = j[th] observation on the response at y_i

n_i = number of observations at i[th] level

m = levels of x_i

$n_i - 1$ = degrees of freedom associated with SS_{PE}

$m - k$ = degrees of freedom associated with SS_{LOF}

Another way to evaluate the model is the lack of fit test. If the mathematical model is well fitted to the experimental data, MS_{LOF} will reflect only the random errors inherent to the system. Additionally, MS_{PE} is also an estimate of these random errors and it is assumed that these two values are not statistically different. This is the key idea of the lack of fit test. It is possible to use the *F* distribution to evaluate if there is some statistical difference between these two media, in the same way that the significance of regression was verified:

Where, *dlof* and *dpe* are the degree of freedom associated with the lack of fit and the pure error respectively. If this ratio is higher than tabulated value of *F*, it is concluded that there is evidence of a lack of fit and that the model needs to be improved. However, if the value is lower than tabulated value, the model fitness can be considered satisfactory. To apply a lack of fit test, the experimental design must be performed with authentic repetitions at least at its central points.

3.7.7 Analysis of variance

Analysis of variance (ANOVA) is a technique for analyzing experimental data in which one or more response (or dependent) variables are measured under various conditions identified by one or more classification variables. In ANOVA, variation in the response is separated into variation attributable to differences between the classification variables and variation attributable to random error. To accomplish this, Sum of squares due to error (SS_E), Sum of squares due to regression (SS_R) and Total Sum of squares (SS_T) are utilized. The (SS_T) is divided into following four parts to measure the deviations of the response from the fitted surface and estimation of the experimental error from center runs (Pecas and Henriques, 2003). Table 3.5 shows the various terms related the Analysis of variance of input functions.

Table 3.5: ANOVA terms used in multiple regressions (Marcos et al., 2008)

Variation Source	Sum of Squares (SS)	Degrees of Freedom	Mean Square (MS)
Regression	$SS_R = \sum_{i=1}^{m}\sum_{j=1}^{n_i}(\hat{y}_i - \bar{y})^2$	$p-1$	$MS_R = \frac{SS_R}{p-1}$
Residuals	$SS_{residual} = \sum_{i=1}^{m}\sum_{j=1}^{n_i}(y_{ij} - \hat{y}_i)^2$	$n-p$	$MS_{residual} = \frac{SS_{residual}}{n-p}$
Lack of fit	$SS_{LOF} = \sum_{i=1}^{m}\sum_{j=1}^{n_i}(\hat{y}_i - \bar{y}_i)^2$	$m-p$	$MS_{LOF} = \frac{SS_{LOF}}{m-p}$
Pure error	$SS_{PE} = \sum_{i=1}^{m}\sum_{j=1}^{n_i}(y_{ij} - \bar{y}_i)^2$	$n-m$	$MS_{PE} = \frac{SS_{PE}}{n-m}$
Total	$SS_T = \sum_{i=1}^{m}\sum_{j=1}^{n_i}(y_{ij} - \bar{y})^2$	$n-1$	

n = number of observations

m = total number of levels in the design

p = number of parameters of model

$\bar{y}$ = overall mean

$\hat{y}_i$ = estimated value by the model for the level *i*;

y_{ij} = replicates performed in each individual levels;

$\bar{y}_i$ = mean of replicates performed in the same set of experimental conditions.

Based upon results obtained from ANOVA, mathematical models consisting of significant terms of individual and interaction effects are built for responses of interest.

3.8 FINITE ELEMENT METHOD

3.8.1 Introduction of FEM

Various methods for modeling and simulation of AFM are reported in the literature. Out of them, the Finite Element Method (FEM) is the most powerful technique. FEM simulates a physical part or assembly's behavior by dividing the geometry of the part into a number of elements of standard shapes, applying loads and constraints, then calculating variables of interest – deflection, stresses, temperature, pressures etc. The behavior of an individual element is usually described by a relatively simple set of equations. Just as the set of elements would be joined together to build the whole structure, the equation describing the behaviors of the individual elements are joined into a set of equations that describe the behaviors of the whole structure.

Definition of FEM is hidden in the word itself. Basic theme is to make calculation at only limited number of points and then interpolate the result for entire domain (surface & volume).

Finite- any continuous object has finite degree of freedom & it's just not possible to solve in this format. Finite Element Method reduces the degree of freedom from infinite to finite with the help of discretization i.e. (nodes & elements).

Element- all the calculations are made at a limited number of points known as nodes. Entity joining nodes and forming a specific shape such as quadrilateral or triangular etc. is known as an element. To get value of variable (say displacement) at where between the calculation points,

interpolation function (as per the shape of the element) is used. In the present study quadrilateral cells have been considered.

Method- There are three methods to solve any engineering problem. Finite Element Analysis belongs to the numerical method category.

A Finite Element program takes the elements you have defined, lists the equations for each unknown value, puts them together as a matrix equation, and then solves all these for the values of the unknown parameters.

The equilibrium equation is of the form:

$$[K]\,[u] = [f]$$

Since it's analogous to the equations of spring deflection, **K** is often called stiffness matrix, **u** is called the deformation vector, and **f** is called the load vector. K is a square matrix, with one row and column for each unknown variable in the problem definition. If there are 100 nodes in a model, and one node has 6 unknowns, then stiffness matrix would be 600 × 600. u and f are each column-matrix which has 1 column and 600 rows.

3.8.2 Flowchart of FEM

The following steps summarize the finite element procedure:

First of all discretization of problem is done and then the problem is divided into number of elements. Interpolation of model is done and behavior of material is done. Equation of elements is derived and then boundary conditions are applied. Then results are found by solving the problem. In the present work Ansys 15 software has been used for preprocessing, analysis and post processing. Above discussed steps have been summarized in the form of flow chart in fig 3.19.

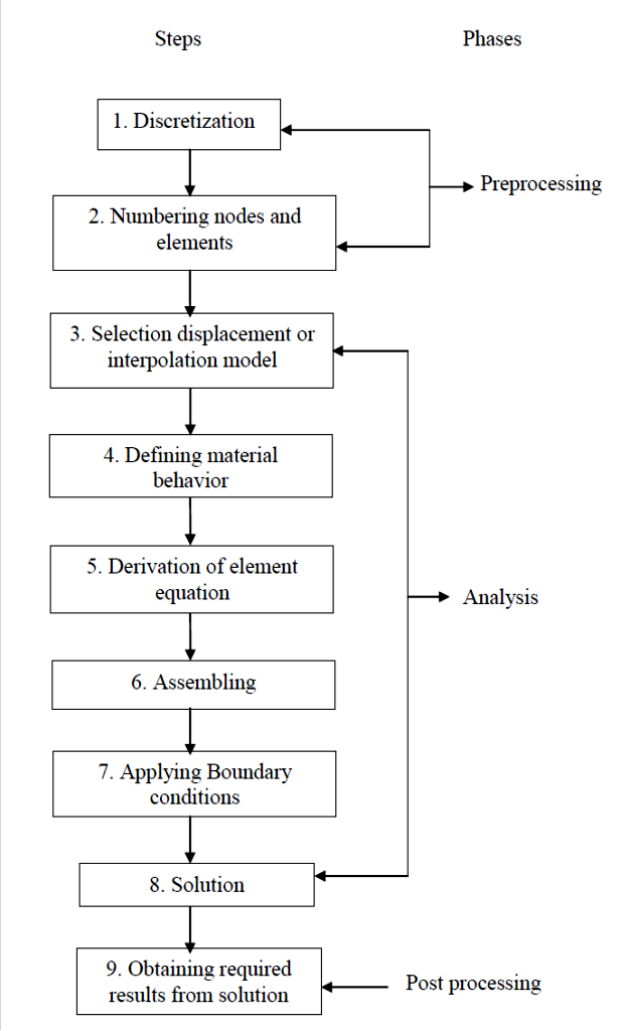

Fig. 3.19: Flowchart of FEM

3.9 BOX- BEHNKEN DESIGN

Box–Behnken designs (BBD) are one class of the experimental designs for response surface methodology. They are rotatable or nearly rotatable based on three-level incomplete factorial designs (Box and Behnken, 1960). Rotatable means that the model would possess a reasonably stable distribution of scaled prediction variance throughout the experimental design region (Montgomery, 2002). The special arrangement of the BBD levels allows the number of design points to increase at the same rate as the number of polynomial coefficients. For example, for three factors, the design can be constructed as three blocks of four experiments consisting of a full two-factor factorial design with the level of the third factor set at zero (Souza et al., 2005).

BBD requires three levels of each factor instead of five as in the case of Central Composite Designs (CCD), which results in fewer experimental trials to evaluate multiple variables and their interactions and is more convenient and less expensive to run than CCD with the same number of factors (Ragonese et al., 2002) as indicated in Table 3.6.

Table 3.6 Number of experiments based on various design approach (Source: www. It1.nist.gov, 2011)

No. of Factors	Number of Experiments		
	Central Composite Design	Full Factorial Design	Box -Behnken Design
2	13	9	11
3	20	27	15
4	30	81	27
5	50	243	46
6	86	729	54
7	152	2187	62

Experiments in phase B have been also designed based on Box Behnken design. Process parameters and their range have been shown in table 3.7.

Table 3.7: Input parameters and their levels (RSM)

Symbol	Factor	Level 1	Level 2	Level 3
A	Extrusion pressure (MPa)	3.5	5.25	7
B	Percentage of oil in Media	10	12.5	15
C	Mesh Number	100	160	220
D	Concentration of abrasives (% of abrasives by weight)	50	55	60
E	Work piece material (% of SiC in SiC/Al)	20	40	60
F	Number of Cycles	100	200	300

3.10 CONSTRAINTS

In response surface methodology, constraints are to be applied to input process parameters. In the table 3.8, different constraints are shown as range of process parameters, whether output response is to be minimized or maximized, importance assigned to process parameters etc.

Table 3.8: Constraints applied to process parameters

Name	Goal	Limit	Limit	Weight	Weight	Importance
Extrusion Pressure (MPa)	is in range	3.5	7	1	1	3
% of oil	is in range	10	15	1	1	3
Mesh no.	is in range	100	220	1	1	3
Conc. of abrasives	is in range	50	60	1	1	3
Work piece material	is in range	20	60	1	1	3
Number of cycles	is in range	100	300	1	1	3
MRR (µg/s)	maximize	2.38	7.62	1	1	3
Change in Surface Roughness	maximize	0.61	1.99	1	1	3

3.11 DESIGN OF EXPERIMENTS

The Box- Behnken method of RSM is applied to design the experiments (Kumar et al. 2013). Based on Box- Behnken design 54 trials with different settings of process parameters are shown in the table number 3.9.

Table 3.9: Box Behnken design

Trial	Ext Pr. (MPa)	% oil (Wt %)	Grit Mesh No.	Conc. Abrasives (Wt %)	W/P material (SiC % in Al/SiC)	No of cycles
1	3.5	10	160	60	40	200
2	5.25	10	160	55	60	100
3	5.25	12.5	160	55	40	200
4	5.25	15	160	55	20	100
5	7	15	160	50	40	200
6	5.25	12.5	160	55	40	200
7	5.25	12.5	220	50	40	100

Trial	Ext Pr. (MPa)	% oil (Wt %)	Grit Mesh No.	Conc. Abrasives (Wt %)	W/P material (SiC % in Al/SiC)	No of cycles
8	5.25	12.5	220	60	40	100
9	5.25	15	100	55	20	200
10	3.5	12.5	160	60	60	200
11	5.25	15	160	55	20	300
12	3.5	12.5	160	50	20	200
13	5.25	10	220	55	20	200
14	7	12.5	100	55	40	300
15	5.25	15	220	55	20	200
16	7	12.5	160	60	20	200
17	5.25	10	160	55	20	100
18	3.5	12.5	220	55	40	300
19	5.25	10	100	55	20	200
20	3.5	12.5	160	60	20	200
21	7	12.5	220	55	40	100
22	5.25	12.5	100	60	40	100
23	3.5	15	160	50	40	200
24	5.25	12.5	160	55	40	200
25	3.5	12.5	100	55	40	100
26	7	12.5	160	50	60	200
27	5.25	15	160	55	60	100
28	5.25	12.5	220	60	40	300
29	5.25	12.5	160	55	40	200
30	7	10	160	50	40	200

Trial	Ext Pr. (MPa)	% oil (Wt %)	Grit Mesh No.	Conc. Abrasives (Wt %)	W/P material (SiC % in Al/SiC)	No of cycles
31	7	12.5	160	50	20	200
32	3.5	12.5	220	55	40	100
33	3.5	12.5	160	50	60	200
34	5.25	12.5	160	55	40	200
35	5.25	15	100	55	60	200
36	5.25	12.5	100	60	40	300
37	5.25	15	160	55	60	300
38	7	15	160	60	40	200
39	7	12.5	220	55	40	300
40	7	12.5	160	60	60	200
41	5.25	12.5	100	50	40	100
42	7	10	160	60	40	200
43	5.25	15	220	55	60	200
44	5.25	10	100	55	60	200
45	5.25	12.5	160	55	40	200
46	5.25	12.5	220	50	40	300
47	7	12.5	100	55	40	100
48	3.5	10	160	50	40	200
49	5.25	10	160	55	20	300
50	5.25	10	220	55	60	200
51	5.25	10	160	55	60	300
52	3.5	15	160	60	40	200
53	5.25	12.5	100	50	40	300
54	3.5	12.5	100	55	40	300

CHAPTER 04

EXPERIMENTATION

4.0 INTRODUCTION

Based on the pilot experimentation and design of experiments, main experiments were conducted. Main experimentation was divided in two phases: phase A and phase B. In phase A experiments were conducted on the basis of design of experiments applying Taguchi method, with L27 orthogonal array. In phase B experiments were conducted applying response surface methodology; experiments were designed using Box-Behnken Design. As already discussed in chapter 3, effect of input process variables fluid extrusion pressure, viscosity of medium (varied by varying the percentage of oil in abrasive medium), mesh number of grit, concentration of abrasives, work piece material, no of cycles has been studied on machining characteristics of MMCs like MRR, SR & Surface Topography.

4.1 MEASUREMENT OF RESPONSE PARAMETERS

4.1.1 Material Removal Rate

Weight of the work piece was measured before and after each trial and time of each operation has been noted. Material removal rate was calculated by using the formula.

$$MRR = \frac{(Initial\ weight - Final\ weight)}{time} \quad (4.1)$$

4.1.2 Change in surface roughness

Surface roughness of initial and finished specimens was measured using Mitutoyo Surftest SJ-400 at Thapar University. Change in surface roughness has been taken as:

Change in surface roughness (ΔRa) = Initial surface roughness - Finished surface roughness (4.2)

4.2 EXPERIMENTAL OBSERVATIONS

Observations were made for each trial and output responses have been tabulated.

4.2.1Observations (phase A for Taguchi method)

Observations for experiments conducted in phase A, based on Taguchi method have been illustrated in table 4.1. Material removal rate and change in surface roughness of each experiment for L_{27} array have been shown.

Table 4.1: Observation table for MRR and ΔRa, after each experiment

Exp.No.	MRR1 µg/s	MRR2 µg/s	MRR3 µg/s	Mean MRR	ΔRa_1 µm	ΔRa_2 µm	ΔRa_3 µm	Mean ΔRa
1	2.20	1.90	1.63	1.91	0.30	0.30	0.60	0.40
2	2.32	3.17	2.84	2.78	0.80	0.60	0.60	0.75
3	5.01	4.78	5.15	4.98	0.67	1.20	0.81	0.90
4	2.11	1.84	2.64	2.20	0.64	1.00	0.56	0.70
5	2.52	4.01	3.09	3.21	0.59	0.86	0.70	0.75
6	5.01	4.10	4.04	4.38	0.72	0.27	0.60	0.58
7	2.52	2.04	2.75	2.44	0.50	1.04	0.55	0.60
8	2.53	3.23	2.81	2.86	0.39	0.18	0.44	0.50
9	4.21	5.01	4.38	4.53	0.72	0.41	0.67	0.80
10	2.54	2.95	2.57	2.69	0.80	0.30	0.71	0.63
11	6.64	5.12	5.00	5.59	1.05	0.71	1.20	0.98
12	7.95	4.43	5.34	5.91	1.20	0.44	1.14	1.13
13	3.23	3.38	2.83	3.15	1.22	0.20	1.00	0.92
14	7.98	6.98	6.35	7.11	1.45	0.09	1.50	1.10
15	4.54	4.62	4.81	4.66	1.30	0.44	1.20	1.13
16	3.43	4.02	3.37	3.61	0.75	0.25	0.90	0.98
17	6.46	6.87	7.09	6.81	0.90	8.09	0.96	0.90
18	4.51	5.48	5.00	5.00	1.30	0.05	1.25	1.18

Exp.No.	MRR1 µg/s	MRR2 µg/s	MRR3 µg/s	Mean MRR	ΔRa_1 µm	ΔRa_2 µm	ΔRa_3 µm	Mean ΔRa
19	9.76	9.77	8.46	9.33	1.24	0.33	1.20	0.90
20	3.98	4.34	3.36	3.90	1.15	0.63	1.30	1.43
21	8.68	8.67	8.89	8.75	1.60	0.42	1.50	1.70
22	9.12	9.97	9.66	9.58	1.23	0.48	1.00	1.15
23	4.13	4.78	4.38	4.43	1.29	2.90	1.40	1.55
24	8.18	8.64	8.26	8.36	1.40	0.25	1.47	1.60
25	9.01	9.23	9.31	9.18	1.30	0.14	1.21	1.30
26	4.32	3.98	4.38	4.23	1.06	2.45	1.21	1.40
27	8.34	8.23	8.19	8.25	1.40	0.43	1.32	1.52

4.2.2 Observations (phase B for RSM)

After completion of experimentation in phase A, experiments based on Box Behnken design have been also done in phase B (Dubey et al., 2008). Response surface methodology is applied and process parameters have been optimized using desirability approach. Observations for each trial are demonstrated in table 4.2.

Table 4.2: Observations for MRR and ΔRa (Box Behnken design)

Trial	Ext Pr. (MPa)	% oil (Wt %)	Grit Mesh No.	Conc. Abrasives (Wt %)	W/P material (SiC % in Al/SiC)	No of cycles	MRR (µg/s)	ΔRa (µm)
1	3.5	10	160	60	40	200	3.89	0.96
2	5.25	10	160	55	60	100	2.38	0.78
3	5.25	12.5	160	55	40	200	5.1	1.25
4	5.25	15	160	55	20	100	4.92	1.16
5	7	15	160	50	40	200	5.83	1.66
6	5.25	12.5	160	55	40	200	5.16	1.01

Trial	Ext Pr. (MPa)	% oil (Wt %)	Grit Mesh No.	Conc. Abrasives (Wt %)	W/P material (SiC % in Al/SiC)	No of cycles	MRR (µg/s)	ΔRa (µm)
7	5.25	12.5	220	50	40	100	3.72	0.93
8	5.25	12.5	220	60	40	100	3.68	0.95
9	5.25	15	100	55	20	200	6.18	1.45
10	3.5	12.5	160	60	60	200	2.78	0.74
11	5.25	15	160	55	20	300	7.62	1.75
12	3.5	12.5	160	50	20	200	4.79	1.2
13	5.25	10	220	55	20	200	6.21	1.45
14	7	12.5	100	55	40	300	7.24	1.99
15	5.25	15	220	55	20	200	6.23	1.46
16	7	12.5	160	60	20	200	6.8	1.82
17	5.25	10	160	55	20	100	4.91	1.16
18	3.5	12.5	220	55	40	300	5.45	1.24
19	5.25	10	100	55	20	200	6.2	1.47
20	3.5	12.5	160	60	20	200	4.8	1.19
21	7	12.5	220	55	40	100	4.18	1.3
22	5.25	12.5	100	60	40	100	3.61	0.94
23	3.5	15	160	50	40	200	3.9	0.97
24	5.25	12.5	160	55	40	200	5.2	1.26
25	3.5	12.5	100	55	40	100	2.45	0.62
26	7	12.5	160	50	60	200	4.72	1.45
27	5.25	15	160	55	60	100	2.38	0.78
28	5.25	12.5	220	60	40	300	6.81	1.49
29	5.25	12.5	160	55	40	200	5.12	1.23
30	7	10	160	50	40	200	5.8	1.63
31	7	12.5	160	50	20	200	6.8	1.82

Trial	Ext Pr. (MPa)	% oil (Wt %)	Grit Mesh No.	Conc. Abrasives (Wt %)	W/P material (SiC % in Al/SiC)	No of cycles	MRR (µg/s)	ΔRa (µm)
32	3.5	12.5	220	55	40	100	2.48	0.61
33	3.5	12.5	160	50	60	200	2.8	0.74
34	5.25	12.5	160	55	40	200	5.14	1.24
35	5.25	15	100	55	60	200	4.21	1.07
36	5.25	12.5	100	60	40	300	6.8	1.54
37	5.25	15	160	55	60	300	6.1	1.46
38	7	15	160	60	40	200	5.82	1.65
39	7	12.5	220	55	40	300	7.25	1.97
40	7	12.5	160	60	60	200	4.71	1.45
41	5.25	12.5	100	50	40	100	3.64	0.96
42	7	10	160	60	40	200	5.85	1.64
43	5.25	15	220	55	60	200	4.16	1.06
44	5.25	10	100	55	60	200	4.17	1.07
45	5.25	12.5	160	55	40	200	5.22	1.24
46	5.25	12.5	220	50	40	300	6.81	1.53
47	7	12.5	100	55	40	100	4.23	1.31
48	3.5	10	160	50	40	200	3.92	0.95
49	5.25	10	160	55	20	300	7.6	1.75
50	5.25	10	220	55	60	200	4.17	1.07
51	5.25	10	160	55	60	300	6.1	1.46
52	3.5	15	160	60	40	200	3.91	0.97
53	5.25	12.5	100	50	40	300	6.82	1.52
54	3.5	12.5	100	55	40	300	5.42	1.23

CHAPTER 05

RESULTS AND DISCUSSION

5.0 INTRODUCTION

Experiments were performed with different combination of input parameters; performance characteristics such as MRR, ΔRa were recorded. In phase A, the statistical investigations of the obtained results have been performed using the Taguchi method, to understand the effect of the selected input process parameters on the output variables. The statistical tools such as signal-to-noise ratio (S/N) and analysis of variance (ANOVA) are used to analyze the results. Optimization of process parameters is also done using the Taguchi methodology. An optimum combination of input parameters is also presented. Theoretical and experimental values have been compared for validation of results. Confirmatory experiments were also conducted based on the identified significant parameters. In phase B, response surface methodology was applied to analyze the effect of input process parameters on response parameters. Desirability approach has been applied for optimization of process parameters. Maximization of both response parameters (MRR and ΔRa) is desirable in our study. To understand the surface topography, microstructure analysis has been also done. Specimens were examined and analyzed using scanning electron microscope and X- ray diffraction techniques.

5.1 ANALYSIS AND OPTIMIZATION USING TAGUCHI METHOD (PHASE A)

Mean values of MRR and ΔRa after each experiment and overall mean values are listed in table number 5.1.

Table 5.1: Mean values for overall MRR and ΔRa

Experiment Number	Mean MRR (µg/s)	Mean ΔRa (µm)	Experiment Number	Mean MRR (µg/s)	Mean ΔRa (µm)
1	1.91	0.40	15	4.66	1.13
2	2.78	0.75	16	3.61	0.98
3	4.98	0.90	17	6.81	0.90
4	2.20	0.70	18	5.00	1.18

Experiment Number	Mean MRR (µg/s)	Mean ΔRa (µm)	Experiment Number	Mean MRR (µg/s)	Mean ΔRa (µm)
5	3.21	0.75	19	9.33	0.90
6	4.38	0.58	20	3.90	1.43
7	2.44	0.60	21	8.75	1.70
8	2.86	0.50	22	9.58	1.15
9	4.53	0.80	23	4.43	1.55
10	2.69	0.63	24	8.36	1.60
11	5.59	0.98	25	9.18	1.30
12	5.91	1.13	26	4.23	1.40
13	3.15	0.92	27	8.25	1.52
14	7.11	1.10	**Overall Mean (27 trials)**	**5.17**	**1.01**

5.1.1 Analysis of variance for MRR

Analysis of variance has been done using Taguchi method on MINITAB software. The average values of MRR (means) for all the six factors at each level are listed in table 5.2. The S/N ratios are listed in table 5.3 for each level of the factors varied during experimentation. Extrusion pressure is found to be the most significant factor, followed by work piece material and number of cycles respectively as shown in table 5.4. It is observed that extrusion pressure is the most significant factor for MRR as demonstrated in table 5.4. As extrusion pressure increases, MRR increases as shown in figure 5.1. This result is in good agreement with findings reported in (Jain et al., 1999). It is found that percentage of oil in media, grit size (mesh number) and concentration of abrasives have little effect on MRR as shown in ANOVA table 5.4 and figure 5.1. Work piece material is also a significant factor as illustrated in table 5.4. It is also observed that MRR first decreases, then increases with an increase in SiC percentage in work material as shown in figure 5.1. This may be due to the random distribution of particles in composite material (Sankar et al., 2009). As the number of cycle increases, MRR gets increased as shown in

figure 5.1. Interaction of extrusion pressure and work piece material is also significant for MRR as illustrated in table number 5.4 and figure 5.2. It can be clearly observed from fig 5.1 that the optimum combination of process parameters for MRR is $A_3\ B_2\ C_1\ D_2\ E_3\ F_3$.

Table 5.2: Response Table for Means

Level	A	B	C	D	E	F
1	3.257	5.221	5.259	5.141	4.902	5.028
2	4.931	5.202	5.074	5.228	4.548	4.983
3	7.339	5.104	5.194	5.158	6.078	5.516
Delta	4.082	0.118	0.185	0.087	1.530	0.533
Rank	1	5	4	6	2	3

Table 5.3: Response Table for Signal to Noise Ratios (Larger is better)

Level	A	B	C	D	E	F
1	9.812	13.390	13.445	13.219	12.028	12.956
2	13.430	13.313	13.215	13.491	12.676	13.031
3	16.801	13.341	13.384	13.335	15.340	14.056
Delta	6.989	0.077	0.231	0.272	3.312	1.100
Rank	1	6	5	4	2	3

Table 5.4: Analysis of variance (ANOVA) for material removal rate

Factors	DOF	Seq SS	Adj MS	F	P	Percentage contribution
A	2	219.920	109.960	295.95	0.003	49.11
B	2	0.028	0.014	0.04	0.964	0.00
C	2	0.257	0.128	0.35	0.743	0.05
D	2	0.335	0.293	0.45	0.689	0.07
E	2	55.467	29.693	74.64	0.013	12.38

Factors	DOF	Seq SS	Adj MS	F	P	Percentage contribution
F	2	6.800	92.016	9.15	0.099	1.51
A X E	4	159.478		107.31	0.009	35.61
A X F	4	2.181		1.47	0.444	0.48
E X F	4	2.537		1.71	0.402	0.56
Error	2	0.743	1.838			0.16
Total	26	447.746				
R-Sq = 99.9%				R-Sq(adj) = 98.8%		

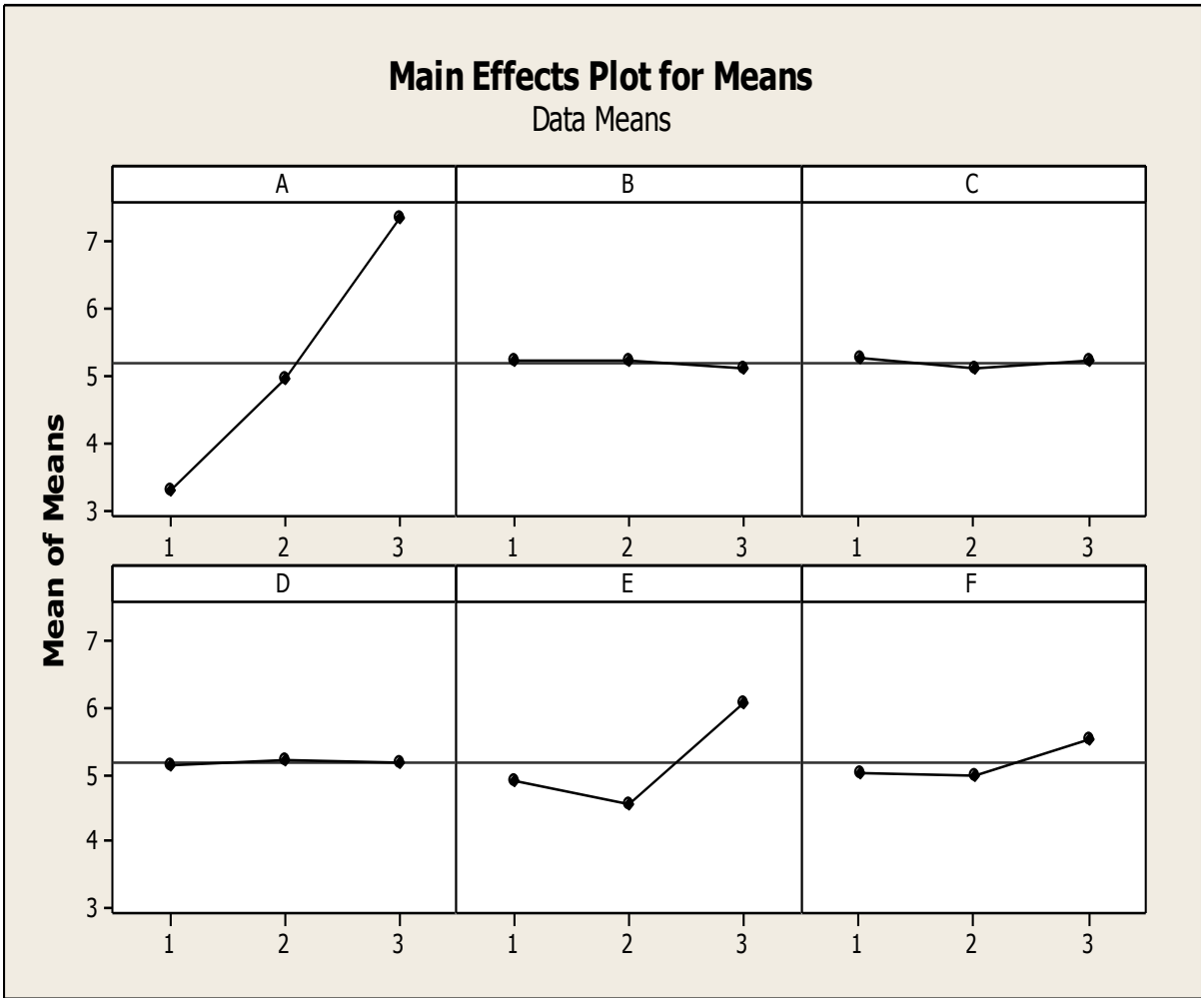

Figure 5.1: Main effects plot for Means of MRR

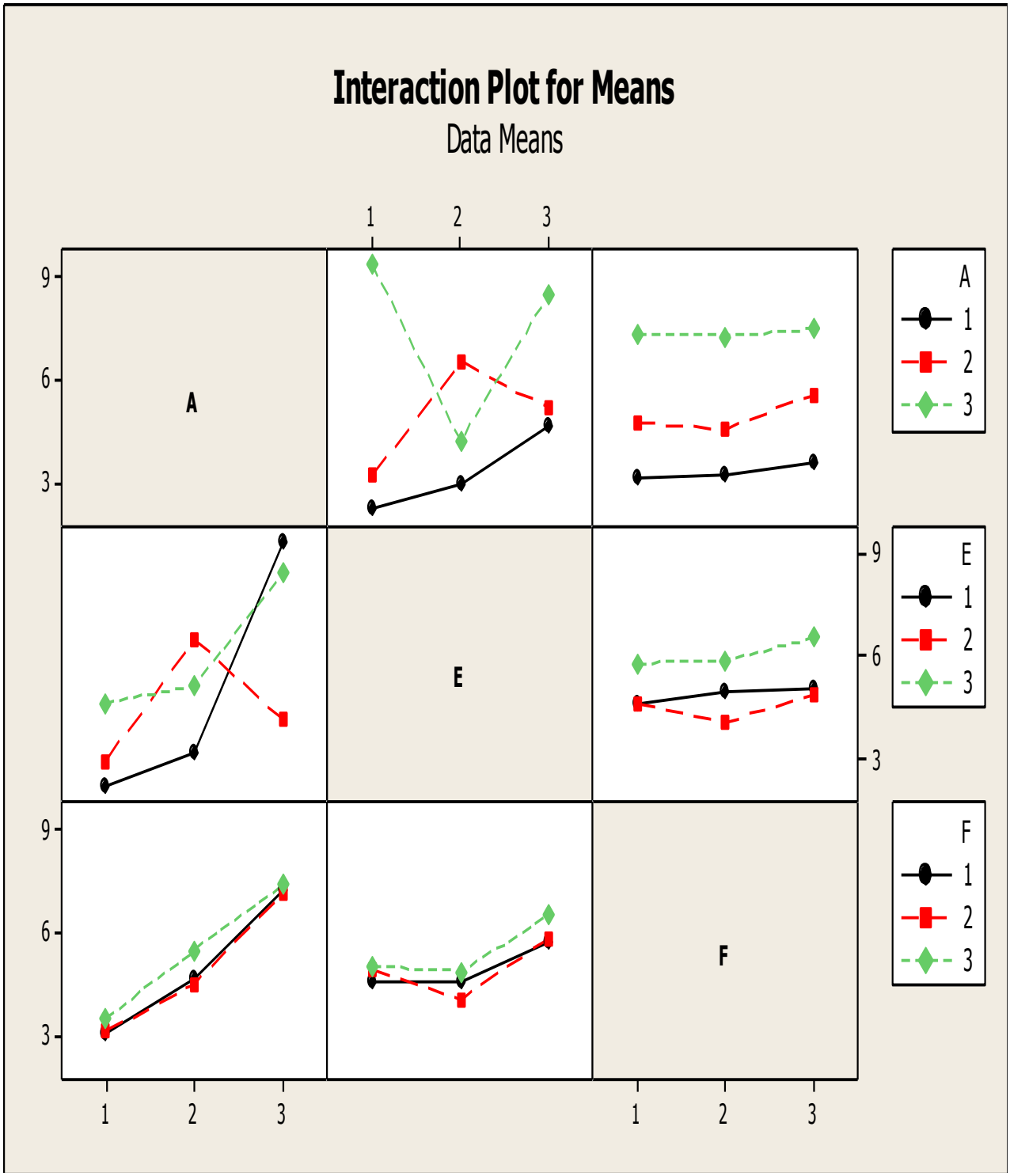

Figure 5.2: Interactions plot for Means of MRR

5.1.2 Optimization of MRR

Mean value of overall MRR can be taken from table number 5.1 as:

Overall MRR (T) = 5.17 μg/s

From figure 5.1, the optimum Taguchi combination can be taken as:

Optimum Taguchi Combination = $A_3\ B_2\ C_1\ D_2\ E_3\ F_3$

Hence, the optimum value of MRR can be calculated as:

MRR (optimum) = $\overline{A_3} + \overline{B_2} + \overline{C_1} + \overline{D_2} + \overline{E_3} + \overline{F_3}$

Considering Significant Parameters

MRR (optimum) = $\overline{A_3} + \overline{E_3} + \overline{F_3} - 2\overline{T}$

=7.339+ 6.078 + 5.516– 2 X 5.17

= 18.933-10.34

= 8.59 μg/s

Confidence Interval, CI is given as

$$CI = \pm\sqrt{\frac{F_{(1,n,\alpha)}V_e}{n_e}}$$

F (1, *n*, α) is the F ratio required, for α (risk), confidence = 1– α

n is the degrees of freedom (d.o.f.) of error

Ve is the variance of pooled error and

ne is the number of replications (effective)

At 95 %, confidence interval

$F_{(1,n,\alpha)}$ = F $_{(1, 2, 0.05)}$ =18.512

$$n_e = \frac{N}{1+\left(dof\ of\ all\ \ factors\ used\ in the estimation\right)}$$

$n_e = 27/(1+6) = 3.857$

Ve = pooled error variance

$Ve = (0.072 + 0.159 + 0.038 + 0.144)/8 = 0.051$

$$CI = \pm\sqrt{\frac{18.512 X\, 0.051}{3.857}}$$

$= \pm 0.494$

So, the optimum value of predicted MRR can be calculated as:

Predicted MRR (optimum) = MRR (optimum) + CI

$= (8.099 < 8.593 < 9.087)\ \mu g/s$

The mean experimental value after confirmation experiments is 8.81μ g/s

Percentage error = (8.81-8.59) /8.81X100= 2.49 %

Percentage error value shows that experimental results are in good agreement with predicted results.

5.1.3 Analysis of variance for ΔRa

The average values of ΔRa (means) for all the six factors at each level are listed in table 5.5. The S/N ratios are listed in table 5.6 for each level of the factors varied during experimentation. ANOVA table 5.7 shows in that extrusion pressure is most significant factor for ΔRa. As extrusion pressure increases, ΔRa increases as shown in figure 5.3 and validated with (Jain et al., 1999). It is found that percentage of oil in media, grit size (mesh number) and concentration of abrasives have little effect on ΔRa as shown in ANOVA table 5.6. Work piece material is also a significant factor as illustrated in table 5.7. ΔRa increases as the percentage of SiC increases in composite material as shown in figure 5.3. As the number of cycle increases, Ra gets increased as shown in figure 5.3. Initially surface roughness improves more but becomes less with further

increase in the number of cycles. This is because initially there are more peaks and valleys. This result supports the findings reported in (Singh and Shan, 2002) and (Wang and Weng, 2007). Interaction of considered factors is not significant for ΔRa as shown in table 5.7 and figure 5.4.

Table 5.5: Response Table for Means (ΔRa)

Level	A	B	C	D	E	F
1	0.6644	1.0256	1.0456	1.0467	0.8422	0.8933
2	0.9944	1.0100	0.9989	1.0133	1.0400	1.0478
3	1.3944	1.0178	1.0089	0.9933	1.1711	1.1122
Delta	0.7300	0.0156	0.0467	0.0533	0.3289	0.2189
Rank	1	6	5	4	2	3

Table 5.6: Response Table for Signal to Noise Ratios (Larger is better)

Level	A	B	C	D	E	F
1	-3.7885	-0.3895	-0.2136	-0.1521	-1.9810	-1.8320
2	-0.1794	-0.5188	-0.5130	-0.3534	-0.1606	0.1067
3	2.7491	-0.3105	-0.4922	-0.7133	0.9227	0.5064
Delta	6.5376	0.2083	0.2994	0.5612	2.9037	2.3384
Rank	1	6	5	4	2	3

Table 5.7: Analysis of variance (ANOVA) for ΔRa

Factors	DOF	Seq SS	Adj MS	F	P	% contribution
A	2	2.405	1.2027	148.89	0.007	72.37
B	2	0.001	0.0005	0.07	0.937	0.03
C	2	0.0108	0.0054	0.67	0.598	0.32
D	2	0.0130	0.0065	0.81	0.553	0.39
E	2	0.493	0.2467	30.54	0.032	14.83

Factors	DOF	Seq SS	Adj MS	F	P	% contribution
F	2	0.227	0.1138	14.10	0.066	6.83
A X E	4	0.080	0.0200	2.48	0.307	2.40
A X F	4	0.032	0.0082	1.02	0.550	0.96
E X F	4	0.042	0.0106	1.32	0.475	1.26
Error	2	0.016	0.0080			0.48
Total	26	3.323				
R-Sq = 99.5 %				R-Sq (adj) = 93.7 %		

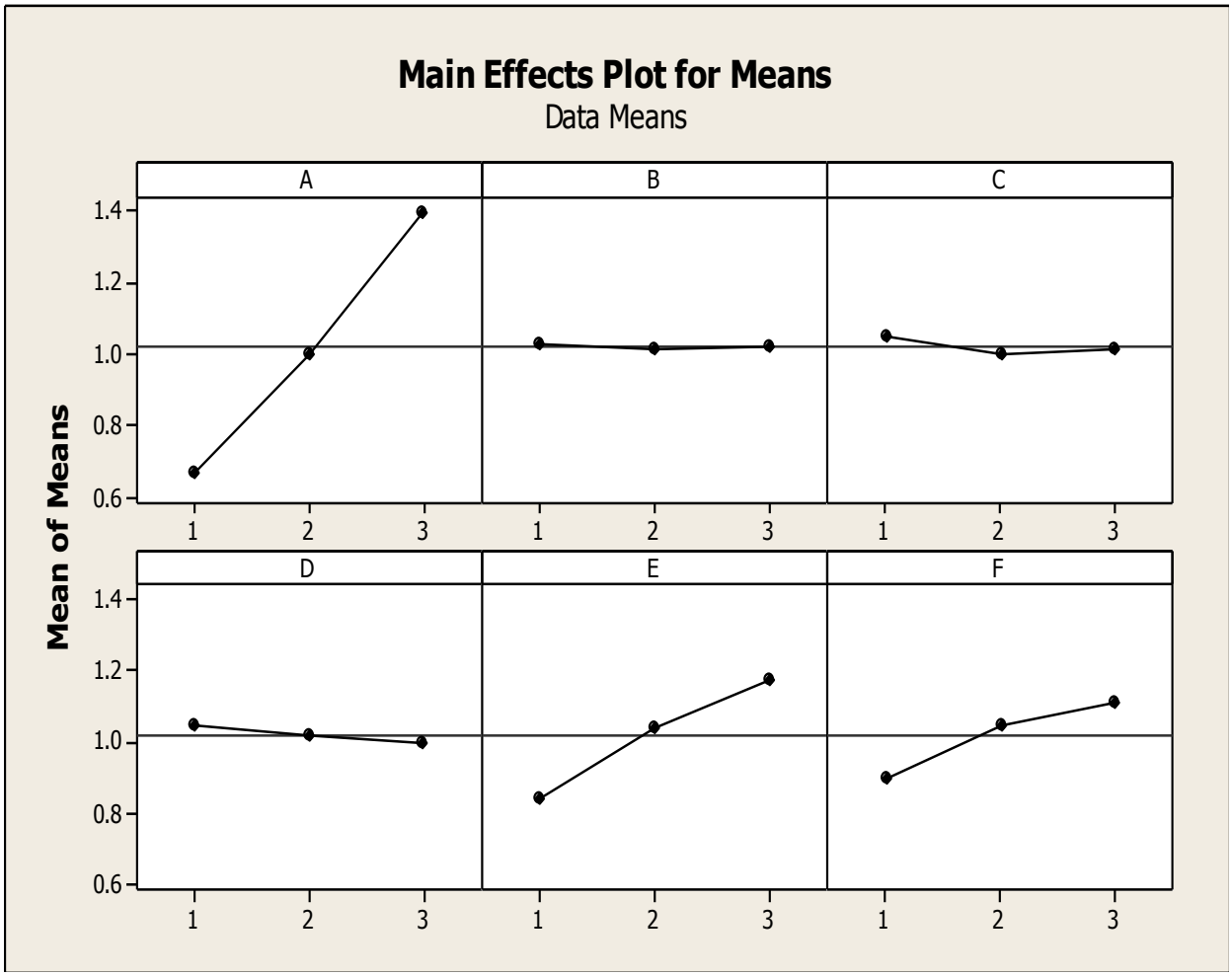

Figure 5.3: Main effects plot for Means of ΔRa

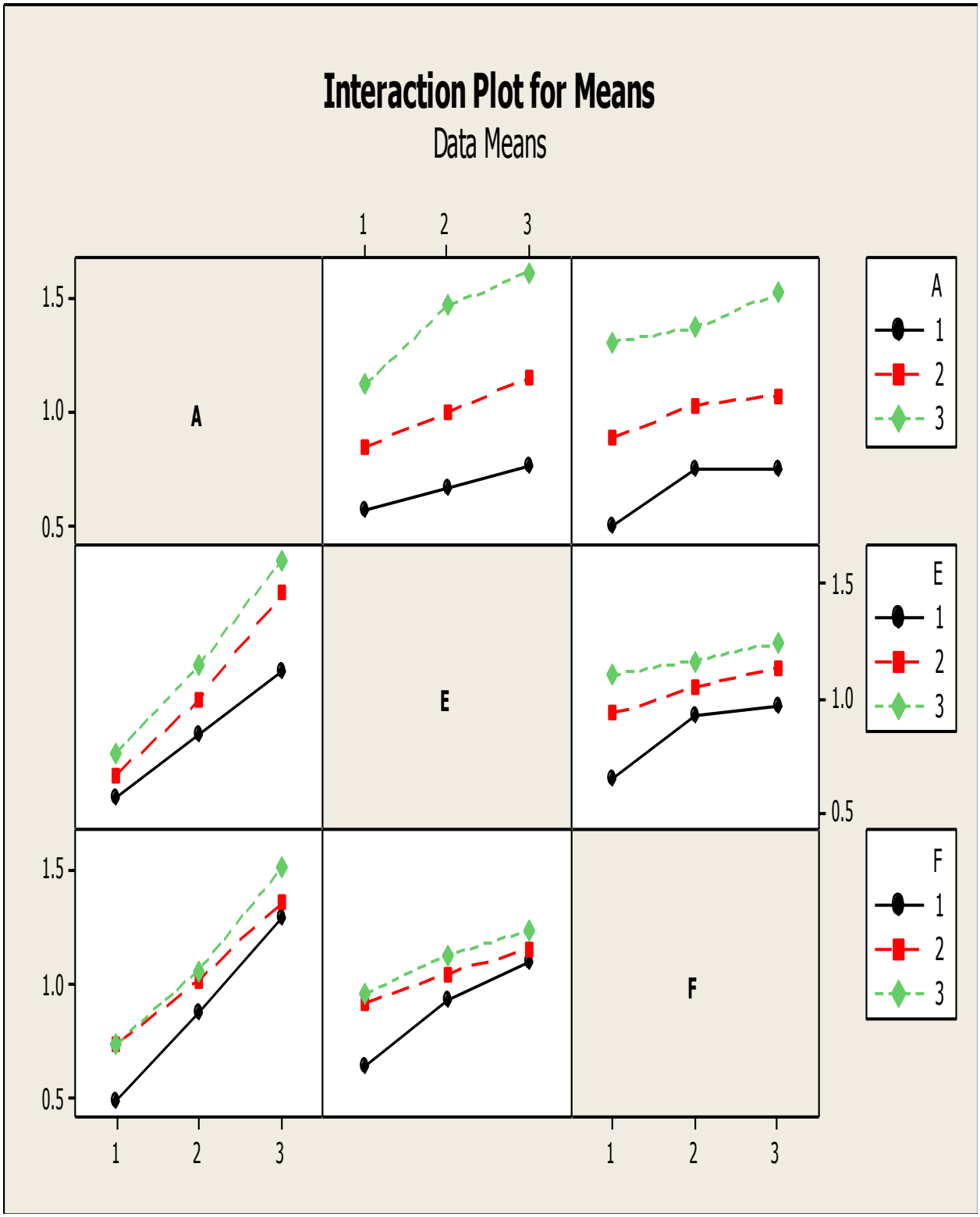

Figure 5.4: Interactions plot for Means of ΔRa

5.1.4 Optimization of ΔRa

Mean value of overall ΔRa can be taken from table number as:

Overall ΔRa (T) = 1.0177 μm

From figure 5.3, the optimum Taguchi combination can be taken as:

Optimum Taguchi Combination $A_3\ B_1C_1\ D_1\ E_3\ F_3$

Hence, the optimum value of ΔRa can be calculated as:

$$\Delta Ra\ (optimum) = \overline{A_3} + \overline{B_1} + \overline{C_1} + \overline{D_1} + \overline{E_3} + \overline{F_3}$$

Considering Significant Parameters

$$\Delta Ra\ (optimum) = \overline{A_3} + \overline{E_3} + \overline{F_3} - 2\overline{T}$$

$$= 1.3944 + 1.1711 + 1.1122 - 2 \text{ X } 1.0177$$

$$= 3.67 - 2.035$$

$$= 1.635\ \mu m$$

Confidence Interval, CI is given as

$$CI = \pm\sqrt{\frac{F_{(1,n,\alpha)}V_e}{n_e}}$$

F (1, *n*, α) is the F ratio required for α (risk), confidence = 1– α,

n is the degrees of freedom(d.o.f.) of error,

Ve is the variance of pooled error, and

ne is the number of replications (effective).

At 95 %, confidence interval

$F_{(1,n,\alpha)}$ = F $_{(1, 2, 0.05)}$ =18.512

$$n_e = \frac{N}{1 + (dof\ of\ all\ \ factors\ used\ in the\ estimation)}$$

$n_e = 27/(1+6) = 3.857$

Ve = pooled error variance

Ve = (0.001 + 0.0108 + 0.0130 + 0.0161)/8 = 0.00511

$$CI = \pm\sqrt{\frac{18.512X0.00511}{3.857}}$$

$= \pm 0.156$

So, the optimum value of predicted ΔRa can be calculated as:

Predicted ΔRa (optimum) = ΔRa (optimum) + CI

= (1.479< 1.635 <1.791)

The mean experimental value after confirmation experiments is 1.72 µm

Percentage error = (1.72-1.63) /1.72X100= 5.23 %

Percentage error value shows that experimental results are in good agreement with predicted results.

5.2 ANALYSIS AND OPTIMIZATION USING RSM (PHASE B)

Response surface methodology has been applied for modeling and analysis of input and output parameters in AFM process. Box-Behnken design has been chosen to design the experiments and analyze the process parameters. The analysis was done to explore the quadratic effects of the parameters on the performances. For Box- Behnken design a quadratic model relating factors and responses is given by

$$Y = \alpha_0 + \sum_{i=1}^{k} \alpha_i x_i + \sum_{i=1}^{k} \alpha_{ii} x_i^2 + \sum_{i<j} \alpha_{ij} x_i x_j \qquad (5.1)$$

Where Y is the preferred response, $x_{i\ (1,\ 2,\ \ldots,\ k)}$ are the independent k quantitative process variables, α_0 is a constant and α_i, α_{ii} and α_{ij} are the coefficients of linear, quadratic and interaction terms, respectively. Input parameters (fluid pressure, percentage of oil in media, grit

size, concentration of abrasives, work piece material and number of cycles) were varied to investigate their effects on output responses (MMR, ΔRa).

The relationship between desired response and independent input variables is as follows:

$$Y = f(P, p, n, c, Wp, N) \quad (5.2)$$

Where, Y is desired response; f is the response function; P is extrusion pressure; p is oil percentage in the media; n is mesh no. /grit size; c is concentration of abrasives; Wp is work piece material; N is the number of cycles.

For approximation of Y, second order polynomial regression, i.e. quadratic model is used. Design expert 6.0, software has been used to compute the values for effect of process variables on material removal rate and change in surface roughness. A model is developed for 95 percent confidence level. Terms having 'Prob > F' less than 0.05 are significant.

5.2.1 ANOVA for MRR

Final Equation for developed model of MRR in Terms of coded factors:

$$MRR = +5.15 + 0.94 \times A + 2.5 \times 10^{-3} \times B - 1.02 \times E + 1.56 \times F - 0.36 \times A^2 + 0.050 \times B^2 + 0.059 \times F^2 + 0.26 \times E \times F \quad (5.3)$$

Final equation for MRR in terms of actual factors:

$$MRR = +0.463 + 1.789 \times \textit{Extrusion Pressure} - 0.200 \times \%\,\textit{of oil} - 0.076 \times \textit{Workpiece material} + 8.108\,X\,10^{-3} \times \textit{Number of cycles} - 0.119 \times (\textit{Extrusion Pressure})^2 + 8.066 \times 10^{-3} \times (\%\textit{of oil})^2 + 5.916 \times 10^{-6} \times (\textit{Number of cycles})^2 + 1.281 \times 10^{-4} \times \textit{Workpiece material} \times \textit{Number of cycles} \quad (5.4)$$

The analysis of variance has been performed for process parameters. For ANOVA the quadratic model for the process parameters is necessary and contributes feasible results. The ANOVA table is shown in table 5.8 which shows that quadratic model lies at 95% confidence level. F-value of model is 4687.69 and p value is <0.0001. It implies that there is only a 0.01% chance that such large F-value of model can occur due to noise. Thus, quadratic model is significant at 95% confidence level. F value for lack of fit of is 1.37 and p value is 0.3941 which implies that it is not significant relative to pure error. The other important coefficient R^2, which is called determination coefficient, is defined as the ratio of the explained variation to the total variation and is a measure of the degree of fit. When R^2 approaches to unity, the response model fits better to the actual data and shows less difference between the predicted and actual values. It was found that the "Pred R-Squared" value of

0.9982 is closely matched with the "Adj R-Squared" value of 0.9986. Effect and significance of the parameters on MRR are also shown in table 5.8. It can be observed from the table that factors A, E and F have a significant effect on response parameters, followed by factor B. MRR and gets increased with increase in extrusion pressure as illustrated in figure 5.5(a). This result supports the findings reported by (Singh and Shan, 2002). Change in percentage of oil has very little effect on MRR as it is clear in figures 5.5(b). As percentage of SiC increases in workpiece, it gets harder and MRR gets decreased as shown in figure 5.5(c). MRR gets increased with an increase in the number of cycles as demonstrated in figures 5.5(d). This result is also in good agreement as reported by (Singh and Shan, 2002). Deviation of effect of parameters from mean value is shown in fig 5.6. Interaction of workpiece material and number of cycles is significant as shown in figure 5.7. Figure 5.8 shows normal probability plot of residuals for MRR. It was observed that residuals fall in straight line which shows that errors are normally distributed as desired. Contour plot of MRR is shown in figure 5.9. 3D plot of MRR is shown in figure 5.10. It can be concluded from contour and 3D plots that MRR gets increased from 3.2 to 6.6 μg/s with simultaneous increase in no. of cycles and decrease in SiC percentage in work piece material.

Table 5.8: Analysis of variance for MRR (RSM)

Source	Sum of Squares	DF	Mean Square	F value	Prob>F	Percentage Contribution	Remarks
Model	107.10	8	13.39	4687.69	< 0.0001		Significant
A	21.36	1	21.36	7477.92	< 0.0001	19.91	Significant
B	0.0001	1	0.00015	0.053	0.8198	0.0003	Not significant
E	24.77	1	24.77	8671.52	< 0.0001	23.30	Significant
F	58.41	1	58.41	20450.29	< 0.0001	54.47	Significant
A^2	1.60	1	1.60	558.49	< 0.0001	1.44	Significant
B^2	0.031	1	0.031	10.68	0.0021	0.0002	Significant
F^2	0.042	1	0.042	14.71	0.0004	0.0003	Significant
EF	0.53	1	0.53	183.93	< 0.0001	0.0049	Significant
Residual	0.13	45	.0028				
Lack of Fit	0.12	40	.0029	1.37	0.3941		Not significant
Pure error	0.011	5	.0021				
Total	107.23	53					
R-Squared	0.9988	Adj R-Squared		0.9986	Pred R-Squared		0.9982

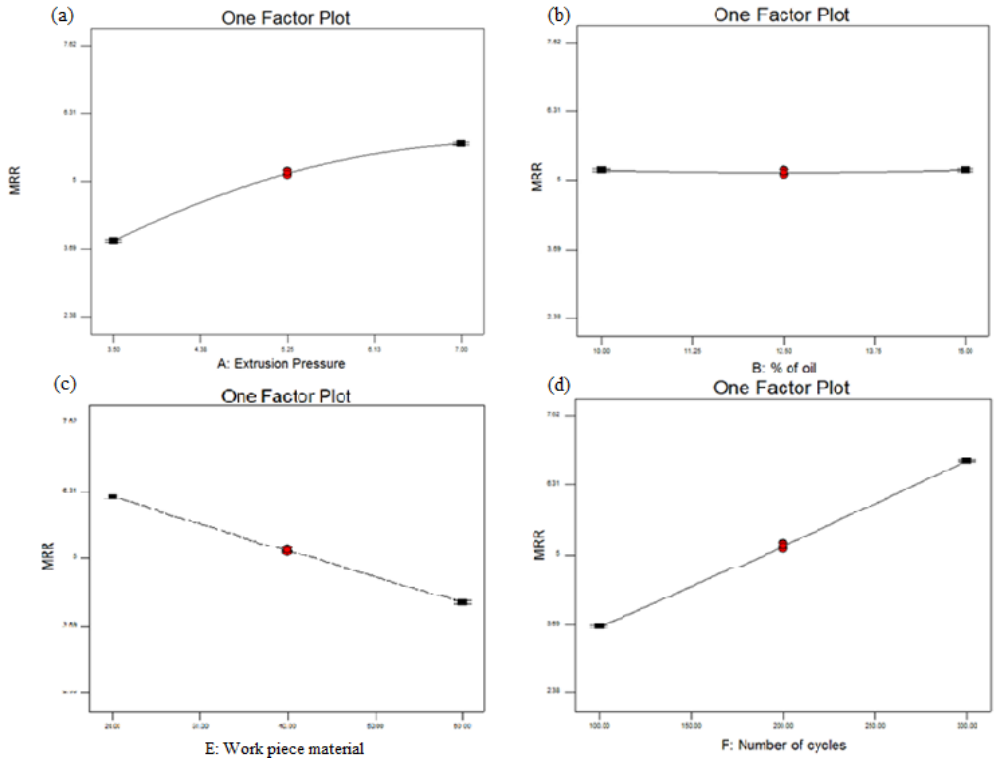

Figure 5.5: One factor plots for MRR

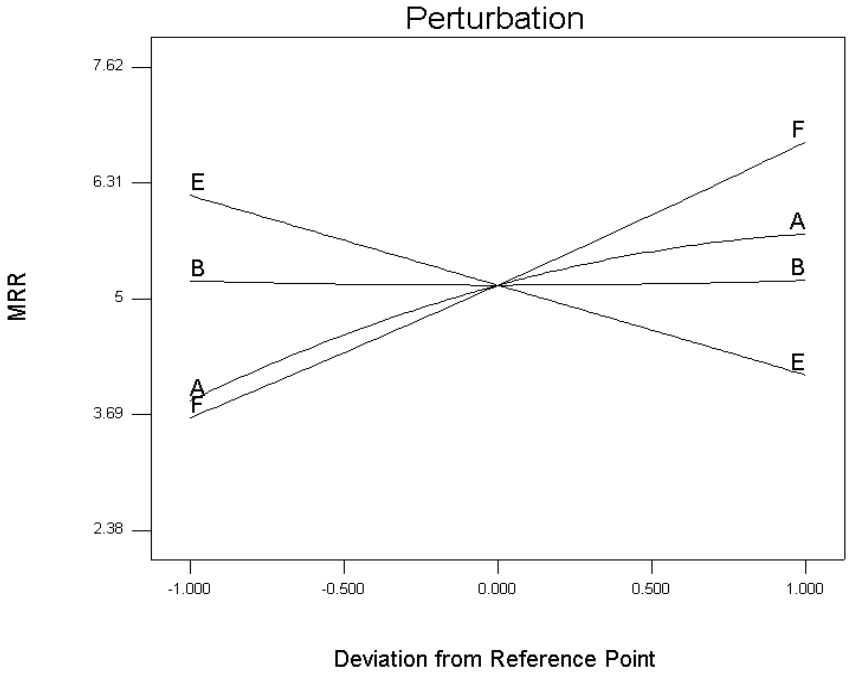

Figure 5.6: Perturbation plot for MRR

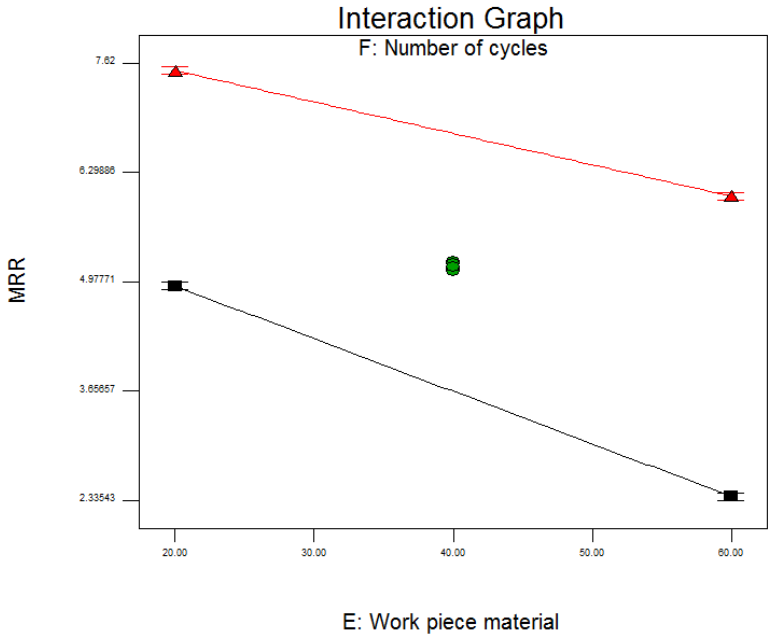

Figure 5.7: Interaction of workpiece material and number of cycles

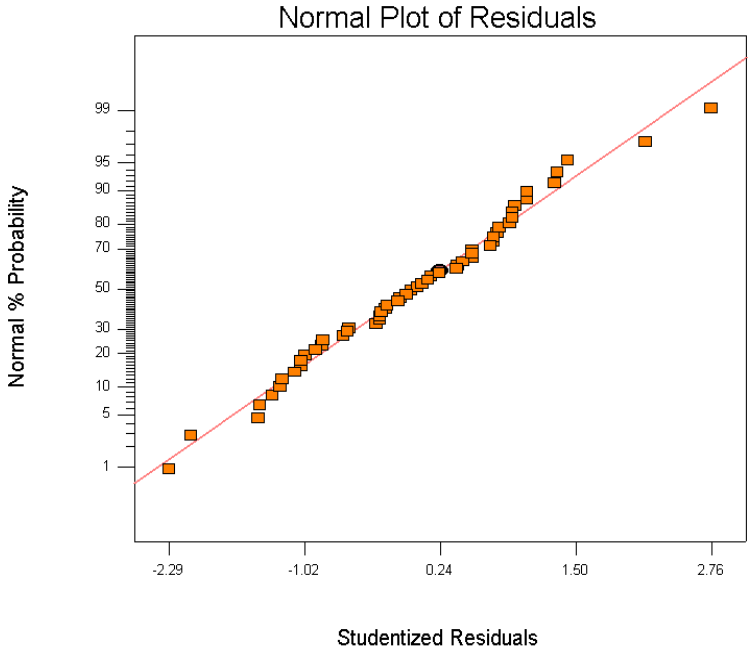

Figure 5.8: Normal probability residual plot

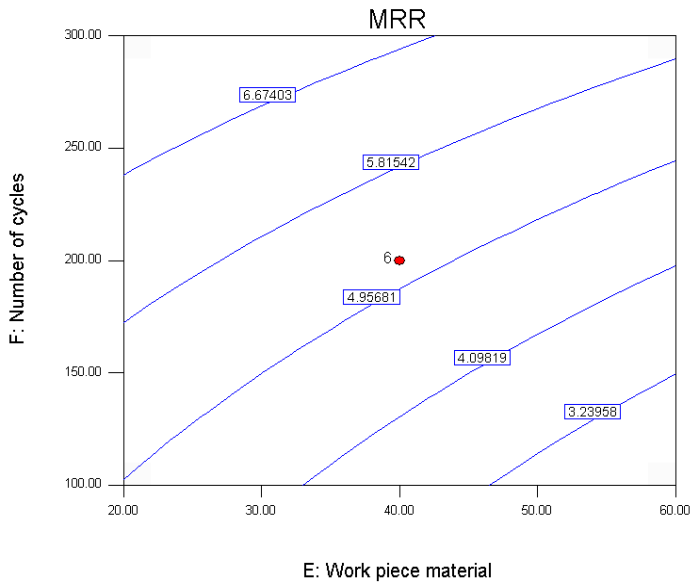

Figure 5.9: Contour plot for MRR

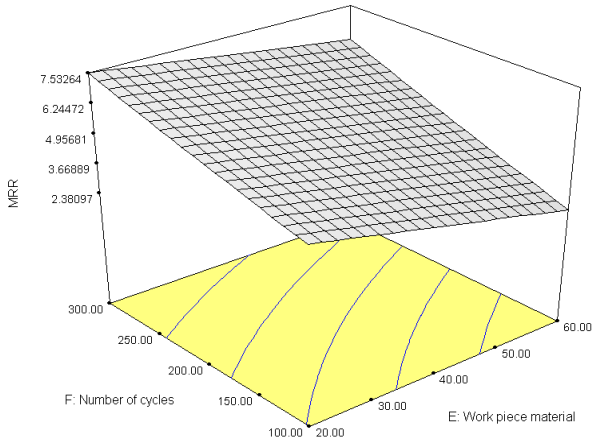

Figure 5.10: 3D plot for MRR

5.2.2 ANOVA for ΔRa

The ANOVA table for ΔRa is shown in table 5.9 which shows that quadratic model lies at 95% confidence level. F-value of model is 553.60 and p value is < 0.0001. It implies that there is only 0.01% chance that such large F- value of model can occur due to noise. Thus, quadratic model is significant at 95% confidence level. F value for lack of fit of is 0.10 and p value is 1.000 which implies that it is not significant relative to pure error. The other important coefficient R^2, which is called determination coefficient, is defined as the ratio of the explained variation to the total

variation and is a measure of the degree of fit. When R^2 approaches to unity, the response model fits better to the actual data and shows less difference between the predicted and actual values. It was found that the "Pred R-Squared" value of 0.9829 is closely matched with the "Adj R-Squared" value of 0.9843. Effect and significance of the parameters on ΔRa are shown in table 5.9. It can be observed from the table that factors A, E and F have a significant effect on ΔRa , followed by factor B. ΔRa gets increased with increase in extrusion pressure as illustrated in figure 5.11(a). Change in percentage of oil has very little effect on ΔRa as it is clear in figure 5.11(b). As percentage of SiC increases in workpiece, it gets harder so ΔRa gets decreased as shown in figure 5.11(c). ΔRa gets increased with an increase in the number of cycles as demonstrated in figure 5.11(d). This result is in good agreement as reported by (Singh and Shan, 2002). Deviation of effect of process parameters from mean value is shown in fig. 5.12. Figure 5.13 shows normal probability plot of residuals for ΔRa . It was observed that residuals fall in straight line which shows that errors are normally distributed as desired. Contour plots of ΔR are shown in figure 5.14. ΔRa gets increased from 1.06 to 1.54 μm with an increase in extrusion pressure with little effect of oil % in media as shown in figure 5.15.

Table 5.9: Analysis of variance for ΔRa

Source	Sum of Squares	DF	Mean Square	F value	Prob>F	Percentage Contribution	Remarks
Model	6.06	6	1.01	553.60	< 0.0001		Significant
A	2.85	1	2.85	1562.38	< 0.0001	46.41	Significant
B	0.0001	1	0.0001	0.057	0.8122	0.00001	Non significant
E	0.86	1	0.86	472.93	< 0.0001	14.00	Significant
F	2.30	1	2.30	1261.11	< 0.0001	37.45	Significant
A^2	0.037	1	0.037	20.35	< 0.0001	0.60	Significant
B^2	0.017	1	0.017	9.27	0.0038	0.02	
Residual	0.086	47	0.0018				
Lack of Fit	0.040	42	0.00094	0.10	1.000		Not Significant
Pure error	0.046	5	0.00923				
Total	6.14	53					
R-Squared	0.9860	Adj R-Squared		0.9843	Pred R-Squared		0.9829

Final equation for developed model of ΔRa in terms of coded factors:

$$\Delta Ra = +1.23 + 0.34 \times A + 2.083 \times 10^{-3} \times B - 0.19 \times E + 0.31 \times F + 0.054 \times A^2 + 0.036 \times B^2 \quad (5.5)$$

Final equation for ΔRa in terms of actual factors:

$$\Delta Ra = +1.33 + 0.012 \times Extrusion\ Pressure - 0.144 \times \%\ of\ oil - 9.479 \times 10^{-3} \times Workpiece\ material + 3.095 \times 10^{-3} \times Number\ of\ cycles + 0.0175 \times (Extrusion\ Pressure)^2 + 5.816 \times 10^{-3} \times (\%\ of\ oil)^2 \quad (5.6)$$

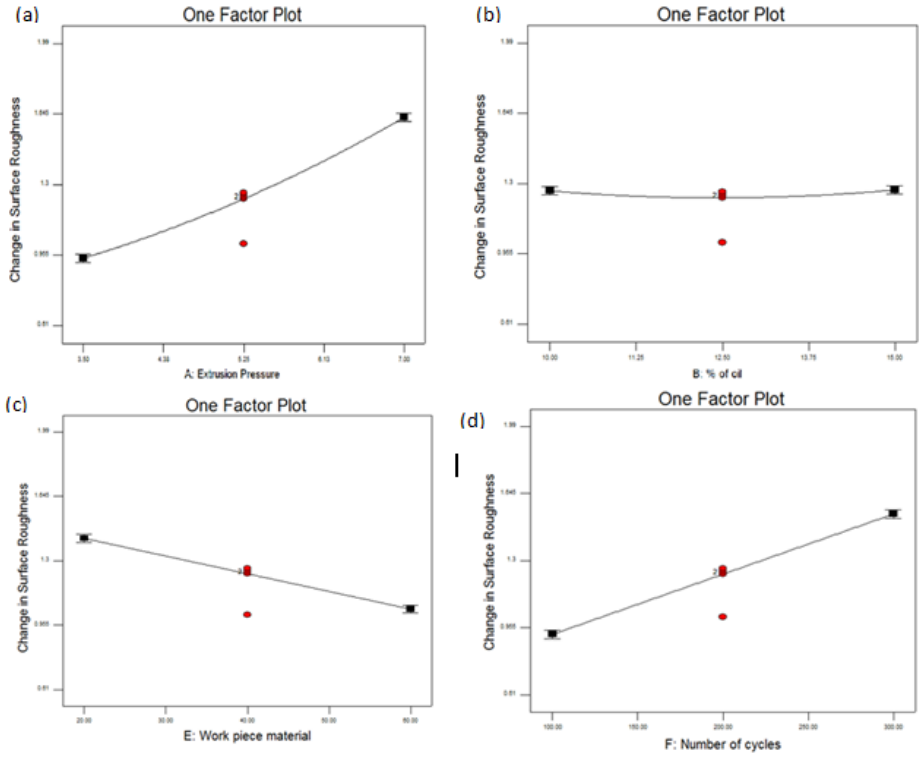

Figure 5.11: One factor plots for MRR

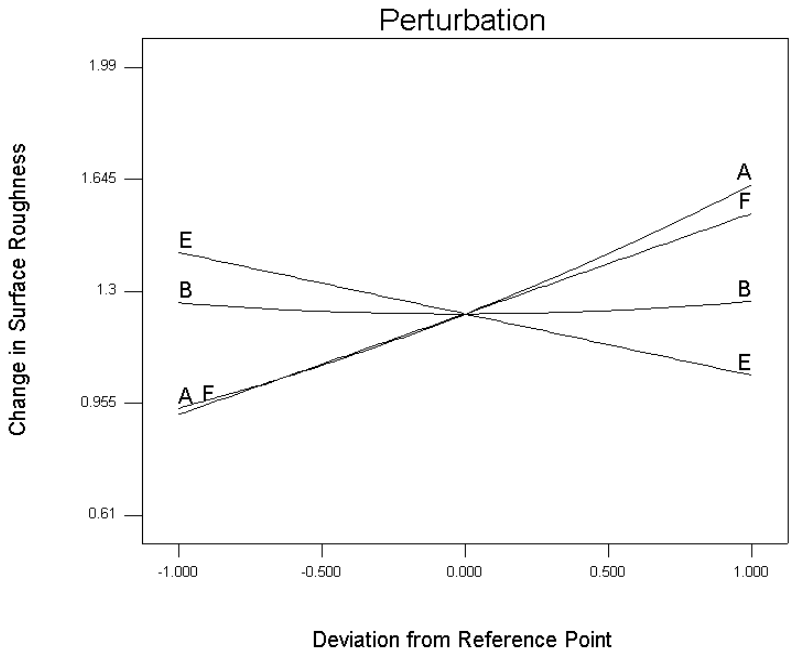

Figure 5.12: Perturbation plot for ΔRa

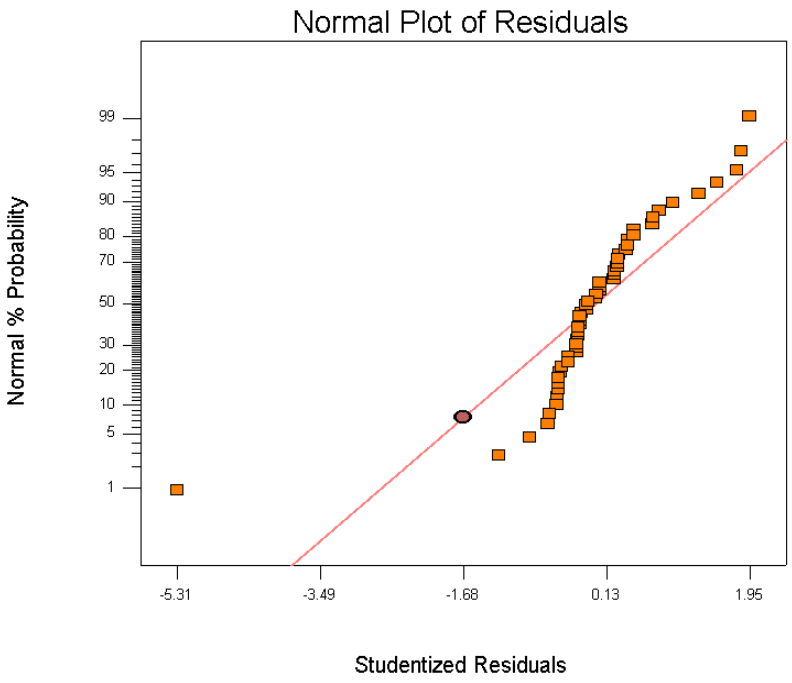

Figure 5.13: Normal probability residual plot

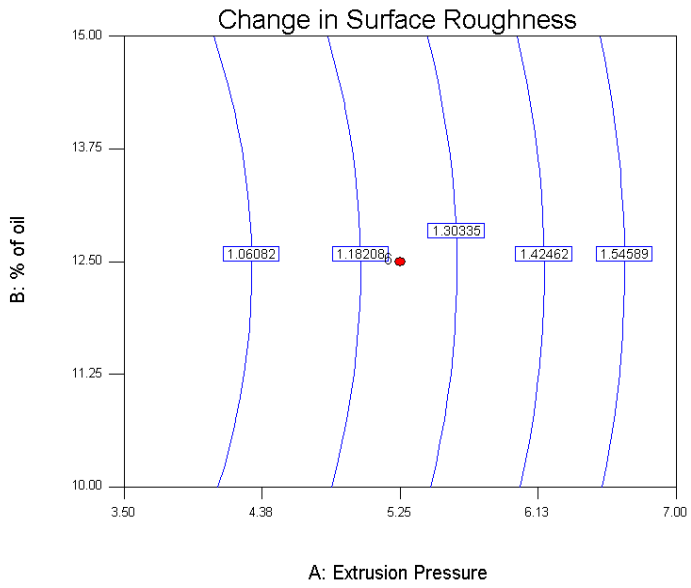

Figure 5.14: Contour plot for ΔRa

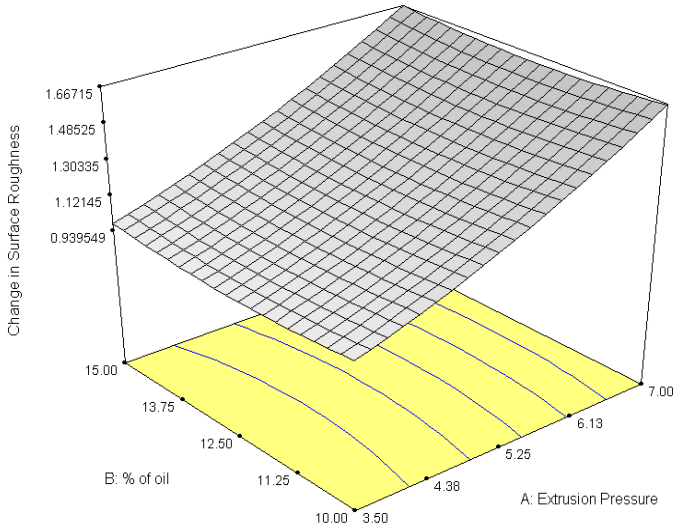

Figure 5.15: 3D plot for effect of extrusion pressure and percentage of oil on ΔRa

5.2.3 Optimization using desirability approach

Multi response optimization is done to achieve multiple objectives like obtaining higher machining rate and higher change in surface roughness. This objective can be achieved using the desirability function approach. The general approach is to first convert each response (Yi) into an individual desirability function (di) and varied over the range $0 \leq di \leq 1$ (Kumar et al., 2013). Where if the response Yi is at its goal, then (di=1). The response is outside an acceptable region (di=0). The simultaneous objective function is a geometric mean of all transformed responses:

$$D= (d_1 \times d_2 \times \ldots\ldots\ldots\ldots\ldots\ldots d_n)^{1/n} \quad (5.7)$$

Where n is the number of responses, here it is 2.

Importance (I) can be given to response parameters. Importance satisfies $0 < Ii < 1$ and

$$I_1 + I_2 + \ldots + I_n = 1$$

$$D = (d_1^{I1} \times d_2^{I2} \times \ldots\ldots\ldots\ldots\ldots\ldots d_n^{In})^{1/n} \quad (5.8)$$

The parameters must be assigned a "Goal" from the choices "none", "maximum", "minimum", "target", or "in range".

The meanings of goal parameters are:

Maximum:

$d_i = 0$ if response < low value

$1 \leq d_i \leq 0$ as response varies from low to high

$d_i = 1$ if response > high value

Minimum:

di = 1 if response < low value

$1 \geq d\,I \geq 0$ as response varies from low to high

di = 0 if response > high value

Target:

di = 0 if response < low value

$0 \leq di \leq 1$ as response varies from low to target

$1 \geq di \geq 0$ as response varies from target to high

di = 0 if response > high value

Range:

di = 0 if response < low value

di = 1 as response varies from low to high

di = 0 if response > high value

The di for "in range" are included in the product of the desirability function D, but are not counted in determining "n": $D = (\pi d_i)^{1/n}$. Constraints of process parameters along with goal and importance assigned are as discussed in chapter 3. Table 5.10 shows 25 solutions of combinations of process parameters that give high desirability.

Table 5.10: Optimal solutions for MRR and ΔRa

No.	Extrusion Pressure (MPa)	Percentage of oil	Mesh number	Conc. of abrasives	Work piece material	Number of cycles	MRR (µg/s)	Change in Surface Roughness (µm)	Desirability
1	6.93	14.38	197.90	56.31	20.25	269.34	7.691	2.035	1
2	6.72	10.83	120.47	58.69	24.00	289.58	7.784	2.002	1
3	6.90	14.50	147.55	56.65	20.52	272.98	7.731	2.039	1
4	6.64	10.64	165.92	51.52	20.04	298.75	8.059	2.052	1
5	6.97	11.35	128.21	55.24	20.27	266.39	7.634	2.020	1
6	6.72	14.85	105.12	57.09	26.70	291.02	7.725	2.000	1
7	6.87	14.94	146.91	59.98	21.21	269.94	7.671	2.027	1
8	6.98	10.32	107.69	59.83	27.42	289.63	7.707	2.047	1
9	6.78	14.61	105.58	52.03	22.43	292.36	7.913	2.051	1
10	6.52	14.84	217.74	50.07	20.14	288.71	7.907	2.006	1
11	6.93	10.52	178.06	56.18	28.03	293.44	7.727	2.035	1
12	6.53	12.07	160.29	56.56	20.49	295.80	7.951	1.994	1
13	6.98	13.67	102.43	51.07	31.85	297.50	7.631	2.011	1
14	6.98	14.41	204.57	53.32	22.23	291.74	7.935	2.097	1
15	6.89	11.58	214.81	59.76	21.11	292.56	7.953	2.070	1
16	6.84	14.99	206.96	55.85	33.18	299.73	7.636	1.999	1
17	6.94	11.24	197.41	50.65	27.84	299.19	7.804	2.043	1
18	6.83	14.09	105.31	59.79	27.07	290.19	7.692	2.002	1
19	6.64	12.86	218.17	57.69	20.59	296.27	7.978	2.021	1
20	6.50	11.15	102.22	59.82	20.02	293.80	7.945	1.993	1
21	6.83	12.82	189.44	59.44	22.17	287.51	7.825	2.025	1
22	6.85	10.78	130.02	54.06	31.73	298.63	7.645	1.990	1
23	6.93	14.91	104.39	59.01	26.85	285.33	7.670	2.033	1
24	6.97	10.41	176.38	56.35	22.94	297.25	7.988	2.106	1
25	6.73	14.88	210.46	58.97	25.21	284.51	7.690	1.996	1

Bar histogram plot for overall desirability has been shown in fig. 5.16. Contour plot for desirability is shown in fig. 5.17. It can be observed from figures 5.16 and 5.17 that overall desirability for response parameters is 1.

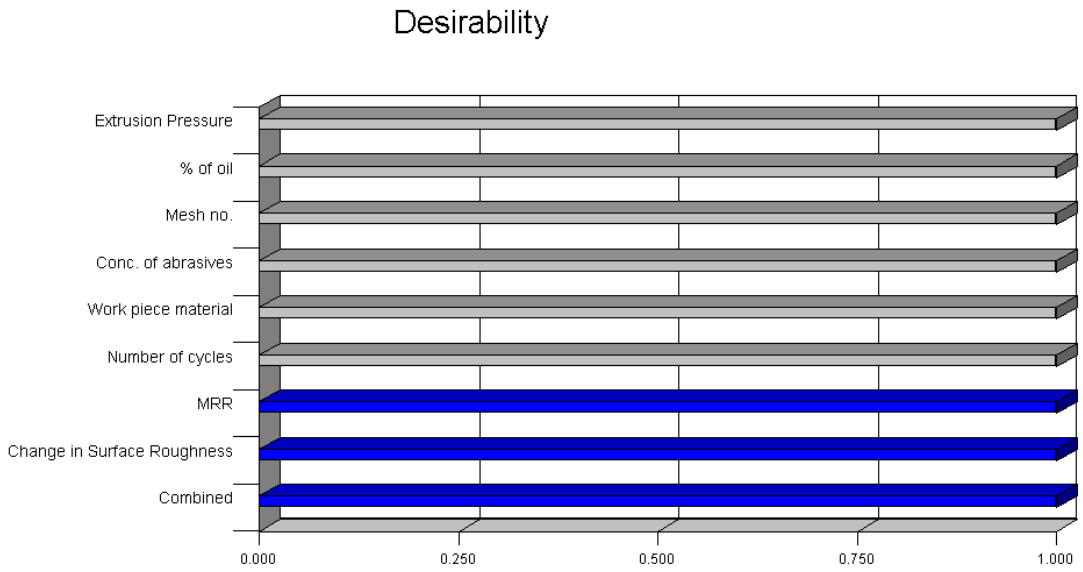

Figure 5.16: Bar histogram plot for desirability

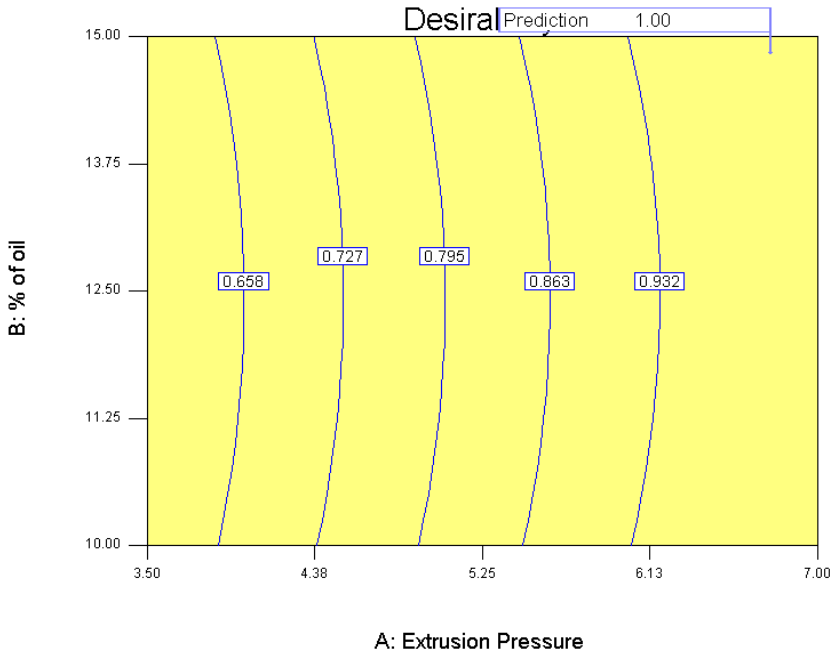

Figure 5.17: Contour plot for desirability

Ramp plot for overall desirability is shown in fig. 5.18. From ramp plot, MRR and ΔRa values at optimum combination of process parameters can be read. It can be observed that desirability is 1.

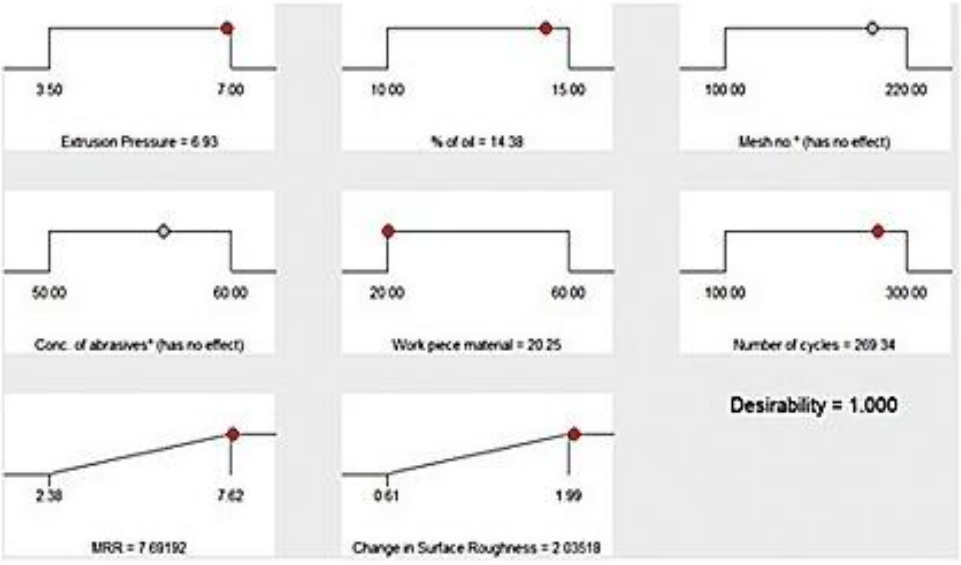

Figure 5.18: Ramp plot for overall desirability

5.3 ANALYSIS OF MICROSTRUCTURE

To study the surface topography of finished and unfinished work pieces, they were examined and analyzed by applying scanning electron microscopy and XRD technique.

5.3.1 Scanning electron microscopy

After finishing by AFM, specimens were examined using scanning electron microscope (SEM model: Super Dry II -Hitachi S-3400 N). Micrographs are taken at x1500 and x1000 magnification. It can be clearly observed from SEM micrographs in figures 5.19, 5.21 and 5.23 that there are surface irregularities before finishing the surfaces using AFM (Jabbaripour et al., 2012), as these surfaces are cut/ machined by EDM process. There are certain defects on surface like crater and cracks as shown in 5.19; recast layers, globules of debris as shown in 5.21 (Kumar et al., 2013); voids, spherical particles etc as shown in 5.23. SEM analysis shows clearly that surface topography has been significantly improved after finishing with AFM as shown in figure 5.20, 5.22 and 5.24. After finishing the surfaces with AFM process, irregularities have been dissolved/ eroded as shown in figures. Recast layer formed by EDM is removed, and

various defects formed by EDM have been abraded by finishing method using AFM. It can also be observed from figures 5.20 and 5.24 that some abrasive particles got embedded on the work piece surface.

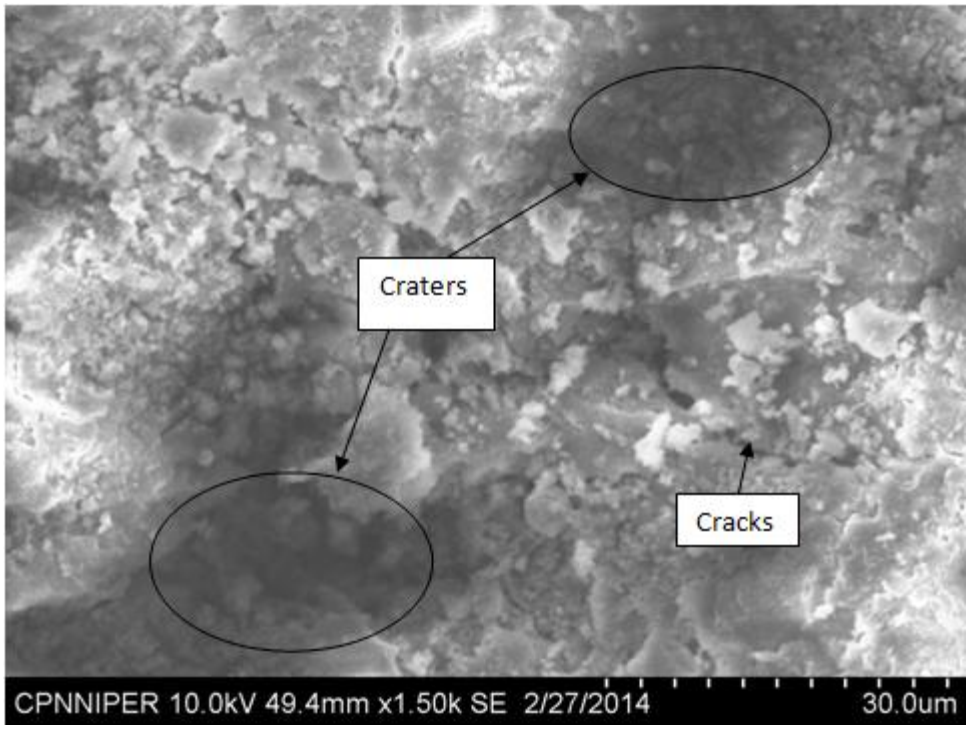

Figure 5.19: SEM micrographs of 20 % SiC in SiC/Al Composite (Before finishing)

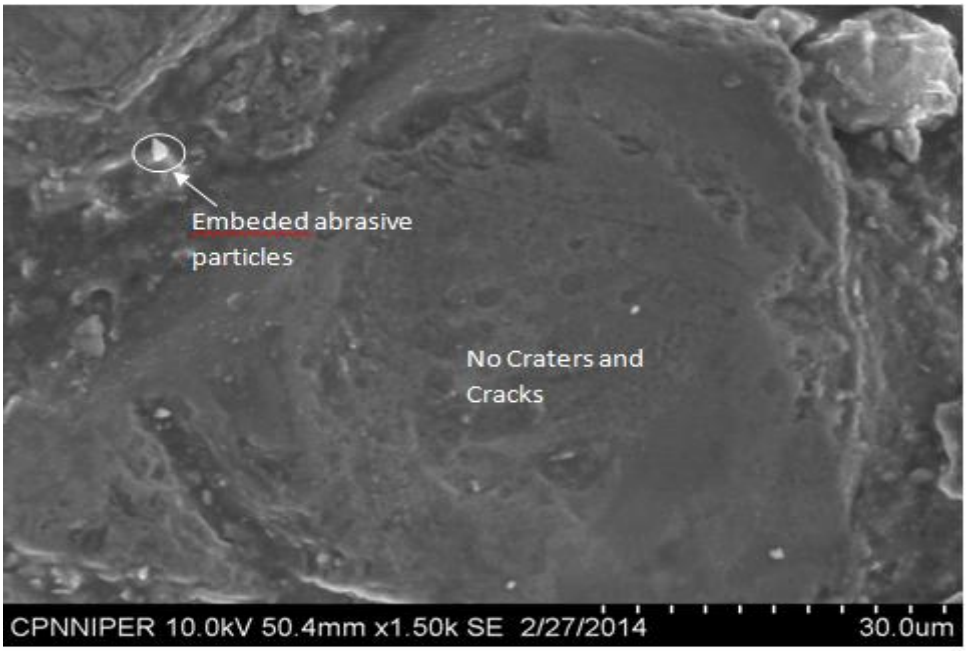

Figure 5.20: SEM micrograph of 20 % SiC in SiC/Al Composite (After finishing)

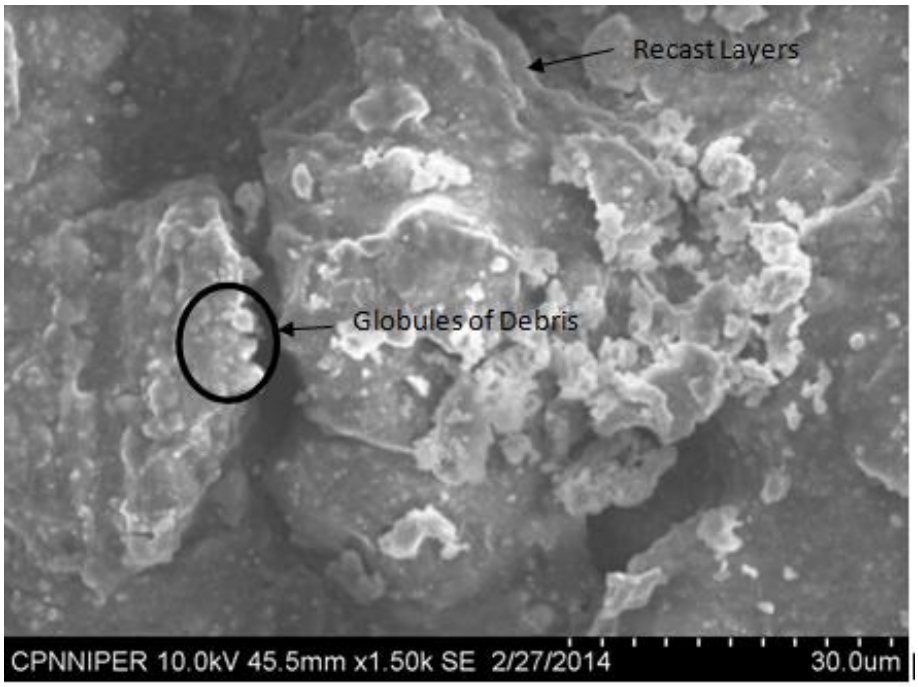

Figure 5.21: SEM micrograph of 40 % SiC in SiC/Al Composite (Before finishing)

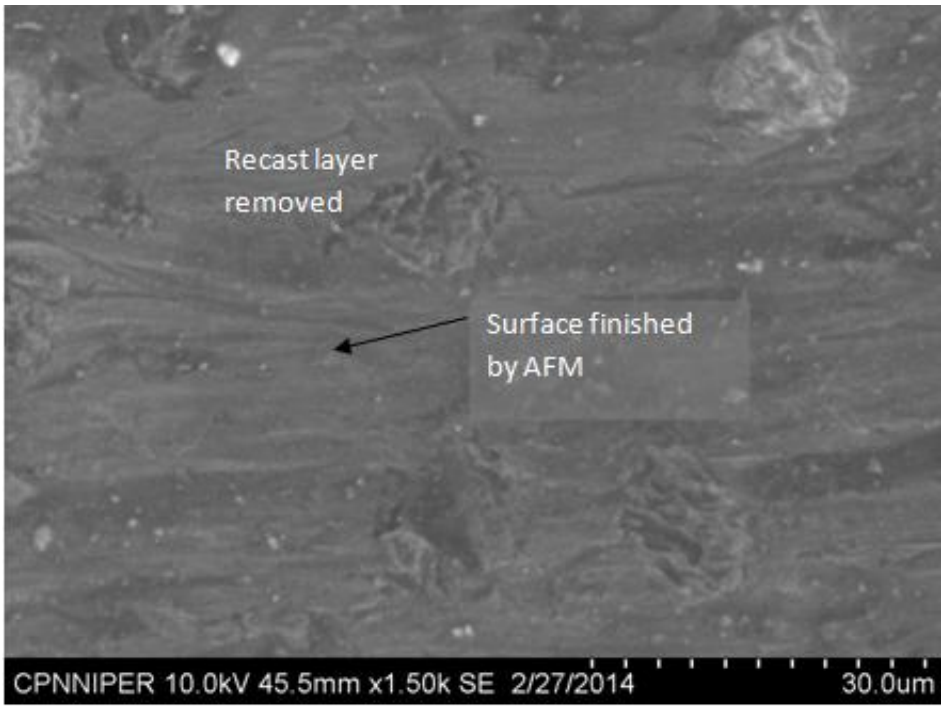

Figure 5.22: SEM micrograph of 40 % SiC in SiC/Al Composite (After finishing)

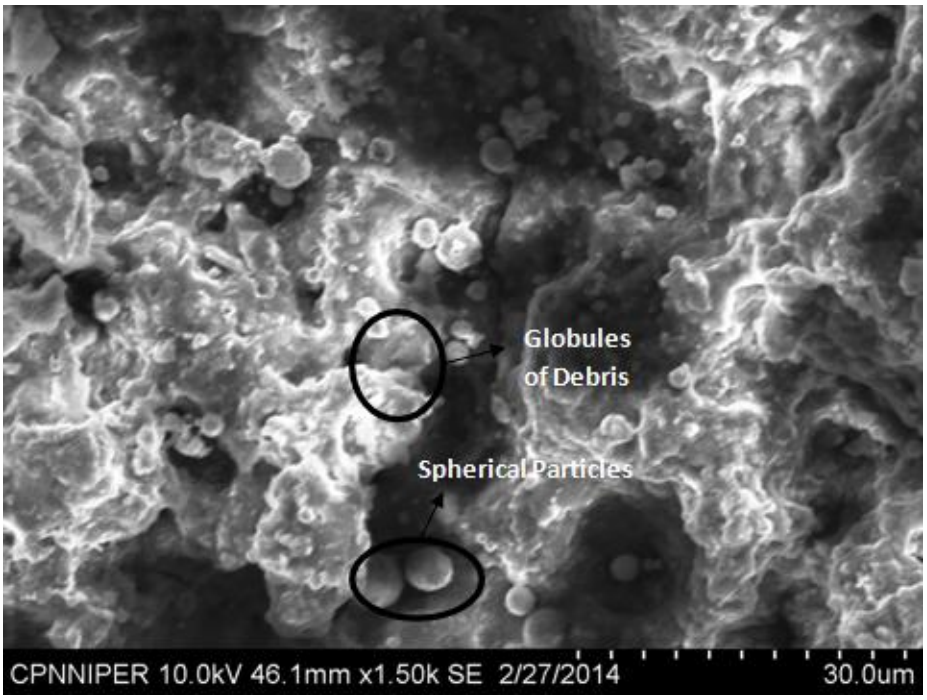

Figure 5.23: SEM micrograph of 60 % SiC in SiC/Al Composite (Before finishing)

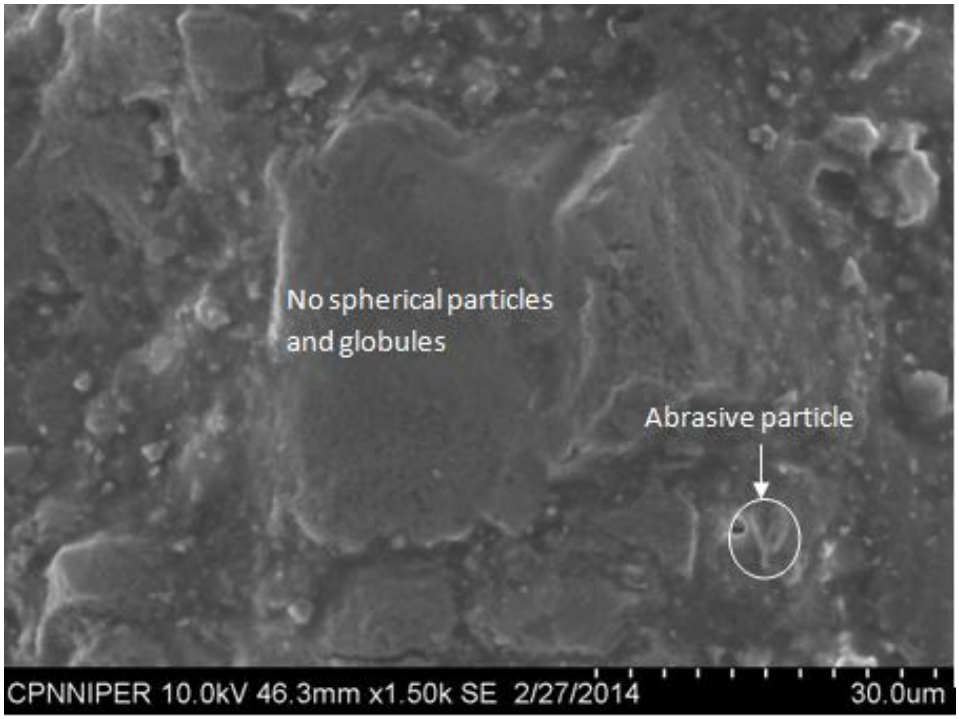

Figure 5.24: SEM micrograph of 60 % SiC in SiC/Al Composite (After finishing)

Some specimens have been also examined at 1000 magnification (50 μm), similar results are found as shown in figures 5.25-5.30. It can be clearly observed from figure 5.25 that there are

cracks and spherical particles on the surface as the surface has been cut using wire EDM. It has been demonstrated in fig 5.26 that cracks and spherical particles have been removed after finishing the surface with abrasive flow machining.

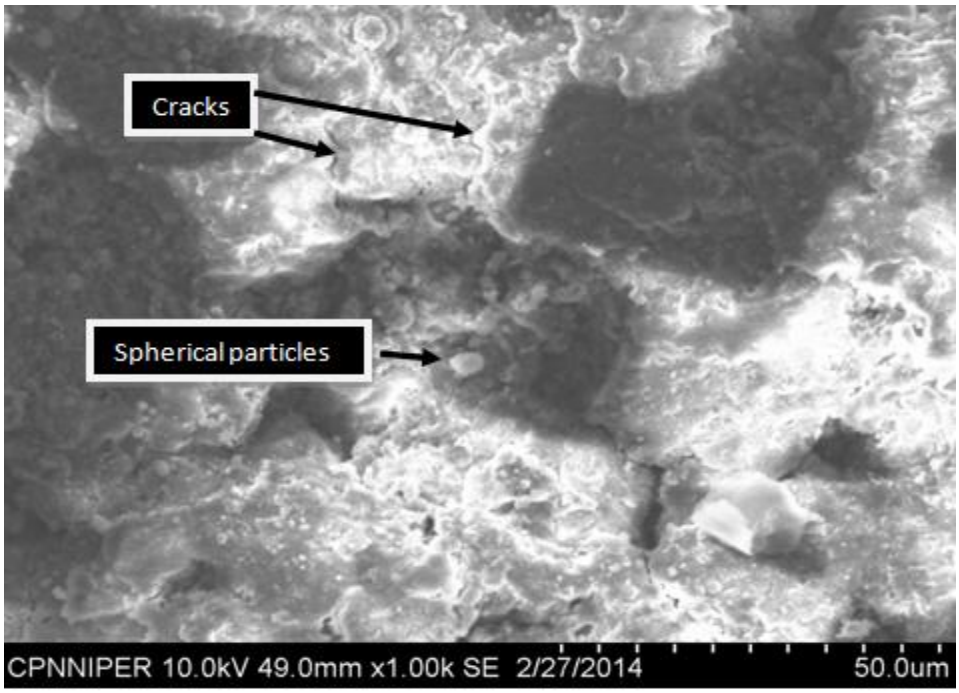

Figure 5.25: SEM micrographs of 20 % SiC in SiC/Al Composite (Before finishing)

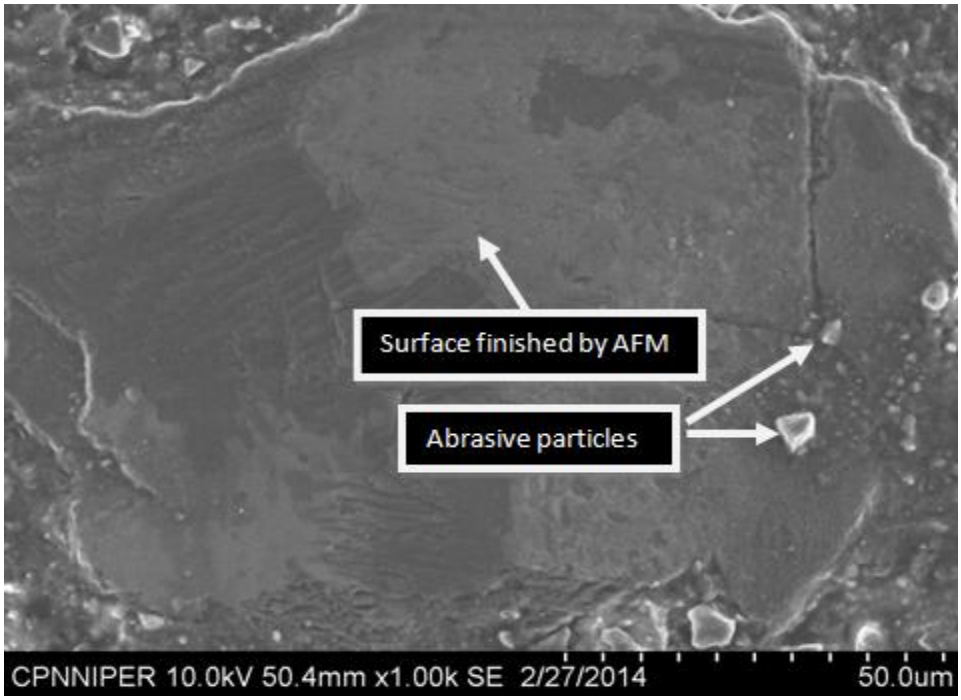

Figure 5.26: SEM micrograph of 20 % SiC in SiC/Al Composite (After finishing)

Some other defects produced during cutting of work pieces using wire EDM such as globules of debris and recast layer are shown in fig. 5.27. These defects have been removed using abrasive flow machining as shown in fig. 5.28.

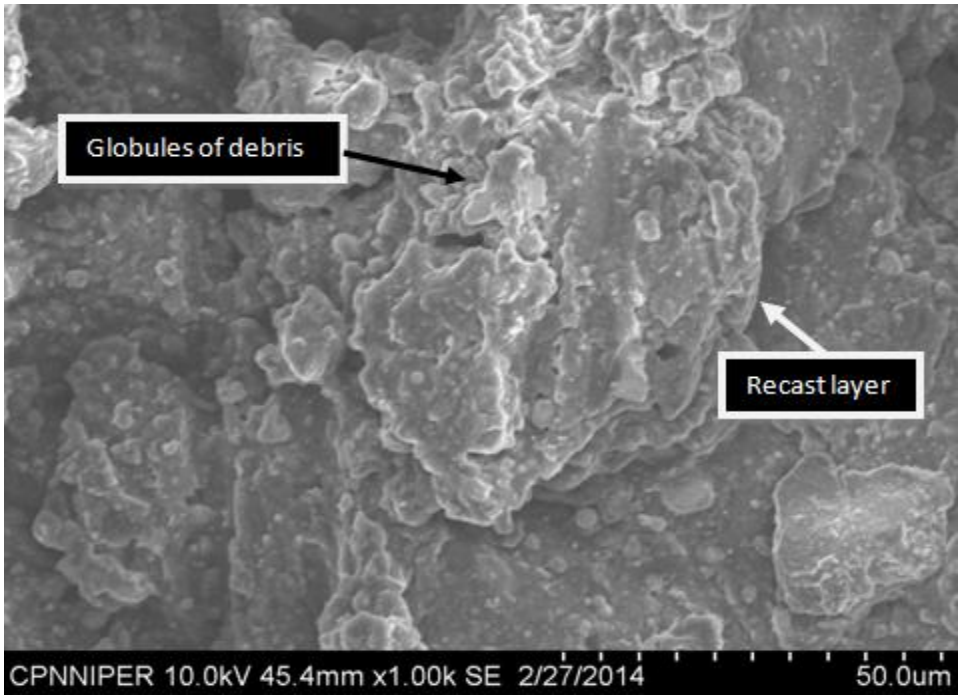

Figure 5.27: SEM micrographs of 40 % SiC in SiC/Al Composite (Before finishing)

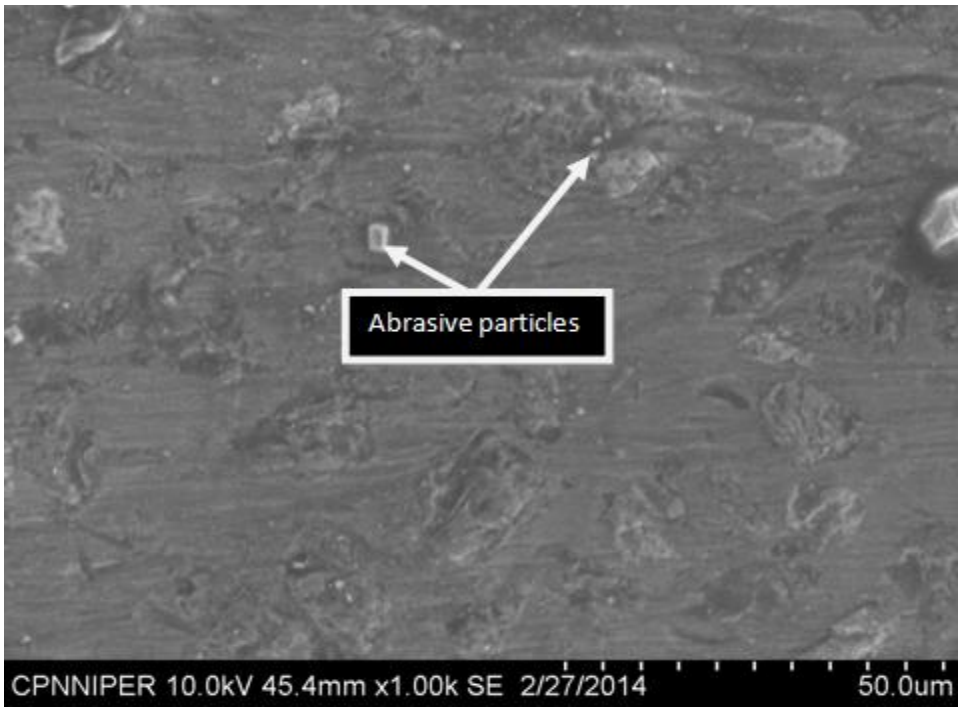

Figure 5.28: SEM micrograph of 40 % SiC in SiC/Al Composite (After finishing)

Pock marks and craters are other defects found on the surface as shown in fig. 5.29, which have been removed by finishing with AFM as shown in fig. 5.30.

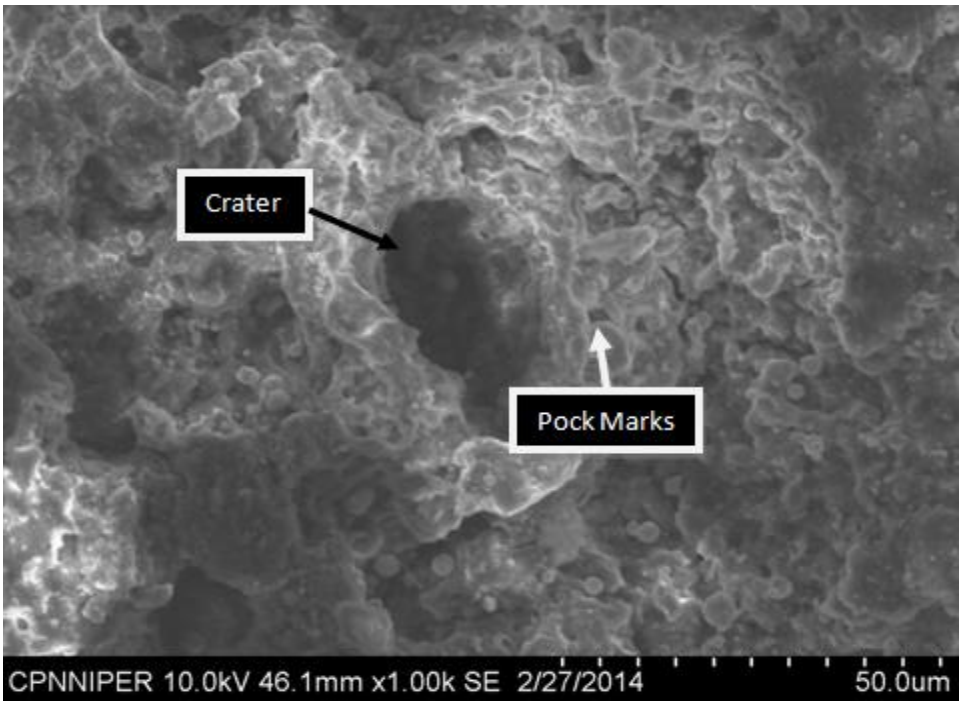

Figure 5.29: SEM micrographs of 60 % SiC in SiC/Al Composite (Before finishing)

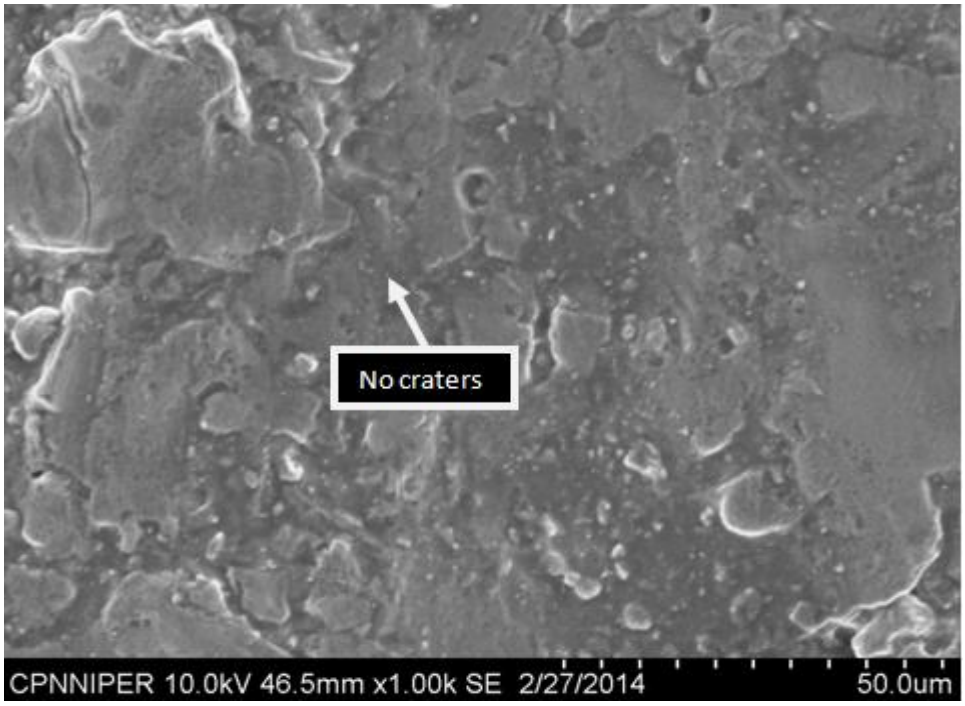

Figure 5.30: SEM micrograph of 60 % SiC in SiC/Al Composite (After finishing)

5.3.2 XRD analysis

XRD analysis of work pieces was also done using X'Pert High Score software. The XRD profiles of Al/SiC composites are shown in figures 5.31, 5.32 and 5.33. It has been examined that most of the peaks are Al and SiC peaks. Highest peak is observed for SiC at 2Θ value of 35.713 (for 20% SiC), 39.091 (for 40% SiC) and 79.207 (for 60% SiC). FeSi was also detected at 36.278. High peak for LiAl5O8 was detected at 2Θ value of 79.207. Some compounds with fewer score have been ignored. Further analysis of some more specimens was also done. Peaks of Al and Si compounds were examined in XRD profiles shown in figures 5.34, 5.35 and 5.36. The highest peak of 20 % SiC in Al/SiC was observed for Al_2SiO_5 at 2Θ value 38.084. The highest peak of 40 % SiC in Al/SiC was observed for $LiAlSiO_4$ at 2Θ value 39.23. The highest peak of 60 % SiC in Al/SiC was observed for Al_2 (SiO_4) O at 2Θ value 48.46. Compounds like Al_2SiO_5, $LiAlSiO_4$, Mn_3Al_2 $(SiO_4)_3$, Si_3Al, Fe_3Al_2 $(SiO_4)_3$, $LiAlSi_3O_8$ were found on finished surfaces.

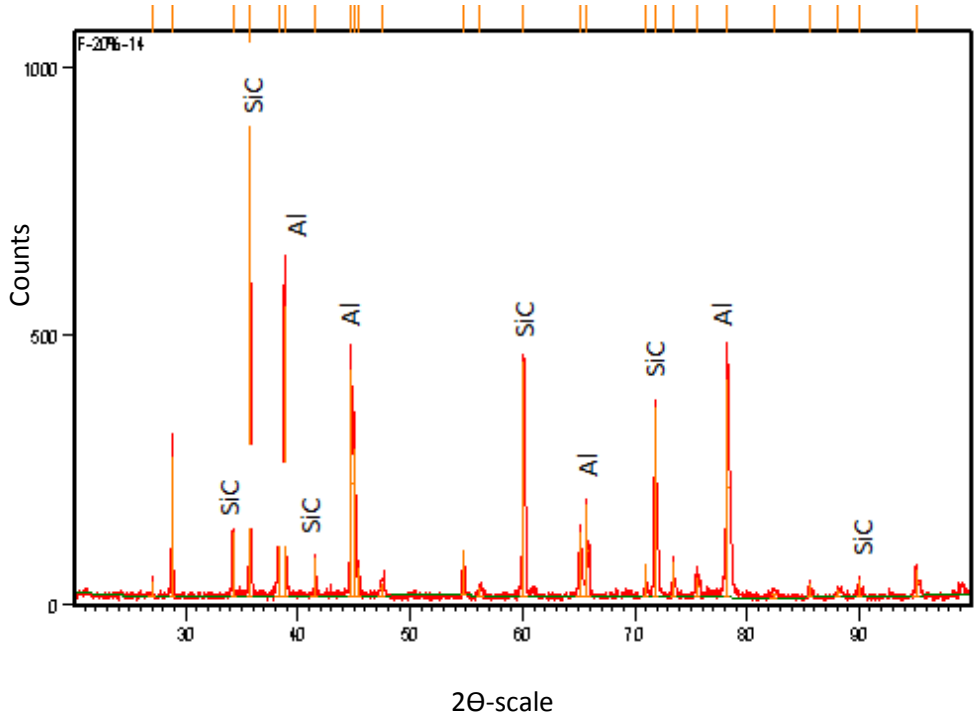

Figure 5.31: XRD for finished work piece with 20% SiC

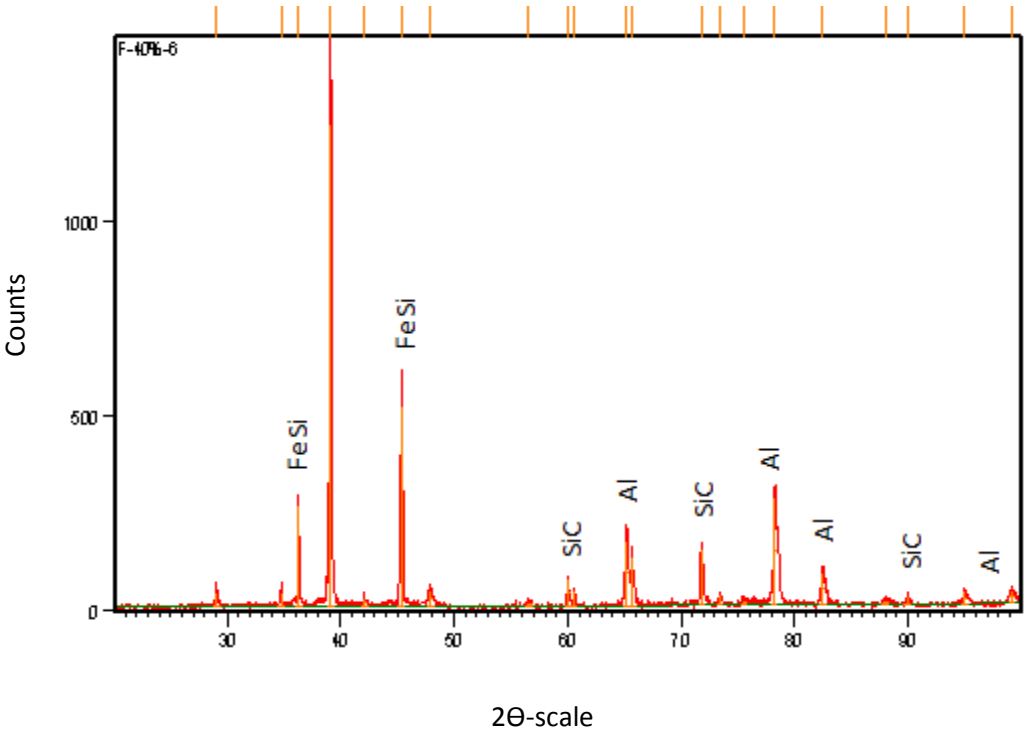

Figure 5.32: XRD for finished work piece with 40% SiC

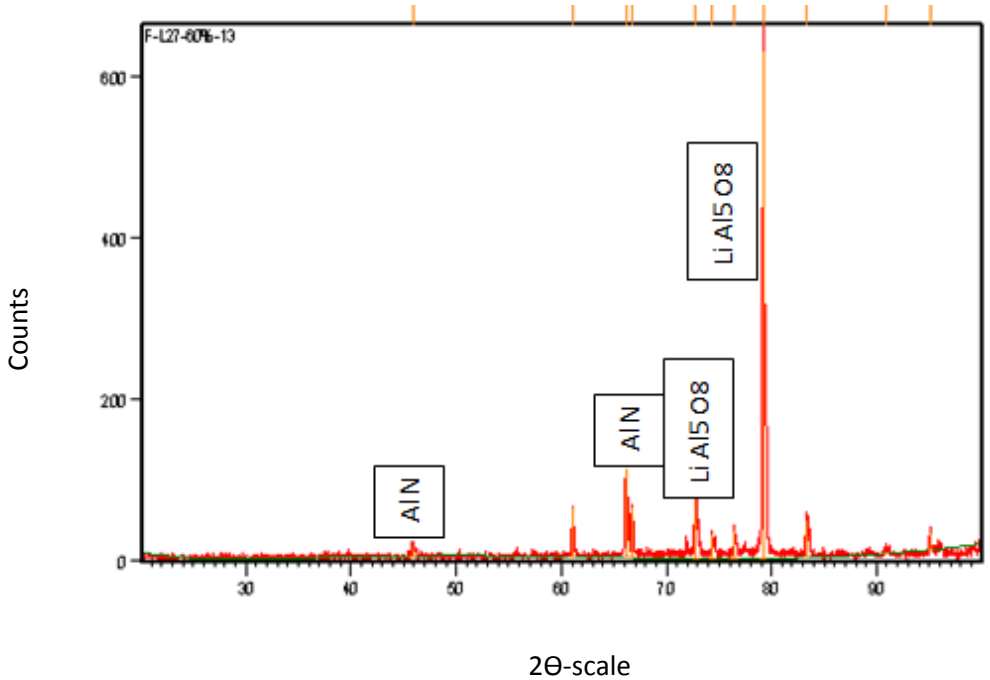

Figure 5.33: XRD for finished work piece with 60% SiC

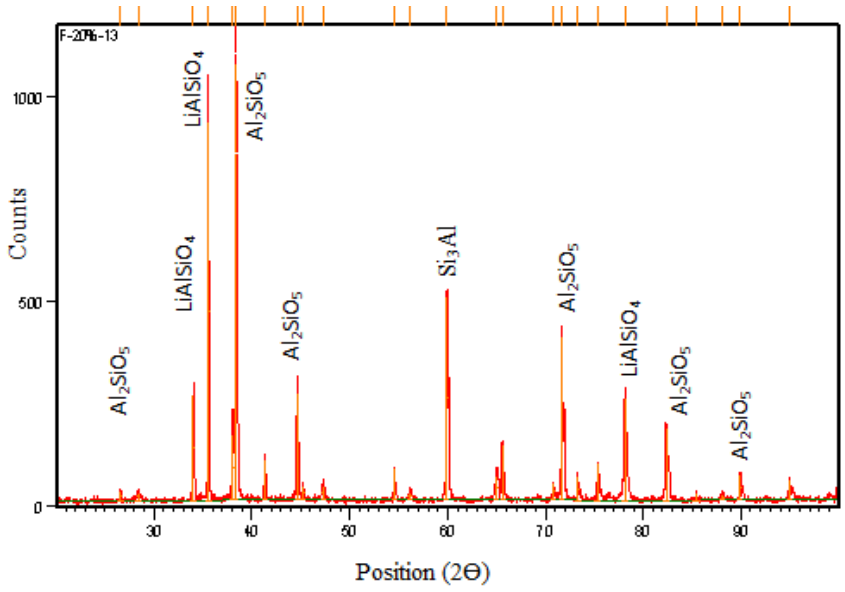

Figure 5.34: XRD for finished work piece with 20% SiC

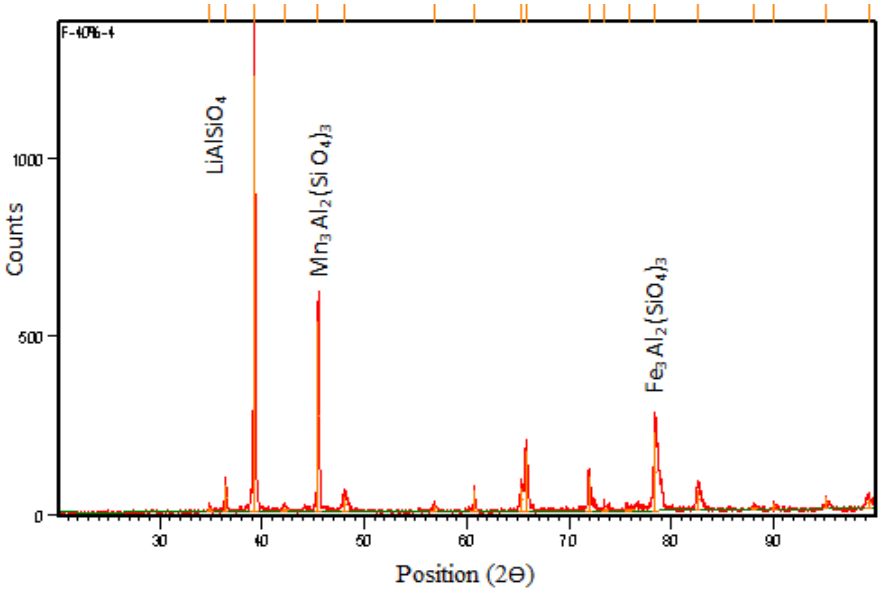

Figure 5.35: XRD for finished work piece with 40% SiC

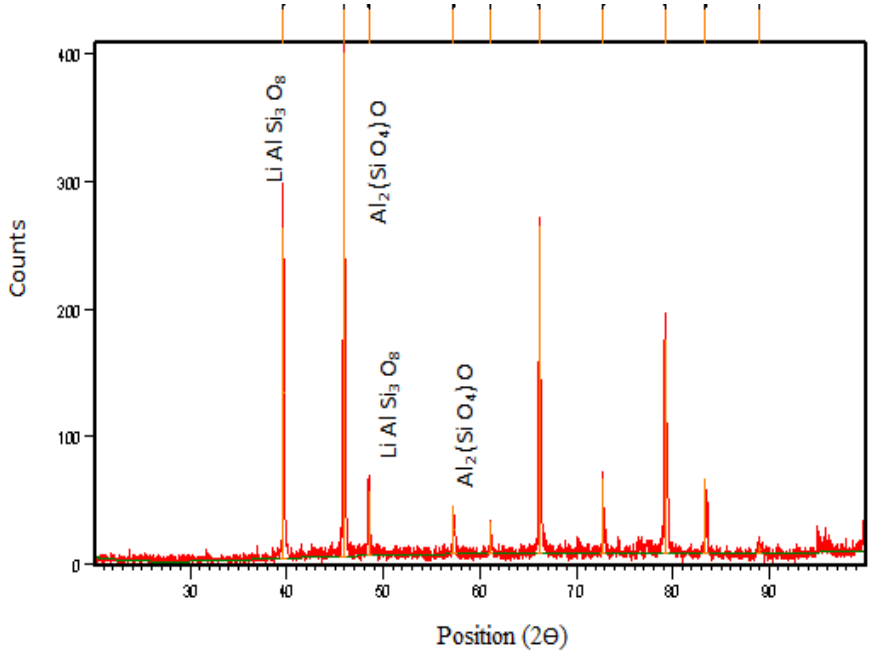

Figure 5.36: XRD for finished work piece with 60% SiC

5.4 MATHEMATICAL MODELING

In the present work a Finite Element Method (FEM) based mathematical model of material removal has been proposed for AFM process. The purpose of the proposed model is to understand the abrasive action during the AFM process. In abrasive flow machining, the abrasion between the abrasive particle and surface to be machined can be divided into microploughing and microcutting (Jain et al., 1999). Microploughing due to a single pass of one abrasive particle may not detach any material from the work piece surface. Material can be removed due to repeated action of single or more abrasive particles. Ploughing may take place because of microfatigue occurring due to repeated passage of particles. Pure microcutting removes chip equal to the volume of the grooves produced. Microploughing and microcutting are the dominant processes for ductile materials while microcutting becomes important for brittle materials. In composite materials also mechanism of material removal is same as discussed above.

An analytical model is proposed which depicts the path of abrasive particles in the work piece passage during AFM. The attempt has been made to develop a model that is as complete as possible and address many aspects of the process such as media velocity, etc. A standard ANSYS package version 15 with FLUENT software has been employed to model the problem

and to evaluate the rate and velocity of impingement and stress distributions in the work piece material. This model depicts the path of an abrasive particle, as it moves in the work piece passage. The simulated path of the movement of the abrasive particles in the work piece, passage can be used for predicting the angle of impingement and the striking velocity of abrasive particles on the work piece surface.

5.4.1 Governing equations

The mathematical representation of the medium in the AFM process includes basic equations of continuity and momentum equations

$$\partial ui/\partial xi = 0 \quad (5.9)$$

$$\rho[(\partial ui\ \partial ui)/\partial xi] = \partial\rho/\partial xi + \partial/\partial xj\ [\mu(\gamma(\partial ui/\partial xj + \partial ui/\partial xi\ )\ )\ ] \quad (5.10)$$

Where ρ is the density of fluid, p is the pressure and u_i is the flow velocity.

In the above equation the shear rate can be derived from the rate of deformation tensor, Dij .

Dij , can be given as (Maity and Tripathy, 2015):

$$\gamma = \sqrt{2\ \text{Dij Dij}} \quad (5.11)$$

Where

$$\text{Dij} = 1/2\ (\partial ui/\partial xj + \partial ui/\partial xi\ ) \quad (5.12)$$

The normal force can be calculated as:

$$F_n = \sigma_{rad} \times A \quad (5.13)$$

$$\text{Where} \qquad A = \pi \times (d_g)^2 \quad (5.14)$$

Where d_g is the diameter of the abrasive particle and σ_{rad} is the radial stress acting on the work piece surface.

The following assumptions were made:

- Incompressible fluid is considered
- Heat generated is not considered
- Quasi steady state is assumed in the study

The indentation diameter can be calculated as:

$$di = \sqrt{dg2} - (\text{dg-} (f_n \times 2 \times 10^{-6}) / (9.81 \times H_{BHN} \pi d_g))^2 \quad (5.15)$$

Where H_{BHN} = Brinell hardness number of the work piece material = 480

The depth of indentation can be calculated as:

$$t = \frac{dg}{2} - \frac{1}{2}\sqrt{\text{d2g} - di2} \quad (5.16)$$

During shearing of the work piece surface the axial shear force F_a is acting, which must be greater than the reaction force on the abrasive particle by the work piece material at the projected area.

The projected area can be calculated as:

$$A' = \frac{d2g}{4} \sin^{-1} \frac{2\sqrt{\text{t (dg}-t)}}{dg} - \sqrt{t(dg-t)(\frac{dg}{2}-t)} \quad (5.17)$$

The volume of the material can be calculated as:

$$V_a = A' \times L_i$$

$$= \frac{d2g}{4} \sin^{-1} \frac{2\sqrt{\text{t (dg}-t)}}{dg} - \sqrt{t(dg-t)(\frac{dg}{2}-t)} \times L_i \quad (5.18)$$

Where L_i is the contact length of the grain, with the work piece.

$$L_i = r \times \theta \quad (5.19)$$

Where θ, is the contact angle of abrasive grain on the work piece.

θ can be calculated as $\cos \theta = d_i / r$ (5.20)

Work piece geometry is defined as shown in fig. 5.37. Different boundaries for work piece have been defined as inlet, outlet, axis and wall as shown in fig. 5.38. It can be clearly observed from fig. 5.39, that strain is the maximum at the wall; hence material is removed from the walls. This is because sharp velocity gradient at the walls. Velocity distribution is demonstrated in fig. 5.40. Velocity is the maximum at the centre and decreases towards the wall. This is because of the

viscosity of the media. Fig. 5.41 illustrates pressure distribution in the work piece. Pressure remains constant up to fixture, and then decreases till exit of the work piece.

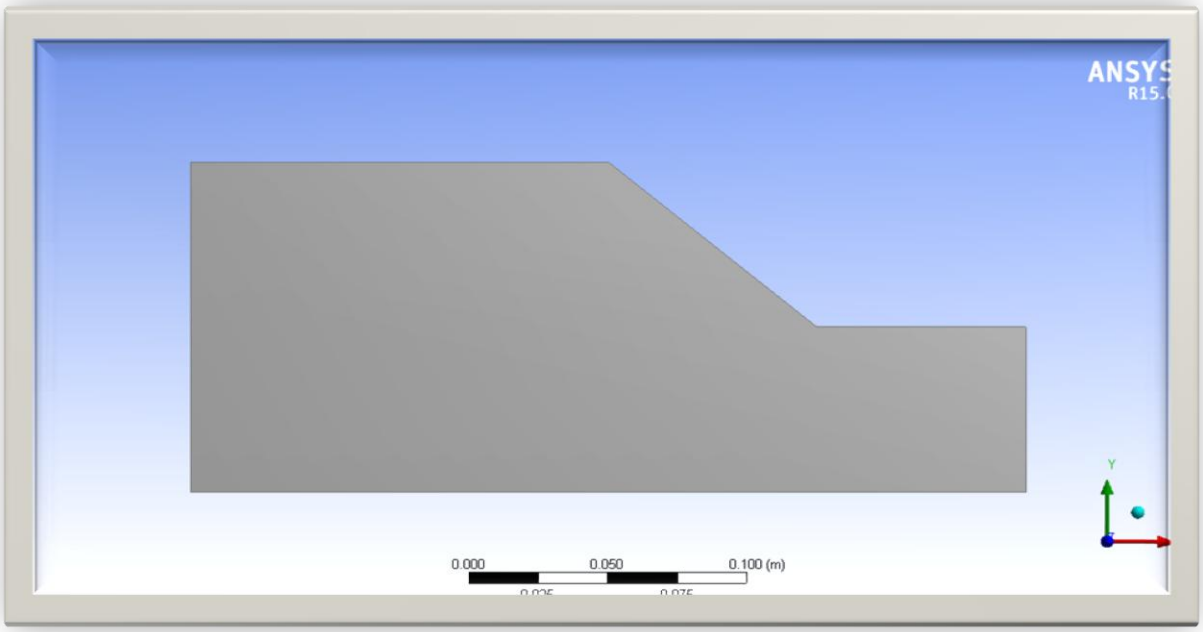

Figure 5.37: Geometry of work piece

Figure 5.38: Boundary conditions as inlet, outlet, axis and wall of work piece

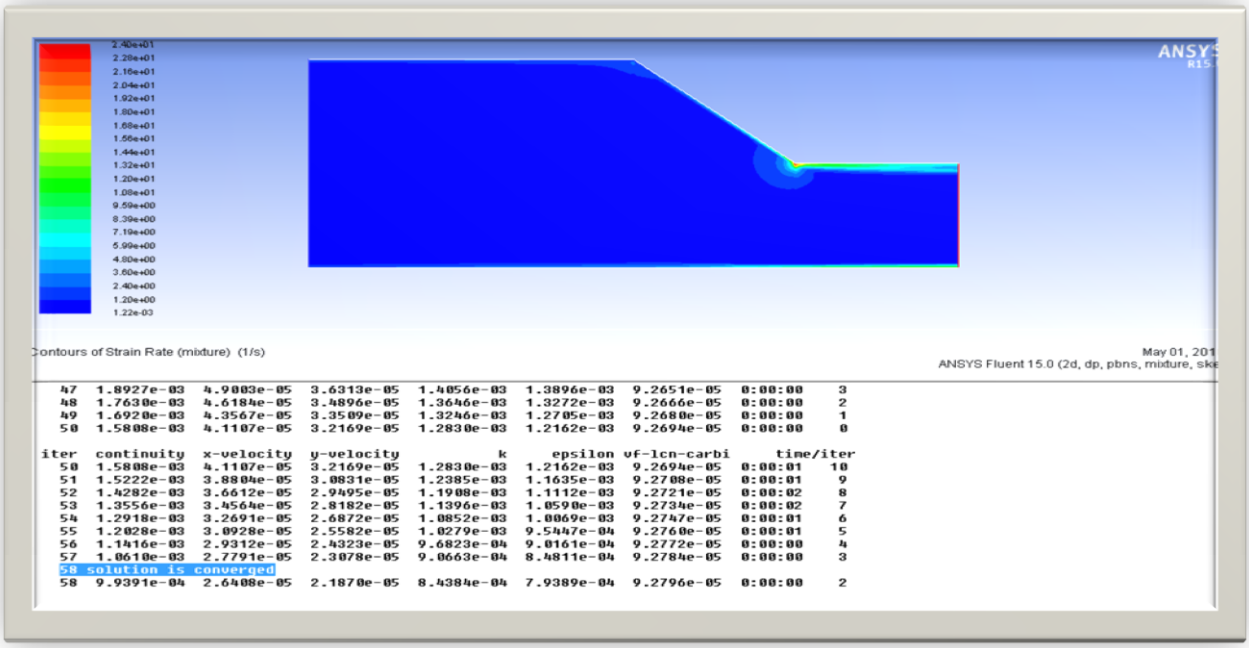


```
   47  1.8927e-03  4.9003e-05  3.6313e-05  1.4056e-03  1.3896e-03  9.2651e-05  0:00:00    3
   48  1.7630e-03  4.6184e-05  3.4896e-05  1.3646e-03  1.3272e-03  9.2666e-05  0:00:00    2
   49  1.6920e-03  4.3567e-05  3.3509e-05  1.3246e-03  1.2705e-03  9.2680e-05  0:00:00    1
   50  1.5808e-03  4.1107e-05  3.2169e-05  1.2830e-03  1.2162e-03  9.2694e-05  0:00:00    0

iter  continuity  x-velocity  y-velocity           k     epsilon vf-lcn-carbi     time/iter
   50  1.5808e-03  4.1107e-05  3.2169e-05  1.2830e-03  1.2162e-03  9.2694e-05  0:00:01   10
   51  1.5222e-03  3.8804e-05  3.0831e-05  1.2385e-03  1.1635e-03  9.2708e-05  0:00:01    9
   52  1.4282e-03  3.6612e-05  2.9495e-05  1.1908e-03  1.1112e-03  9.2721e-05  0:00:02    8
   53  1.3556e-03  3.4564e-05  2.8182e-05  1.1396e-03  1.0590e-03  9.2734e-05  0:00:02    7
   54  1.2918e-03  3.2691e-05  2.6872e-05  1.0852e-03  1.0069e-03  9.2747e-05  0:00:01    6
   55  1.2028e-03  3.0928e-05  2.5582e-05  1.0279e-03  9.5447e-04  9.2760e-05  0:00:01    5
   56  1.1416e-03  2.9312e-05  2.4323e-05  9.6823e-04  9.0161e-04  9.2772e-05  0:00:00    4
   57  1.0610e-03  2.7791e-05  2.3078e-05  9.0663e-04  8.4811e-04  9.2784e-05  0:00:00    3
solution is converged
   58  9.9391e-04  2.6408e-05  2.1870e-05  8.4384e-04  7.9389e-04  9.2796e-05  0:00:00    2
```

Figure 5.39: Strain distribution

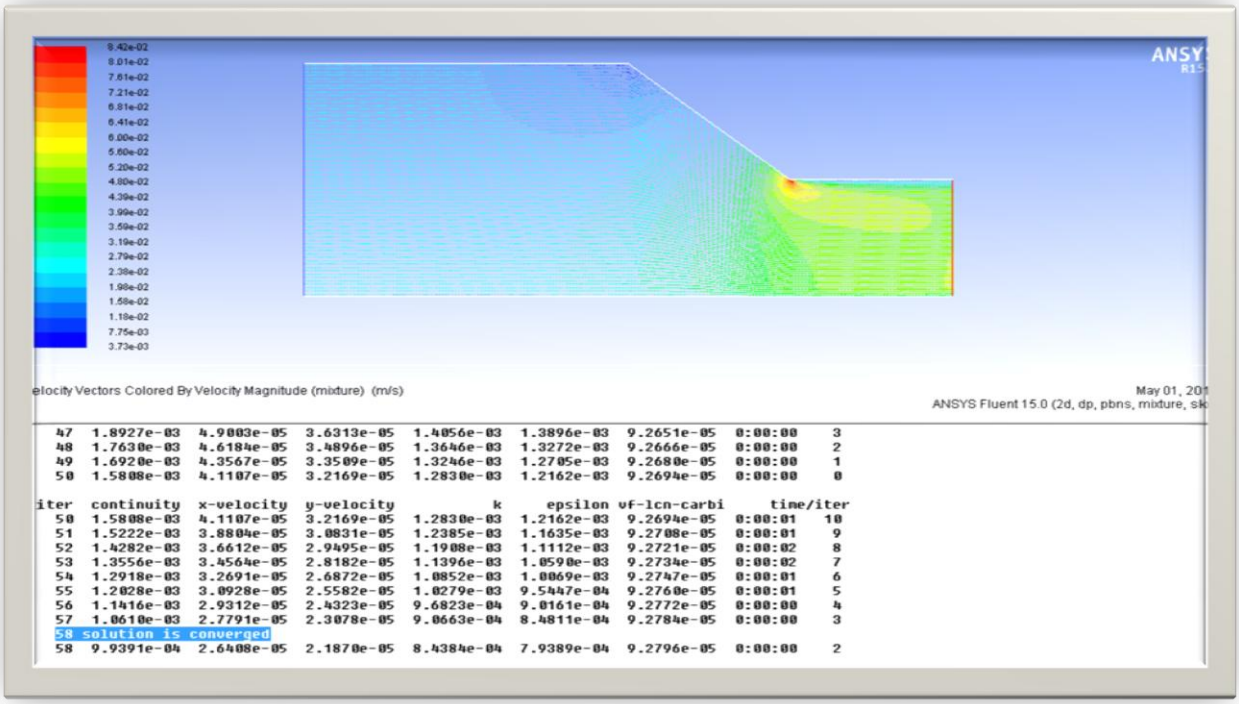


```
   47  1.8927e-03  4.9003e-05  3.6313e-05  1.4056e-03  1.3896e-03  9.2651e-05  0:00:00    3
   48  1.7630e-03  4.6184e-05  3.4896e-05  1.3646e-03  1.3272e-03  9.2666e-05  0:00:00    2
   49  1.6920e-03  4.3567e-05  3.3509e-05  1.3246e-03  1.2705e-03  9.2680e-05  0:00:00    1
   50  1.5808e-03  4.1107e-05  3.2169e-05  1.2830e-03  1.2162e-03  9.2694e-05  0:00:00    0

iter  continuity  x-velocity  y-velocity           k     epsilon vf-lcn-carbi     time/iter
   50  1.5808e-03  4.1107e-05  3.2169e-05  1.2830e-03  1.2162e-03  9.2694e-05  0:00:01   10
   51  1.5222e-03  3.8804e-05  3.0831e-05  1.2385e-03  1.1635e-03  9.2708e-05  0:00:01    9
   52  1.4282e-03  3.6612e-05  2.9495e-05  1.1908e-03  1.1112e-03  9.2721e-05  0:00:02    8
   53  1.3556e-03  3.4564e-05  2.8182e-05  1.1396e-03  1.0590e-03  9.2734e-05  0:00:02    7
   54  1.2918e-03  3.2691e-05  2.6872e-05  1.0852e-03  1.0069e-03  9.2747e-05  0:00:01    6
   55  1.2028e-03  3.0928e-05  2.5582e-05  1.0279e-03  9.5447e-04  9.2760e-05  0:00:01    5
   56  1.1416e-03  2.9312e-05  2.4323e-05  9.6823e-04  9.0161e-04  9.2772e-05  0:00:00    4
   57  1.0610e-03  2.7791e-05  2.3078e-05  9.0663e-04  8.4811e-04  9.2784e-05  0:00:00    3
solution is converged
   58  9.9391e-04  2.6408e-05  2.1870e-05  8.4384e-04  7.9389e-04  9.2796e-05  0:00:00    2
```

Figure 5.40: Velocity distribution

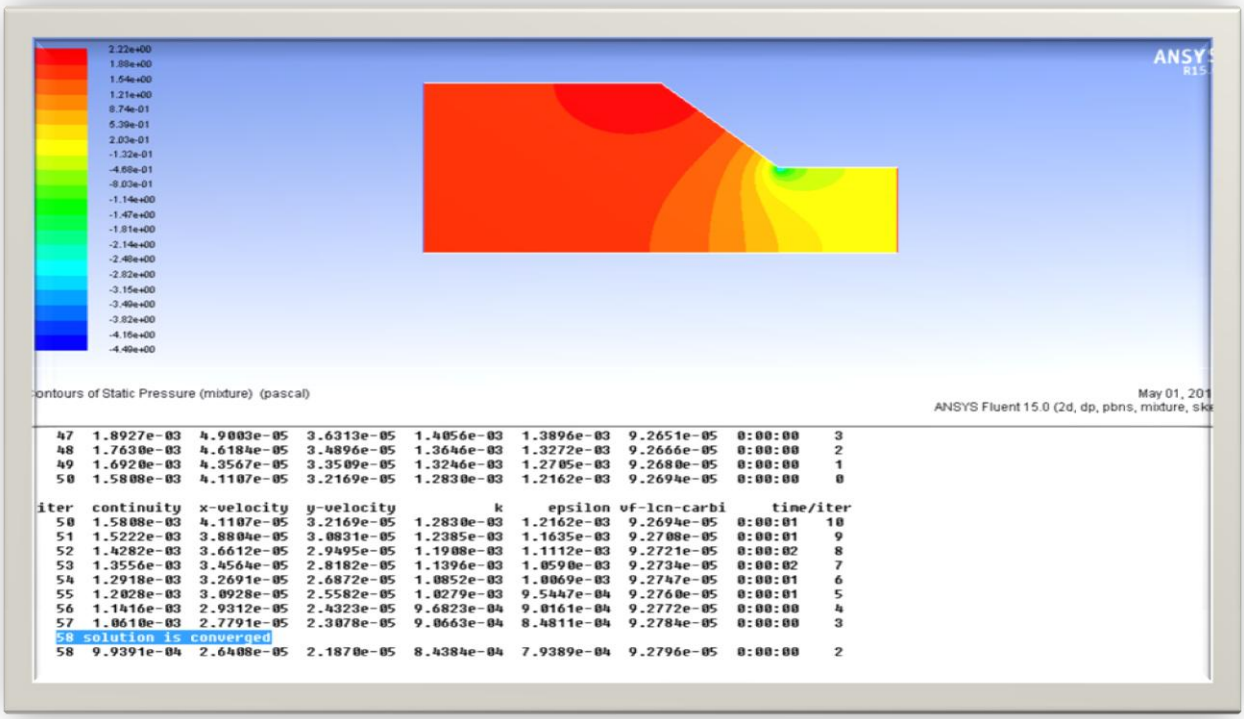


```
  47  1.8927e-03  4.9003e-05  3.6313e-05  1.4056e-03  1.3896e-03  9.2651e-05  0:00:00    3
  48  1.7630e-03  4.6184e-05  3.4896e-05  1.3646e-03  1.3272e-03  9.2666e-05  0:00:00    2
  49  1.6920e-03  4.3567e-05  3.3509e-05  1.3246e-03  1.2705e-03  9.2680e-05  0:00:00    1
  50  1.5808e-03  4.1107e-05  3.2169e-05  1.2830e-03  1.2162e-03  9.2694e-05  0:00:00    0

iter  continuity  x-velocity  y-velocity           k     epsilon vf-lcn-carbi     time/iter
  50  1.5808e-03  4.1107e-05  3.2169e-05  1.2830e-03  1.2162e-03  9.2694e-05  0:00:01   10
  51  1.5222e-03  3.8804e-05  3.0831e-05  1.2385e-03  1.1635e-03  9.2708e-05  0:00:01    9
  52  1.4282e-03  3.6612e-05  2.9495e-05  1.1908e-03  1.1112e-03  9.2721e-05  0:00:02    8
  53  1.3556e-03  3.4564e-05  2.8182e-05  1.1396e-03  1.0590e-03  9.2734e-05  0:00:02    7
  54  1.2918e-03  3.2691e-05  2.6872e-05  1.0852e-03  1.0069e-03  9.2747e-05  0:00:01    6
  55  1.2028e-03  3.0928e-05  2.5582e-05  1.0279e-03  9.5447e-04  9.2760e-05  0:00:01    5
  56  1.1416e-03  2.9312e-05  2.4323e-05  9.6823e-04  9.0161e-04  9.2772e-05  0:00:00    4
  57  1.0610e-03  2.7791e-05  2.3078e-05  9.0663e-04  8.4811e-04  9.2784e-05  0:00:00    3
solution is converged
  58  9.9391e-04  2.6408e-05  2.1870e-05  8.4384e-04  7.9389e-04  9.2796e-05  0:00:00    2
```

Figure 5.41: Pressure distribution

5.4.2 Calculation of volumetric material removal

The shear stress profile is shown in fig. 5.42. The wall shear stress is on y-axis versus position on x-axis. This plot demonstrates the radial wall shear stress, which is required to calculate volumetric material removal analytically.

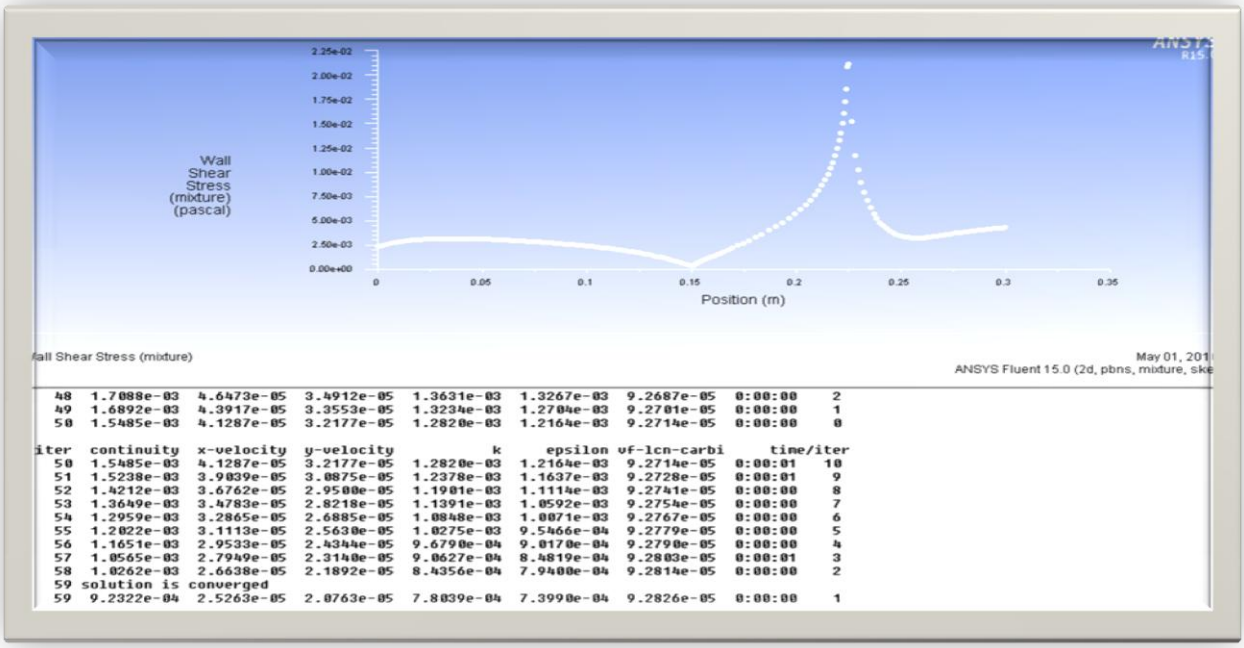


```
  48  1.7088e-03  4.6473e-05  3.4912e-05  1.3631e-03  1.3267e-03  9.2687e-05  0:00:00    2
  49  1.6892e-03  4.3917e-05  3.3553e-05  1.3234e-03  1.2704e-03  9.2701e-05  0:00:00    1
  50  1.5485e-03  4.1287e-05  3.2177e-05  1.2820e-03  1.2164e-03  9.2714e-05  0:00:00    0

iter  continuity  x-velocity  y-velocity          k     epsilon vf-lcn-carbi     time/iter
  50  1.5485e-03  4.1287e-05  3.2177e-05  1.2820e-03  1.2164e-03  9.2714e-05  0:00:01   10
  51  1.5238e-03  3.9839e-05  3.0875e-05  1.2378e-03  1.1637e-03  9.2728e-05  0:00:01    9
  52  1.4212e-03  3.6762e-05  2.9508e-05  1.1981e-03  1.1114e-03  9.2741e-05  0:00:00    8
  53  1.3649e-03  3.4783e-05  2.8218e-05  1.1391e-03  1.0592e-03  9.2754e-05  0:00:00    7
  54  1.2959e-03  3.2865e-05  2.6885e-05  1.0848e-03  1.0071e-03  9.2767e-05  0:00:00    6
  55  1.2022e-03  3.1113e-05  2.5630e-05  1.0275e-03  9.5466e-04  9.2779e-05  0:00:00    5
  56  1.1651e-03  2.9533e-05  2.4344e-05  9.6798e-04  9.0170e-04  9.2790e-05  0:00:00    4
  57  1.0565e-03  2.7949e-05  2.3140e-05  9.0627e-04  8.4819e-04  9.2803e-05  0:00:01    3
  58  1.0262e-03  2.6638e-05  2.1892e-05  8.4356e-04  7.9408e-04  9.2814e-05  0:00:00    2
  59 solution is converged
  59  9.2322e-04  2.5263e-05  2.0763e-05  7.8039e-04  7.3998e-04  9.2826e-05  0:00:00    1
```

Figure 5.42: Shear stress profile

From CFD simulation (fig. 5.42) we get, radial stress as:

$$\sigma_r = 0.0225 \text{ Pa}$$

$$F_n = 3.8 \times 10^{-10} \text{ N}$$

Now the indentation diameter can be calculated by putting the value of F_n in equation no. 5.13

$$d_i = 75 \times 10^{-6} \text{ m}$$

Putting the value of d_i in equation number 5.14, we get

Depth of indentation, $t = 3 \times 10^{-9}$ m

Then projected area can be calculated as putting the value t, in equation no. 5.15

$$A' = 9.79 \times 10^{-12} \text{ m}^2$$

Also from the equation number 5.18 we get (Shakti and Maity, 2013),

$$2\theta = 176.09$$

Also, we know $2\theta = L_i / r$

So $Li = 1.2386 \times 10^{-5}$ m

Volumetric material removal by a single grain can be calculated as:

$$V_a = A' \times L_i$$

$$= 1.212 \times 10^{-16}\ m^3$$

5.5 VALIDATION OF FEM MODEL

We have calculated volumetric removal by a single grain, Va = 1.212×10^{-16} m^3

Time taken in one cycle = 20 s

MRR (by a single grain) = 1.212×10^{-16} /20 = 0.606×10^{-17} m^3/s

Experimental value of volumetric MRR = 5.17 μg/s

Density of work piece material = 3.00 g/cm^3

Volumetric material removal $= \frac{5.17\ \mu g/s}{3.00\ g/cm^3}$

$= \frac{5.17\ \mu g/s}{3.00 \times 10^{12}\ \mu g/m^3}$

$= 1.72 \times 10^{-12} m^3/s$

Radius of abrasive particle used (spherical) = 37 μm

Volume of abrasive particle used $= \frac{4}{3} \times 3.14 \times \left(37\ (10^{-4})\right)^3$

$= 2.1 \times 10^{-7}\ cm^3$

Volume of media taken for experiment = 200 cm^3

Volume for 50 % concentration of abrasives = 100 cm^3

Number of striking abrasive particles possible $= \frac{100}{2.1 \times 10^{-7}}$

$= 0.47 \times 10^5$(Approx.)

Hence volume of material removed by single grain $= \frac{1.72 \times 10^{-12} m^3/s}{0.47 \times 10^5}$

$= 3.65 \times 10^{-17} m^3/s$

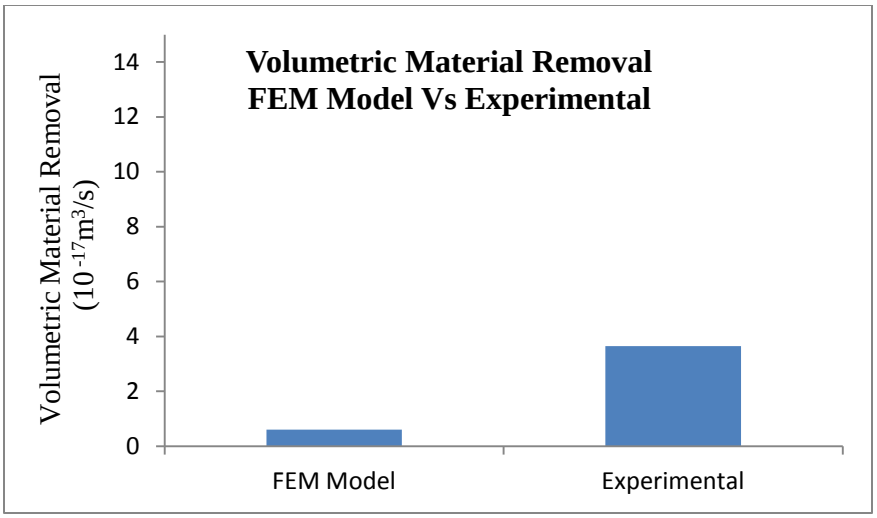

Figure 5.43 Validation of FEM model with experimental results

As shown in figure number 5.43 volumetric material removal by a single grain calculated by FEM model is in good agreement with experimental volumetric material removal, FEM model is validated with experimental results.

CHAPTER 06

CONCLUSIONS

In the present work, Al/SiC MMCs with different percentage of SiC (20, 40 and 60 percent) were machined by electrical discharge machining process, and then surface finishing was done using abrasive flow machining. Experiments have been performed on the experimental set up designed and developed in the laboratory. Experimental investigation has been done for input parameters like extrusion pressure, percentage of oil in media, mesh number of grit, concentration of abrasives, work piece material and number of cycles and response parameters as MRR, ΔRa and surface topography. Analysis and optimization of process parameters has been done using Taguchi method and response surface methodology. Work specimens were examined by applying scanning electron microscopy and XRD analysis. Based on the experimental investigation and microstructure analysis, some of the conclusions are presented as below:

1. Extrusion pressure was observed as the most significant factor for MRR and ΔRa. MRR increases with an increase in extrusion pressure as axial and radial stresses increases with increase in extrusion pressure. ΔRa also increases with an increase in extrusion pressure.
2. It can be observed from ANOVA that change in percentage of oil in media has very little effect on response parameters. MRR plot shows that MRR decreases with increase in percentage of oil in the media as viscosity of media decreases with increase in percentage of oil.
3. Mesh number of abrasives and concentration of abrasives have been observed as non significant parameters as shown in ANOVA table and main effect plots.
4. Work piece material (20, 40 & 60 percent SiC in SiC/Al MMC) is also a significant factor. MRR first decreases then increases with the percentage increase in SiC, because hardness of work material increases with percentage increase of SiC in aluminium. ΔRa increases with the percentage increase in SiC in the work piece material.
5. MRR increases with an increase in the number of cycles. ΔRa also increases with an increase in the number of cycles. ΔRa is more initially and less with further increase in the number of cycles. This is because initially there are more peaks and valleys which dissolve at a fast rate initially.

6. The material removal rate was observed from 1.91 to 9.33 µ g/s. From confirmation experiments, optimum MRR is found to be 8.81µg/s and predicted value is 8.59µg/s. The percentage error between predicted and experimental value is 2.49%. This shows that experimental results are in good agreement with theoretical results.
7. ΔRa was observed from 0.40 to 1.70 µm. Optimum ΔRa from confirmation experiment is found to be 1.72 µm and predicted value is 1.63µm. The percentage error between predicted and experimental value is 5.23 %.
8. It can also be observed from response surface methodology analysis that extrusion pressure (19.91 % contribution), work piece material (23.30 % contribution) and number of cycles (54.47) were found to be the most important factors affecting the material removal rate. Percentage change of oil in the media has very little effect on material removal rate.
9. Extrusion pressure (46.41 % contribution), work piece material (14 % contribution) and number of cycles (37.45 % contribution) were found to be the most important factors affecting the change in surface roughness. Percentage change of oil in the media has very small effect on change in surface roughness.
10. The material removal rate varied from 2.38 to 7.62 µg/s and ΔRa varied from 0.62 to 1.97 µm.
11. The error between the predicted value and experimental values of MRR is 5.64% and ΔRa is 4.24 %. This confirms validation of results for predicted values and experimental values.
12. From a multi objective optimization using desirability approach, the optimum combination of parameters is observed as extrusion pressure 6.93 MPa, percentage of oil in media 14.38, grit size 197 (mesh number), concentration of abrasives 56 %, work piece material 20 % SiC and the number of cycles 270.
13. It is clear from SEM that surface defects produced while cutting the work pieces using an EDM process such as cracks, crater, recast layer; globules of debris, spherical particles, pock marks etc. have been removed by AFM process. Surface roughness has been also improved.
14. Compounds like SiC, Al, FeSi, AlN and LiAlO8 have been observed on the finished surface through XRD analysis using X'Pert High Score software.

15. Analysis of abrasive flow machining has been done using FEM. Then by getting the outputs from the FLUENT software of ANSYS 15.0 and putting these values in the equation, MRR has been calculated.

1. Antony, Design of experiments for engineers and scientists, Butterworth and Heinman, USA, 2003.
2. Bahre D., Brunnet H. and Swat M., Investigation of one-way abrasive flow machining and in-process measurement of axial forces, Procedia CIRP 1, 2012, 419 – 424.
3. Basavarajappa S., Chandramohan G., et al., Application of Taguchi Technique to Study Dry-sliding Wear Behaviour of Metal Matrix Composites, Materials and Design, 28, 2007, 1393-1398.
4. Bhondwe K.L., Yadava V. and Kathiresan G., Finite element prediction of material removal rate due to electro-chemical spark machining", International Journal of Machine Tools and Manufacture, 46, 2006, 1699–1706.
5. Box P. and Behnken D., Technometrics, 1960, Taylor & Francis, United Kingdom.
6. Brar B. S., Walia R. S. and Singh V. P., State of art abrasive flow machining, National Conference on Advancements and Futuristic Trends in Mechanical and Materials Engineering, 2010.
7. Brar B.S., Walia R.S., Singh V.P. and Sharma M., A Robust Helical Abrasive Flow Machining (HLX-AFM) Process**.** Journal of the Institution of Engineers (India): Series C, 94, 2013, 21-29.
8. Cherian J. and Dr Issac J. M., Effect of process variables in Abrasive Flow Machining, International Journal of Emerging Technology and Advanced Engineering (ISSN 2250-2459, ISO 9001:2008 Certified Journal, 3(2), 2013.
9. Dabade U. and Joshi S., Analysis of chip formation mechanism in machining of Al/SiCp metal matrix composites, Journal of Materials Processing Technology, 209, 2009, 4704-4710.
10. Das M., Jain V. K. and Ghoshdastidar P. S., Fluid flow analysis of magnetorheological abrasive flow finishing (MRAFF) process, International Journal of Machine Tools & Manufacture, 48, 2008, 415–426.

11. Das M., Jain V.K. and Ghoshdastidar P.S., The Out-of-Roundness of the Internal Surfaces of Stainless Steel Tubes Finished by the Rotational–Magnetorheological Abrasive Flow Finishing Process, Materials and manufacturing Processes, 26 (8), 2011, 1073-1084.
12. Derringer G., Suich R., Simultaneous optimization of several response variables, J Qual Technol, 12, 1980, 214–219.
13. Dubey A. and Yadava V., Multi-objective optimisation of laser beam cutting process, Optics & Laser Technology, 40, 2008, 562–570.
14. El-Hofy H. A.-G, Advanced Machining Processes, McGraw-Hill, Production Engineering Department, Alexandria University, Egypt.
15. Fang L., Zhao J., Li B. and Sun K., Movement patterns of ellipsoidal particle in abrasive flow machining, Journal of Materials Processing Technology, 209, 2009 6048–6056.
16. Fang L., Zhao J., Sun K., Zheng D. and Ma D., Temperature as sensitive monitor for efficiency of work in abrasive flow machining, wear, 266, 2008, 678–687.
17. Ferreira S.L., Bruns R.E., Ferreira H.S., et al., Box–Behnken design: an alternative for the optimization of analytical methods, Anal. Chim. Acta, 597, 2007, 179–186.
18. Garanayak S. R. and Maity K. P., CFD analysis and optimization of Abrasive Flow Machining, ME thesis, NIT Rourkela, 2013.
19. Ghosh R., Sarkar R. and Paul S., Development of machinable hydroxyapatite-lanthanum phosphate composite for biomedical applications, materials and design, 106, 2016, 161-169.
20. Gorana V.K, Jain V.K. and Lal G.K., Prediction of surface roughness during abrasive flow machining, International Journal of Advanced Manufacturing Technology, 2006, 258–267.
21. Gorana V.K., Jain V. K. and Lal G. K., Forces prediction during material deformation in abrasive flow machining, wear, 260, 2006, 128–139.
22. Gorana V.K., Jain V.K.and Lal G.K., Experimental investigation into cutting forces and active grain density during abrasive flow machining, Int J Mach Tool Maunuf , 44, 2003, 201–211.

23. Gunaraj V. and Murugan N., Application of response surface methodologies for predicting weld base quality in submerged arc welding of pipes, Journal of Materials Processing Technology, 88, 1999, 266–275.
24. Gurgel A. G., Sales W. F., Barcellos C.S. de., Bonney J. and Ezugwu E.O., An element-free Galerkin method approach for estimating sensitivity of machined surface parameters, International Journal of Machine Tools & Manufacture, 46, 2006, 1637–1642.
25. Howard M. and Cheng K., An integrated systematic investigation of the process variables on surface generation in abrasive flow machining of titanium alloy 6Al4V, Proc I MechE, Part B: J Eng Manuf, 228(11), 2014, 1419–1431.
26. Jabbaripour B., Sadeghi M. H., Faridvand S. and Shabgard M.R., Investigating the Effects of EDM Parameters on Surface Integrity, MRR and TWR in Machining of Ti–6Al–4V. Machining Science Technology: An International Journal 2012, 16,419–444.
27. Jain N. K. and Jain V.K., Modeling of material removal in mechanical type advanced machining processes: a state-of-art review, International Journal of Machine Tools & Manufacture 41, 2001, 1573–1635.
28. Jain R.K and Jain V.K., Optimum selection of machining conditions in abrasive flow machining using neural network, Journal of Materials Processing Technology, 108, 2000, 62-67.
29. Jain R.K and Jain V.K., Stochastic simulation of active grain density in abrasive flow machining, Journal of Materials Processing Technology, 152, 2003, 17–22.
30. Jain R.K. and Jain V.K., Specific energy and temperature determination in abrasive flow machining process, International Journal of Machine Tools & Manufacture 41, 2001, 1689–1704.
31. Jain R.K., Jain V.K. and Dixit P.M., Modeling of material removal and surface roughness in abrasive flow machining process, International Journal of Machine Tools & Manufacture, 39, 1999, 1903–1923.
32. Jain V. K., Advanced machining processes, 16th edition, Allied Publishers Pvt. Limited., New Delhi, ISBN 81-7764-294-4, 2012.

33. Jain V.K. and Adsul S.G., Experimental investigations into abrasive flow machining (AFM), Int J Mach Tool Maunuf, 40, 2000, 1003–1021.
34. Jain V.K., Kumar R., Dixit P.M. and Sidpara A., Investigations into abrasive flow finishing of complex workpieces using FEM, Wear, 267, 2009, 71–80.
35. Jain, V.K., Magnetic field assisted abrasive based micro-/nano-finishing, Journal of Materials Processing Technology 209, 2009, 6022–6038.
36. Jayswal S.C., Jain V.K. and Dixit P.M., Modeling and simulation of magnetic abrasive finishing process", Int J Adv Manuf Technology, 26, 2005, 477–490.
37. Jeong D.K. and Kyung D.K., Deburring of burrs in spring collets by abrasive flow machining, International Journal of Advanced Manufacturing Technology, 2004, 469–473.
38. Judal K.B., Yadava V. and Pathak D., Experimental Investigation of Vibration Assisted Cylindrical–Magnetic Abrasive Finishing of Aluminum Workpiece, Materials and manufacturing Processes, 28(11), 2013, 1196-1202.
39. Jung D., Wang W.L., Knafl A., Jacobs T.J., Hu S. J. and Assanis, D.N. , Experimental investigation of abrasive flow machining effects on injector nozzle geometries, engine performance, and emissions in a di diesel engine, International Journal of Automotive Technology, 2008, 9-15.
40. Kamal K. K., Ravikumar N.L., Piyushkumar B. Tailor, Ramkumar J., Sathiyamoorthy D., Performance evaluation and rheological characterization of newly developed butyl rubber based media for abrasive flow machining process, journal of materials processing technology 209, 2008, 2212–2221.
41. Kamble P.D., Untawale S.P. and Sahare S.B., Use of Magneto Abrasive Flow Machining to Increase Material Removal Rate and Surface Finish VSRD International Journal of Mechanical, Auto. & Prod. Engg., 2 (7), 2012.
42. Kant G. and Sangwan K. S., Prediction and optimization of machining parameters for minimizing power consumption and surface roughness in machining, Journal of Cleaning Production, 2014, 151-164.
43. Kenda J., Pusavec F., Kermouche G. and Kopac J., Surface Integrity in Abrasive Flow Machining of Hardened Tool Steel AISI D2, Procedia Engineering, 19, 2011, 172–177.

44. Ko S. L., Baron Y. M. and Park J. I., Micro deburring for precision parts using magnetic abrasive finishing method, J of Mater Process Tech, 187-188, 2007, 19–25.
45. Kumar A., Kumar V. and Kumar J., Investigation of machining parameters and surface integrity in wire electric discharge machining of pure titanium, Proc I MechE, Part B: J Eng Manuf, 227 (7), 2013, 972–992.
46. Kumar A., Kumar V. and Kumar J., Multi-response optimization of process parameters based on response surface methodology for pure titanium using WEDM process. International Journal of Advance Manufacturing Technology, 68, 2013, 2645-2668.
47. Kwak J.S., Application of Taguchi and response surface methodologies for geometric error in surface grinding process, International Journal of Machine Tools Manufacturing, 45, 2005, 327–334.
48. Lau S, Yue M, Lee C, et al.., Un-conventional machining of composite materials, J of Mater Proc Tech, 48, 1995, 199–205.
49. Lee H.S., Kim D. I., An J.H., Lee H.J., Kim K.H. and Jeong H., Hybrid polishing mechanism of single crystal SiC using mixed abrasive slurry (MAS), CIRP Annals - Manufacturing Technology, 59, 2010 333–336.
50. Lin H., Min W., Cailou C. and Xiusheng J., FEM Analysis of Spring-backs in Age Forming of Aluminum Alloy Plates, Chinese Journal of Aeronautics, 20, 2007, 564-569.
51. Lung Kwang Pan, Wang Che Chung, Wei Shien Long and Hai Feng Sher, Optimizing multiple quality characteristics via Taguchi method-based Grey analysis, Journal of Materials Processing Technology, 182, 2007, 107–116.
52. Maity K. P. and Tripathy K. C., Modelling and optimization of abrasive flow machining of al alloy. 4M/ICOM, 450, 2015.
53. Mali H.S. and Manna A., Optimum selection of abrasive flow machining conditions during fine finishing of Al/15 wt% SiC-MMC using Taguchi method, International Journal of Advanced Manufacturing Technology, 2010, 1013–1024.
54. Mali H.S. and Manna A., Simulation of surface generated during abrasive flow finishing of Al/SiCp-MMC using neural networks, International Journal Advanced Manufacturing Technology, 2012, 1263–1268.

55. Mamilla R. S., Ramkumar J. and Jain V. K., Experimental investigation and mechanism of material removal in nano finishing of MMCs using abrasive flow finishing (AFF) process, wear, 266, 2009, 688–698.
56. Mamilla R.S., Jain V.K. and Ramkumar J., Experimental investigations into rotating workpiece abrasive flow finishing, wear, 267, 2009, 43–51.
57. Miracle B., Metal matrix composites from science to technological significance, Composites Science and Technology, 65, 2005, 2526-2540.
58. Mkaddem A. and Mansori M. E., Finite element analysis when machining UGF-reinforced PMCs plates: Chip formation, crack propagation and induced-damage, Materials and Design, 30, 2009, 3295–3302.
59. Montgomery D.C., Design and Analysis of Experiments, 4th ed., 2002, Wiley, New York.
60. Muguthu, J. N. and Gao D., Profile Fractal Dimension and Dimensional Accuracy Analysis in Machining Metal Matrix Composites (MMCs), Materials and manufacturing Processes, 28 (10), 2013, 1102-1109.
61. Mulik R.S. and Pandey P.M., Experimental Investigations and Modeling of Finishing Force and Torque in Ultrasonic Assisted Magnetic Abrasive Finishing. Journal of Manufacturing Science and Engineering, 134, 2012, 1-12.
62. Muller F. and Monaghan J., Non-conventional machining of particle reinforced metal matrix composites, Journal of Materials Processing and Technology, 118, 2001, 278-285.
63. Myers R.H. and Montgomery D.C., Response Surface Methodology: process and product optimization using designed experiments, John Wiley & Sons, 2002, New York.
64. Ozden Sedat, Ekici Recep and Nair Fehmi, Investigation of impact behaviour of aluminium based SiC particle reinforced metal–matrix composites, Composites: Part A, 38, 2007, 484–494.
65. Paiva R. M. M., Antonio C. A. C. and Da Silva L. F. M., Multiobjective optimization of mechanical properties based on the composition of adhesives, International Journal of Mechanics and Materials in Design, 6(1), 2015, 1-24.
66. Pandey P. C. and Shan H. S., Modern machining processes, 27th edition, Tata

McGraw-Hill Publishing Company Limited., New Delhi, ISBN 0-07-096553-6, 2005.

67. Paulo D. J., Maranhao C., Faria P., Abrao A., Rubio J. C. and Silva L. R., Precision radial turning of AISI D2 steel, International Journal of Advanced Manufacturing Technology, Springer, 42, (2009), 842-849.
68. Paulo D. J., Mranhao C., et al., Performance of cutting tools in machining Cu/W alloys for application in EDM electrodes, Int. J. Refractory Metals and Hard Materials, 27, 2009, 676-682
69. Pecas P. and Henriques E.A., Influence of silicon powder nixed dielectric on conventional discharge machining, International Journal of Machine Tools and Manufacture, 43, 2003, 1465-1471.
70. Rantatalo M., Jan-Olov A., Bo Goransson and Norman P., Milling machine spindle analysis using FEM and non-contact spindle excitation and response measurement, International Journal of Machine Tools & Manufacture, 47, 2007, 1034–1045.
71. Rao R. and Yadava V., Multi-objective optimization of Nd:YAG laser cutting of thin super alloy sheet using grey relation a analysis with entropy measurement, Optics and Laser Technology, 41, 2009, 922–30.
72. Rosso M., Ceramic and metal matrix composites: route and properties, Journal of Materials Processing Technology, 175, 2006, 364-375.
73. Sadiq A. and Shunmugam M.S., A novel method to improve finish on non-magnetic surfaces in magneto- rheological abrasive honing process, Tribology International, 43, 2010, 1122–1126.
74. Sangwan K.S., Saxena S., et al., Optimization of machining parameters to minimize surface roughness using integrated ANN-GA approach, Procedia CIRP, 29, 2015, 305-310.
75. Sankar M. R., Jain V. K. and Ramkumar J., Abrasive flow machining (AFM): An Overview, 2011.
76. Sankar M.R., Jain V.K., Ramkumar J. and Josh Y.M., Rheological characterization of styrene-butadiene based medium and its finishing performance using rotational abrasive flow finishing process. International Journal of Machine Tools & Manufacture, 51, 2012, 947–957.

77. Sehijpal S. and Shan H.S., Development of magneto abrasive flow machining process, Int J Mach Tool Maunuf, 42, 2002, 953-959.
78. Sharma R. K., Kumar D. and Kumar P., Manufacturing excellence through TPM implementation: a practical analysis, Industrial management and data systems, 106(2), 2006, 256-280.
79. Shuren Zhang, Weina Liu, Lifeng Yang, Chunfeng Zhu, Chun Li,Junye Li and Xin Li, Study on Abrasive Flow Ultra-Precision Polishing Technology of Small Hole, Proceedings of the 2009 IEEE International Conference on Mechatronics and Automation, August 9 - 12, 2009, Changchun, China.
80. Sidhu S.S., Batish A. and Kumar S., Study of Surface Properties in Particulate-Reinforced Metal Matrix Composites (MMCs) Using Powder-Mixed Electrical Discharge Machining (EDM), Materials and manufacturing Processes, 29 (1), 2014, 495-500.
81. Singh D.K., Jain V.K. and Raghuram V., Parametric study of magnetic abrasive finishing process. Journal of Materials Processing Technology, 149, 2004, 22–29.
82. Singh R. and Walia R. S., Hybrid Magnetic Force Assistant Abrasive Flow Machining Process Study for Optimal Material Removal, International Journal of Applied Engineering Research, 7(11), 2012, ISSN 0973-4562.
83. Singh R., Walia R. S. and Suri N. M., Study Of Parametric Effect On Surface Roughness Improvement For Hibrid Centrifugal Force Assisted Abrasive Flow Machining Process, International Journal of Latest Research in Science and Technology, 1(3), 2012, 198-201.
84. Singh S., Kumar P. and Shan H.S., Quality Optimization of surface finishing by magnetic field assisted abrasive flow machining through Taguchi technique, International Journal of Computer Applications in Technology, 27(1), 2006.
85. Sirahbizu L., Mahapatra M. Mohan, et al., Influence of Reinforcement Type on Microstructure, Hardness, and Tensile Properties of an Aluminum Alloy Metal Matrix Composite. Journal of Minerals and Materials Characterization and Engineerin, 1, 2013, 124-130.
86. Souza A.S., Dos S., Walter N.L., et al., Application of Box–Behnken design in the optimization of an on-line pre-concentration system using knotted reactor for

cadmium determination by flame atomic absorption spectrometry, Spectrochimica Acta Part-B, 609, 2005, 737–742.

87. Srivatsan T. S., Al-Hajri M., Smith C. and Petraroli M., The tensile response and fracture behavior of 2009 aluminium alloy metal matrix composite. Mater Sci Eng, 346, 2003, 91–100.
88. Sun C., Zhu D., Li Z. and Wang L., Application of FEM to tool design for electrochemical machining freeform surface, Finite Elements in Analysis and Design, 43, 2006, 168 – 172.
89. Tofigh A. and Shabani O., Efficient optimum solution for high strength Al alloys matrix composites, Ceramics Int., 39, 2013, 7483-7490.
90. Tzeng Hsinn-Jyh, Yan Biing-Hwa, Hsu Rong-Tzong and Lin Yan-Cherng, Self-modulating abrasive medium and its application to abrasive flow machining for finishing micro channel surfaces, Int J Adv Manuf Technol, 32, 2007, 1163–1169.
91. Uhlmann E., Mihotovic V., Coenen A., Modelling the abrasive flow machining process on advanced ceramic materials, Journal of Materials Processing Technology, 209, 2009, 6062–6066.
92. Venkata B., Ganguly I**.** and Srinivasarao G**.,** Machinability of Aluminum Metal Matrix Composite Reinforced with In-Situ Ceramic Composite Developed from Mines Waste Colliery Shale, Mat Manuf Proc, 28, 2013, 1082-1089.
93. Walia R. S., Shan H.S. and Kumar P., Abrasive flow machining with additional centrifugal force applied to the media, Machining science and technology, 10, 2006, 341-354.
94. Wang A.C. and Weng S.H., Developing the polymer abrasive gels in AFM processs, J of Materials Processing Technology, 192–193, 2007, 486–490.
95. Wang A.C., Liu C.H., Liang K.Z. and Pai S.H., Study of the rheological properties and the finishing behavior of abrasive gels in abrasive flow machining, Journal of Mechanical Science and Technology, 2007, 1593-1598.
96. Wang, Z., Geng X., Chi G. and Wang Y., Surface Integrity Associated with SiC/Al Particulate Composite by Micro-Wire Electrical Discharge Machining, Materials and manufacturing Processes, 29 (5), 2014, 532-539.

97. Wani A. M., Yadava V. and Khatri A., Simulation for the prediction of surface roughness in magnetic abrasive flow finishing (MAFF), J of Mater Process Tech, 190, 2007, 282–290.
98. Weller E. J., Non-Traditional machining processes, Society of Manufacturing Engineers, 1984, 15-71.
99. Yamaguchi H., Srivastava A. K., Tan M. A., Riveros R. E. and Hashimoto F., Magnetic abrasive finishing of cutting tools for machining of titanium alloys, CIRP Annals - Manufacturing Technology, 61, 2012, 311–314.
100. Yan B., Tsai H., Chung, Huang Yuan, et al., Examination of wire electrical discharge machining of Al2O3p/6061Al composites, J Mach Tools Manuf, 45, 2005, 251–259.
101. Yin X. and Komvopoulos K., A slip-line plasticity analysis of abrasive wear of a smooth and soft surface sliding against a rough (fractal) and hard surface. International Journal of Solids and Structures, 49, 2012, 121–131.
102. Zhong-He C., Wei-qiang W. and Le-Wen Z., FEM analyses of stress and deformation of a flexible inner pressure bolt, J China Univ Mining & Technol, 18, 2008, 584–587.

APPENDICES

Nomenclature

SEM:	scanning electron microscope
XRD:	X-RAY diffraction technique
MMC:	Metal matrix composite
SiC:	silicon carbide (%wt)
SiC/Al MMC:	wt % of SiC in MMC
MRR:	material removal rate
ΔRa :	Change in surface roughness
Y:	Desired response
F:	Response function
P:	Extrusion pressure
p:	Oil percentage in media
n:	Mesh no. /grit size
c:	Concentration of abrasives
Wp:	Work piece material
N:	Number of cycles

L27 STANDARD ORTHOGONALARRAY (SIX FACTORS, 3 LEVELS EACH

Experiment No.	A	B	C	D	E	F
1.	1	1	1	1	1	1
2.	1	1	1	1	2	2
3.	1	1	1	1	3	3
4.	1	2	2	2	1	1
5.	1	2	2	2	2	2
6.	1	2	2	2	3	3
7.	1	3	3	3	1	1
8.	1	3	3	3	2	2
9.	1	3	3	3	3	3
10.	2	1	2	3	1	2
11.	2	1	2	3	2	3
12.	2	1	2	3	3	1
13.	2	2	3	1	1	2
14.	2	2	3	1	2	3
15.	2	2	3	1	3	1
16.	2	3	1	2	1	2
17.	2	3	1	2	2	3
18.	2	3	1	2	3	1
19.	3	1	3	2	1	3
20.	3	1	3	2	2	1
21.	3	1	3	2	3	2
22.	3	2	1	3	1	3
23.	3	2	1	3	2	1
24.	3	2	1	3	3	2
25.	3	3	2	1	1	3
26.	3	3	2	1	2	1
27.	3	3	2	1	3	2

Pictorial view of SEM machine used for micro structure analysis

F Table for alpha= 95% confidence F (0.05)

DF	1	2	3	4	5	6	7	8	9	10	12	15
1	161.4476	199.5000	215.7073	224.5832	230.1619	233.9860	236.7684	238.8827	240.5433	241.8817	243.9060	245.9499
2	18.5128	19.0000	19.1643	19.2468	19.2964	19.3295	19.3532	19.3710	19.3848	19.3959	19.4125	19.4291
3	10.1280	9.5521	9.2766	9.1172	9.0135	8.9406	8.8867	8.8452	8.8123	8.7855	8.7446	8.7029
4	7.7086	6.9443	6.5914	6.3882	6.2561	6.1631	6.0942	6.0410	5.9988	5.9644	5.9117	5.8578
5	6.6079	5.7861	5.4095	5.1922	5.0503	4.9503	4.8759	4.8183	4.7725	4.7351	4.6777	4.6188
6	5.9874	5.1433	4.7571	4.5337	4.3874	4.2839	4.2067	4.1468	4.0990	4.0600	3.9999	3.9381
7	5.5914	4.7374	4.3468	4.1203	3.9715	3.8660	3.7870	3.7257	3.6767	3.6365	3.5747	3.5107
8	5.3177	4.4590	4.0662	3.8379	3.6875	3.5806	3.5005	3.4381	3.3881	3.3472	3.2839	3.2184
9	5.1174	4.2565	3.8625	3.6331	3.4817	3.3738	3.2927	3.2296	3.1789	3.1373	3.0729	3.0061
10	4.9646	4.1028	3.7083	3.4780	3.3258	3.2172	3.1355	3.0717	3.0204	2.9782	2.9130	2.8450
11	4.8443	3.9823	3.5874	3.3567	3.2039	3.0946	3.0123	2.9480	2.8962	2.8536	2.7876	2.7186
12	4.7472	3.8853	3.4903	3.2592	3.1059	2.9961	2.9134	2.8486	2.7964	2.7534	2.6866	2.6169
13	4.6672	3.8056	3.4105	3.1791	3.0254	2.9153	2.8321	2.7669	2.7144	2.6710	2.6037	2.5331
14	4.6001	3.7389	3.3439	3.1122	2.9582	2.8477	2.7642	2.6987	2.6458	2.6022	2.5342	2.4630
15	4.5431	3.6823	3.2874	3.0556	2.9013	2.7905	2.7066	2.6408	2.5876	2.5437	2.4753	2.4034
16	4.4940	3.6337	3.2389	3.0069	2.8524	2.7413	2.6572	2.5911	2.5377	2.4935	2.4247	2.3522
17	4.4513	3.5915	3.1968	2.9647	2.8100	2.6987	2.6143	2.5480	2.4943	2.4499	2.3807	2.3077
18	4.4139	3.5546	3.1599	2.9277	2.7729	2.6613	2.5767	2.5102	2.4563	2.4117	2.3421	2.2686

19	4.3807	3.5219	3.1274	2.8951	2.7401	2.6283	2.5435	2.4768	2.4227	2.3779	2.3080	2.2341
20	4.3512	3.4928	3.0984	2.8661	2.7109	2.5990	2.5140	2.4471	2.3928	2.3479	2.2776	2.2033
21	4.3248	3.4668	3.0725	2.8401	2.6848	2.5727	2.4876	2.4205	2.3660	2.3210	2.2504	2.1757
22	4.3009	3.4434	3.0491	2.8167	2.6613	2.5491	2.4638	2.3965	2.3419	2.2967	2.2258	2.1508
23	4.2793	3.4221	3.0280	2.7955	2.6400	2.5277	2.4422	2.3748	2.3201	2.2747	2.2036	2.1282
24	4.2597	3.4028	3.0088	2.7763	2.6207	2.5082	2.4226	2.3551	2.3002	2.2547	2.1834	2.1077
25	4.2417	3.3852	2.9912	2.7587	2.6030	2.4904	2.4047	2.3371	2.2821	2.2365	2.1649	2.0889
26	4.2252	3.3690	2.9752	2.7426	2.5868	2.4741	2.3883	2.3205	2.2655	2.2197	2.1479	2.0716
27	4.2100	3.3541	2.9604	2.7278	2.5719	2.4591	2.3732	2.3053	2.2501	2.2043	2.1323	2.0558
28	4.1960	3.3404	2.9467	2.7141	2.5581	2.4453	2.3593	2.2913	2.2360	2.1900	2.1179	2.0411
29	4.1830	3.3277	2.9340	2.7014	2.5454	2.4324	2.3463	2.2783	2.2229	2.1768	2.1045	2.0275
30	4.1709	3.3158	2.9223	2.6896	2.5336	2.4205	2.3343	2.2662	2.2107	2.1646	2.0921	2.0148
40	4.0847	3.2317	2.8387	2.6060	2.4495	2.3359	2.2490	2.1802	2.1240	2.0772	2.0035	1.9245
60	4.0012	3.1504	2.7581	2.5252	2.3683	2.2541	2.1665	2.0970	2.0401	1.9926	1.9174	1.8364
120	3.9201	3.0718	2.6802	2.4472	2.2899	2.1750	2.0868	2.0164	1.9588	1.9105	1.8337	1.7505
inf	3.8415	2.9957	2.6049	2.3719	2.2141	2.0986	2.0096	1.9384	1.8799	1.8307	1.7522	1.6664